A Modular Plasmid System for Expression of Genes in *Neisseria gonorrhoeae*

A thesis

submitted in partial fulfilment

of the requirements for the degree

of

Master of Science (Research) in Cellular and Molecular Biology

at

The University of Waikato

by

Chloe Dale Flemming

THE UNIVERSITY OF
WAIKATO
Te Whare Wānanga o Waikato

2023

Abstract

Neisseria gonorrhoeae is the causative agent of the sexually transmitted infection, gonorrhoea. Antimicrobial resistance in *N. gonorrhoeae* is of increasing concern and there is no current vaccine. Over the last 80 years, *N. gonorrhoeae* has become highly resistant to many frontline antibiotics, and as such, there are now limited treatment options. Research and development is critical for the discovery of new diagnostic assays, antimicrobials, and vaccines that combat *N. gonorrhoeae*.

To date, there are a variety of genetic tools available for generating mutations, gene deletions, and gene complementation in *N. gonorrhoeae*. Plasmids are available for the introduction of new genes of interest and complementation, however replicating plasmids are often unstable, time consuming to manipulate, and suffer from poor transformation efficiencies.

Here, this project aimed to resolve the current issues with *N. gonorrhoeae* plasmid systems by using a Golden Gate assembly technique to design a modular cloning system specifically to enable custom gene expression in *N. gonorrhoeae*. Golden Gate cloning uses Type IIS restriction endonucleases to allow the assembly of complex multipart plasmids from reusable DNA parts. These include the gonococcal-specific cryptic plasmid maintenance region from pEG2, the Opa promoter, antibiotic resistance genes encoding kanamycin and erythromycin resistance, fluorescent proteins, and a ColE1 origin of replication for propagation in *Escherichia coli*. Our system was designed to be more efficient by enabling the rapid generation of very small, customised plasmids capable of replication in both *E. coli* and *N. gonorrhoeae*.

Currently, there are vast gaps in our knowledge of *N. gonorrhoeae* biology. This thesis offers a new system that is an efficient tool for custom gene expression in *N. gonorrhoeae* to improve our understanding of this pathogen. Improving research approaches, such as mutagenesis and complementation, will contribute to drug and vaccine discovery efforts searching for reliable treatments for this devastating pathogen.

Acknowledgements

I would like to thank my primary supervisor Dr Joanna Hicks and secondary supervisor Dr Will Kelton. The support and guidance you two have given me is incredible, I always felt I could ask any question at any time, and you both responded quickly and comprehensively. There was always passion in your speech and gestures, making everything exciting and fun. You gave me confidence to work independently and the knowledge to question deeper. I am extremely grateful for the effort you have invested in me and the time you have taken to guide me. I appreciate both of you greatly.

Thank you to the past and present members of the Proteins and Microbes lab team. The friendliness and positive environment you surrounded me with made every day enjoyable. A special thanks to Emma Walker, Stacy van Niekerk, and Kyrin Hanning for your advice and direction when I needed it. I am utmost grateful.

Thank you to the University of Waikato for my MSc Research Scholarship and for providing the opportunity to study in such a welcoming manner.

To my closest friends, Zia Tilsley and Megan Buchanan, I want to thank you for the incredible support you both gave me and the enthusiasm you encouraged me with. You always relieved my concerns and reminded me to be proud of my achievements. I cannot appreciate you both enough.

To my amazing partner, Matthew Cranefield, I want to thank you for your constant support and comfort when I needed it most. You listened to me when I needed to talk through my work and helped me through all the hardest times. I will always be grateful for your kindness and patience.

I would like to give special thanks to my Nana Pauline. In my toughest times of being a student, you gave me support and the warmest love. I cannot thank you enough.

Finally, yet importantly, I want to thank my wonderful family, Alan, Leigh, Amber, Cody, and Kyle. You are my anchor, my deepest support, and the reason I have the strength to achieve. From showing interest in my work, to providing a home cooked meal, I will forever appreciate your care and pride in what I do.

Table of Contents

List of Figures

List of Tables

Glossary

amp	Ampicillin Resistance
AMR	Antimicrobial Resistance
BLAST	Basic Local Alignment Search Tool
bp	Base Pair
CDC	Centre of Disease and Control
CFU	Colony Forming Units
ColE1	Colicin E1
cPCR	Colony Polymerase Chain Reaction
cppA	Cryptic Plasmid Protein A
ddH_2O	Double Distilled Hydrogen Dioxide
DNA	Deoxyribose Nucleic Acid
dsDNA	Double Stranded DNA
DUS	DNA Uptake Sequence
EFGR	Epidermal Growth Factor Receptor
Erm	Erythromycin Resistance
GC	Gonococcal
GCB	Gonococcal Base
GFP	Green Fluorescent Protein
GMO	Genetically Modified Organism
HIV	Human Immunodeficiency Virus
HP	Hypothetical Protein
HSPG	Heparan Sulphate Proteoglycan
KO	Knock Out
Kan	Kanamycin Resistance
LB	Luria Broth
lctP	Lactate Permease
LOS	Lipooligosaccharides
LP	Long Pass
MM	Master Mix
MoClo	Molecular Cloning

OD	Optical Density
ORF	Open Reading Frame
Opa	Opacity Protein
Ori	Origin of Replication
PAMP	Pathogen Associated Molecule Patterns
PBP2	Penicillin Binding Protein 2
PBS	Phosphate Buffered Saline
PCR	Polymerase Chain reaction
pDNA	Plasmid DNA
Por	Porin Ion Chanel Protein
pTet	Tetracycline Promoter
QV	Quality Value
RMP	Reduction Modifiable Protein
RPM	Revolutions Per Minute
rsGFP	Red Shift GFP
sfGFP	Super Fold GFP
SOC	Super Optimal Broth with Catabolite Repression
STI	Sexually Transmitted Infection
TAE	Tris-acetate-EDTA
TetR	Tetracycline Resistance
Tm	Melting Temperature
trp	Tryptophan Operon
vapD	Virulence-associated Protein D
WHO	World Health Organisation
WT	Wild Type

Chapter One

Introduction

1.1 Introduction

The bacterium *Neisseria gonorrhoeae* (gonococcus) is a human obligate pathogen that is widely known to cause the sexually transmitted infection, gonorrhoea. Gonorrhoea primarily infects the mucosa of the urogenital tract, but is also capable of infecting other exposed mucosal sites such as the pharynx, rectum, and conjunctivae (Kirkcaldy et al., 2019). Gonorrhoea infection can present in both men and women as symptomatic and asymptomatic with a higher rate of asymptomatic infection in females. Symptomatic infection usually presents as urethritis in males and endo- or ectocervicitis in females. When left untreated, gonorrhoea can lead to complications such as pelvic inflammatory disease, infertility, blindness or sores in the eyes of new-born babies, a higher risk of contracting Human Immunodeficiency Virus (HIV) (Mayo Clinic, n.d.), and even death (Green et al., 2022). In 2021, there were 6458 cases reported in Aotearoa New Zealand (ESR, n.d.) and in 2020, the World Health Organisation (WHO) estimated 82 million cases of gonorrhoea worldwide, most of which were in the African and Western Pacific Region (WHO, n.d.). Compounding increasing rates of gonorrhoea infection is the rise of antibiotic resistant *N. gonorrrhoeae* strains, reducing treatment options. Additionally there is no vaccine for gonorrhoea, due to the near lack of immunological memory in the human body, even after repeated infection (Green et al., 2022).

1.2 Antimicrobial resistance

Over the past 80 years *N. gonorrhoeae* has developed resistance to every antibiotic used for its treatment, leading to the bacterium gaining 'superbug' status making it a candidate to cause an untreatable disease (Figure 1.1). The Centre for Disease Control and Prevention (CDC) has estimated there are 550,000 resistant strains of *N. gonorrhoeae* yearly in the United States (Adamson & Klausner, 2021). Resistance to antibiotics in *N. gonorrhoeae* develops due to spontaneous mutation and/or gene acquisition. Once established these resistance elements can be transferred to other gonococci by transformation, which facilitates the spread of resistance alleles. Transformation has played a significant role in the evolution of antimicrobial resistance

in *N. gonorrhoeae*, who are naturally competent for DNA transformation over their entire lifecycle. They are highly competent for transformation by their own DNA and to a lesser extent although still significant that of closely related bacteria, mainly commensal Neisseria species and the other pathogenic Neisseria species, *Neisseria meningitidis*. For example, during asymptomatic pharyngeal gonorrhoea, gonococci encounter other Neisseria species, that may promote the initial emergence of antibiotic resistance by transformation in the gonococci. For example, donor DNA from commensal Neisseria species has created mosaic genes in *N. gonorrhoeae* such as the *penA* mosaic alleles that encodes variant of the penicillin binding protein 2 (PBP2) that have reduced affinity for β-lactam antibiotics (Unemo & Shafer, 2011). These resistance alleles can then spread amongst *N. gonorrhoeae* strains via horizontal gene transfer. The natural competence of *N. gonorrhoeae* has quickly led to the spread of antibiotic resistant strains, making treatment for gonorrhoea increasingly difficult (Dillard, 2011). Research and development is desperately needed for assays, new antimicrobials, and vaccines against *N. gonorrhoeae*.

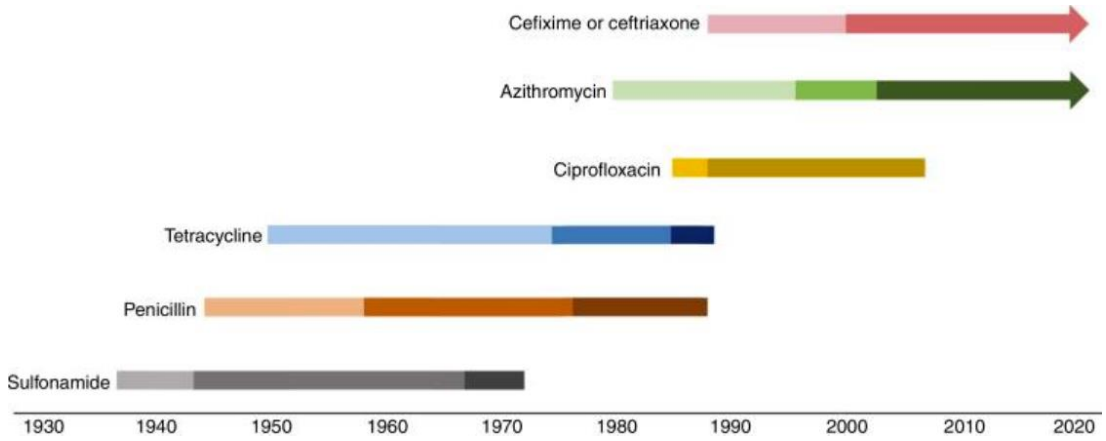

Figure 1.1: History of antimicrobial resistance in *N. gonorrhoeae*. Antimicrobial resistance of sulfonamide, penicillin, tetracycline, ciprofloxacin, azithromycin, and cefixime or ceftriaxone have been reported in *N. gonorrhoeae* over time. The colour variations represent events that affected the level of resistance. Image from (Costa-Lourenço et al., 2017).

1.3 Adaptation to the host

N. gonorrhoeae is capable of infecting a wide range of host mucosa and possesses an array of surface molecules to bind and invade various types of tissue. The bacterium expresses three primary outer membrane proteins, the colony opacity associated (Opa) proteins, the porin ion channel protein (Por) and the reduction modifiable protein (RMP), along with two pathogen associated molecular patterns (PAMPs), lipooligosaccharides (LOS) and the type IV pili (J. L. Edwards & Apicella, 2004). Many of these surface molecules possess the ability to undergo both phase and antigenic variation. In part this explains why it is difficult for the human immune system to develop immunological memory. In addition to constant surface variation *N. gonorrhoeae* is able to manipulate host cell signalling events to promote its survival and pathogenesis, primarily through its key outer membrane antigens.

1.3.1 Exploitation of host epithelial cells

N. gonorrhoeae can exploit host cell pathways such as epithelial cell exfoliation. Exfoliation of epithelial cells is an innate immune response that aims to avert colonisation of bacteria by shedding a small fraction of cells (Walker et al., 2023). Two characteristics of gonococci play a large role in this exploitation: Opa proteins and pili. Opa proteins are variable proteins that reside on the outer membrane of gonococcal cells that interact with host cells during infection. Opa proteins commonly interact with the carcinoembryonic antigen cell adhesion molecules (CEACAMs) which assist in cell-cell recognition and regulate other cellular mechanisms such as cell shedding (Kuespert et al., 2006). Pili are known for their role in adhesion to host cells and colonisation and when retracted by gonococci, the Opa protein to host cell interaction is strengthened (Walker et al., 2023) enabling tight binding to host cells.

Exfoliation of host cells is exploited via gonococci that express the Opa protein, which bind to CEACAM receptors of the host epithelial cells (Figure 1.2). This modifies the expression of genes such as CD105 by allowing nitric oxide to diffuse into the host cell. This expression of CD105 activates integrin (important receptors in cell adhesion), and lowers phosphorylation of β-catenin, maintaining the epithelial cell bond and preventing cell shedding (Walker et al., 2023).

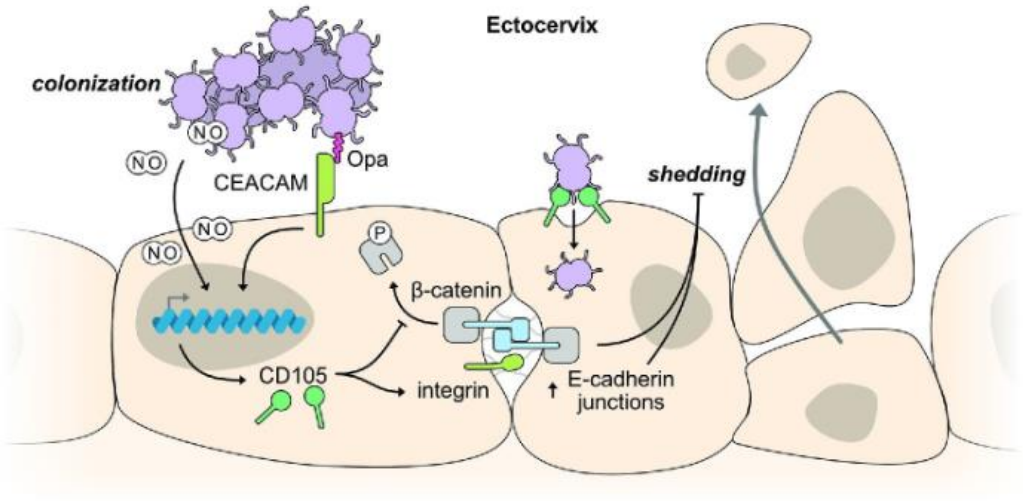

Figure 1.2: Exfoliation of host cells exploitation. Exfoliation of host cells is exploited via gonococci that express the Opa protein (pink), which bind to CEACAM receptors (green left) of the host epithelial cells. This modifies the expression of the gene CD105 (neon green) by allowing nitric oxide (NO) to diffuse into the host cell. Expression of CD105 activates integrin (green right), lowering phosphorylation (P) of β-catenin (grey), and maintaining the epithelial cell bond and preventing cell shedding. Image adapted from (Walker et al., 2023).

N. gonorrhoeae is also capable of invading endocervical cells of the transition zone in the female reproductive tract. Binding to the bacteria to endocervical cells initiates cell invasion by promoting cytoskeletal rearrangements and weakening of cell junctions. CEACAM expression is reduced in the endocervical cells, therefore *N. gonorrhoeae* interacts with the HSPG receptor leading to activation of the EFGR receptor (V. L. Edwards et al., 2013). This results in decreased integrin expression, increased phosphorylation of B-catenin and movement of E-cadherin junction proteins to the membrane under the bacteria (V. L. Edwards et al., 2013). This weakens cell junctions and alongside phosphorylation of NMII and rearrangement of actin filaments results in cell invasion (Wang et al., 2017). Although only a small number of gonococci cross the epithelial barrier via this intracellular route, they can cause both local and disseminated infections.

1.3.2 Evasion of host immune mechanisms

N. gonorrhoeae has adapted to the host immune response through coevolution, and as such is well evolved to bypass immune responses in humans via a range of mechanisms. These evasion mechanisms generally limit the host protective immune response leaving the host unable to mount an immune response upon reinfection and making vaccine design difficult. *N. gonorrhoeae* is capable of manipulating both innate and adaptive immune responses. For example, to dampen the innate response it expresses lysozyme inhibitors, reduces complement activity, manipulates neutrophils for intracellular survival, reprogrammes macrophages, induces an anti-inflammatory phenotype in dendritic cells, and manipulates pro- and anti-inflammatory cytokine responses. Additionally, *N. gonorrhoeae* can hinder the development of both B and T cell immunity by hindering antibody production and function and inducing a Th17 cell response at the expense of a Th1/Th2 cell response which is critical for lasting adaptive immunity.

For example, *N. gonorrhoeae* can avoid macrophages, which detect and destroy harmful bacteria in the body via phagocytosis (Lendeckel et al., 2022). This is due to the cell membrane of *N. gonorrhoeae* containing LOS which are used by the cells to imitate carbohydrates in order to lower recognition by the body's phagocytic cells, evading phagocytosis by macrophages by constantly changing its surface proteins and not allowing antibodies to bind (Green et al., 2022). This is potentially the reason for why human immune memory is weak and a vaccine is so difficult for *N. gonorrhoeae* as the changing surface proteins make it challenging to target (Green et al., 2022).

Further understanding of mechanisms of *N. gonorrhoeae* infection and immune evasion will contribute to the development of gonococcal vaccines. Alongside vaccines, new antimicrobials are needed to combat antimicrobial resistance. Central to vaccine and antimicrobial research and development is the ability to genetically manipulate *N. gonorrhoeae* easily and quickly.

1.4 Tools for genetic manipulation of *Neisseria gonorrhoeae*

Genetic manipulation plays a large role in research of *N. gonorrhoeae*. It allows researchers to modify DNA for reasons such as inserting or deleting genes, creating fluorescent strains of bacteria, or fusing proteins to different tags. Currently, there are

few studies improving the contemporary treatments for *N. gonorrhoeae* through genetic manipulation tools. However, there a multiple aspects of manipulation that need to be considered before proceeding.

1.4.1 General considerations for genetic manipulation of *N. gonorrhoeae*

N. gonorrhoeae is naturally transformable, making genetic manipulation easy via spot or liquid transformation. However, the DNA being transformed in gonococci requires an important feature called the gonococcal DNA uptake sequence (DUS). This DUS was identified to be a 10 bp sequence of 5' GCCGTCTGAA 3' (Burnstein et al., 1988; Goodman & Scocca, 1988; Graves et al., 1982) and later found to be most efficient as a 12 bp sequence of 5' ATGCCGTCTGAA 3' by Smith, Gwinn, and Salzberg in 1999, increasing transformation by two-fold in gonococci (Smith et al., 1999). The DUSs are commonly found throughout the gonococcal genome as short conserved sequences, assisting in the exchange of DNA from the environment, and therefore necessary when attempting to manipulate genetics (Spencer-Smith et al., 2016).

Facilitating transformation efficiency in *N. gonorrhoeae* is the inclusion of resistance marker genes such as an ampicillin resistance gene (*amp*), kanamycin resistance gene (*kan*) or erythromycin resistance genes (*erm*). Although marker-less constructs are feasible in the gonococcus the inclusion of a resistance marker allows for more efficient screening of colonies that have successfully taken up DNA, as when grown on antibiotic plates, only the colonies with the extracellular DNA inside will be present.

1.4.2 Methods of genetic manipulation

A paper from 2011 titled "Genetic Manipulation of *Neisseria gonorrhoeae*" (Dillard, 2011) recognises the increased antibiotic resistance of the bacterium and how the rate of natural transformation has aided in this problem. This study takes advantage of the transformation efficiency by genetically manipulating the gonococci, finding mutants through screening with and without selection, using constructs designed to encourage genetic mutation, complementation, and heterologous gene expression (Dillard, 2011). This paper lays out majority of the staple methods needed to work with and grow *N. gonorrhoeae*, such as the media it needs to thrive, how to select for piliated and Opa positive colonies, create transformants, and analyse the data.

1.4.2.1 Spot transformation

The paper outlines the genetic manipulation of *N. gonorrhoeae* via either a liquid or spot transformation with DNA that contains the DUS and uses electroporation for when this sequence not used. The Dillard paper recognised that this DUS was essential in their constructs for transformation of *N. gonorrhoeae*. However, they state that only piliated colonies were naturally transformable and that piliation was phase-dependant during growth.

In their methods, the spot transformations are performed by soaking spots of highly concentrated DNA containing the DUS on a plate and streaking the bacteria through the spots, producing colony forming units (CFU) of up to 20 – 50%. This method is stated to be more efficient than the liquid transformations but not as time efficient. As spot transformations are so efficient, it is possible to insert mutations that have no antibiotic resistance gene in the plasmid, using PCR to screen. However, this method is often used when transforming plasmids with mutated constructs that were first cloned into *Escherichia coli* with a selectable marker chosen for insertion into the chromosome. These constructs are prepared for gonococcal transformation by flanking the marker with gonococcal DNA on both sides for double-crossover homologous recombination and linearisation of the construct to prevent inserting the entire insertion of the construct or selection of colonies that have only had a single-crossover recombination. Linearisation is said to be unnecessary if the plasmid is 8 kb or larger as *N. gonorrhoeae* will process fragments of this size before DNA uptake when transforming naturally.

The Dillard paper also states that it is also possible to use the spot transformation method to perform insertion-duplication mutagenesis for incorporating plasmids into the chromosome of the bacteria. This is done by inserting a single fragment of gonococcal DNA into the plasmid when cloning into *E. coli*, using an antibiotic resistance marker for selection, and single-crossover recombination will insert the circularised plasmid into the chromosome of *N. gonorrhoeae* during transformation.

1.4.2.2 Liquid transformation

A liquid transformation can also be done for the same outcomes however this is considered less efficient but faster as frozen stocks of bacteria can be prepared

previously to the transforming. It is also less likely to produce colonies of mixed populations, unlike the spot transformation method.

1.4.2.3 Electroporation

Electroporation is a rarely used method for transformation of DNA into *N. gonorrhoeae* as it is far less efficient, but can be useful when transforming a nonpiliated strain or when transforming with DNA that does not contain the gonococcal DUS (Dillard, 2011). Although this may be the only method to use at times, it can be difficult to keep cells viable, as the washing conditions used to remove salts in this method are harsh on the bacteria and therefore must be done quickly.

The transformation methods outlined in the Dillard 2011 paper aim to insert DNA into *N. gonorrhoeae* for genetic manipulation. This can be achieved in multiple ways, most of which involve the use of a vector, otherwise known as a plasmid.

1.4.3 Gene insertion

A common way to insert genes of interest is via a plasmid. Plasmids allow for horizontal gene transfer of genetic information, such as fluorescent markers or antibiotic resistance markers, making it easy to manipulate the genetics of bacteria. An essential component for gene expression is making sure the plasmid being used will both duplicate and maintain the plasmid DNA as well as the desired DNA insert.

Plasmids were first discovered in the early 1950s and plasmid-based gene expression was first used by Stanley Cohen, Herbert Boyer, and Charles Brinton in 1972 (Kazi et al., 2022). The earliest discovery of a plasmid in gonococci was the cryptic plasmid pJD1, which was found to be in 96% of gonococci strains, and about 4.2 kb in size (Cehovin & Lewis, 2017). It did not appear to have a phenotype or function but curiously had many inverted repeat regions. The plasmid contains the DUS, aiding in DNA uptake during transformations. It has also been suggested that this cryptic plasmid can delete regions of itself and take up DNA to replace it, providing genetic flexibility, and potentially uses the repeat regions as a way of protecting the DNA via the formation of secondary structures to physically disable enzymatic activity (Davies & Normark, 1980).

Plasmids are widely used to insert genetic material directly into the chromosomes of bacteria. Plasmids can either be an extra element in addition to the chromosome (not integrated) or deliver DNA for chromosome integration via double-crossover recombination.

1.4.4 Double-crossover recombination

Homologous recombination in bacteria is where DNA from another cell is inserted into the genome of a recipient cell (Vos, 2009). It is generally used by bacteria to create genetic variation, potentially providing survival advantages. A double-crossover recombination event is where a fragment of the chromosome is exchanged in two areas that share regions of homology, creating a section in the middle that has new DNA and the outer parts the same (Figure 1.3). A double-crossover event can be used to manipulate the genetics of bacteria by inserting a fragment of DNA into the chromosome via a plasmid construct.

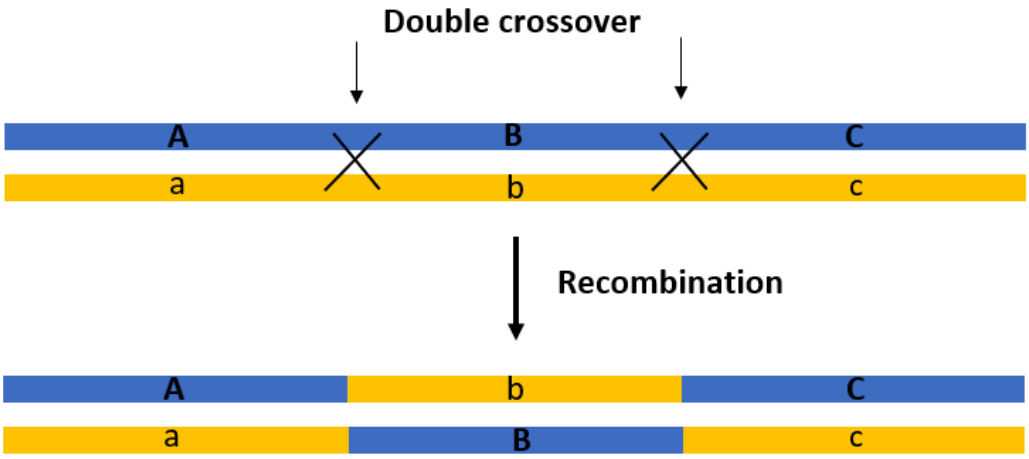

Figure 1.3: A double crossover recombination event. Chromosomes can exchange genetic information during a double crossover recombination event when they share two regions of homology (x marks on figure) with another chromosome. The two regions of homology are switched, resulting in a transfer of the fragment between the two regions (**B** and **b** fragments are switched).

With the exception of the cryptic plasmid, plasmid stability is a known issue in the gonococcus due to the activity of restriction endonucleases. Therefore, the preferred method of complementing a gene deletion is via integration of the deleted gene into a known region of the gonococcal chromosome. A study done by Ramsey et al. developed complementation constructs for the genetic manipulation of *N. gonorrhoeae*. The plasmid constructs have regions of homology with the chromosome of *N. gonorrhoeae* and guide a gene of interest into DNA between the coding genes *iga* and *trpB* (Ramsey et al., 2012). Other existing plasmids for complementation use different areas for gene insertion, such as between *lctP* and *aspC*, however some regions can cause issues if they are open reading frames, leading to unwanted modifications of growth or pathogenesis (Ramsey et al., 2012). The new constructs created by Ramsey et al. have regions of homology with *N. gonorrhoeae* and genes for direct insertion, as well as resistance markers, transcriptional terminators, promotors, and respective repressors (Figure 1.4).

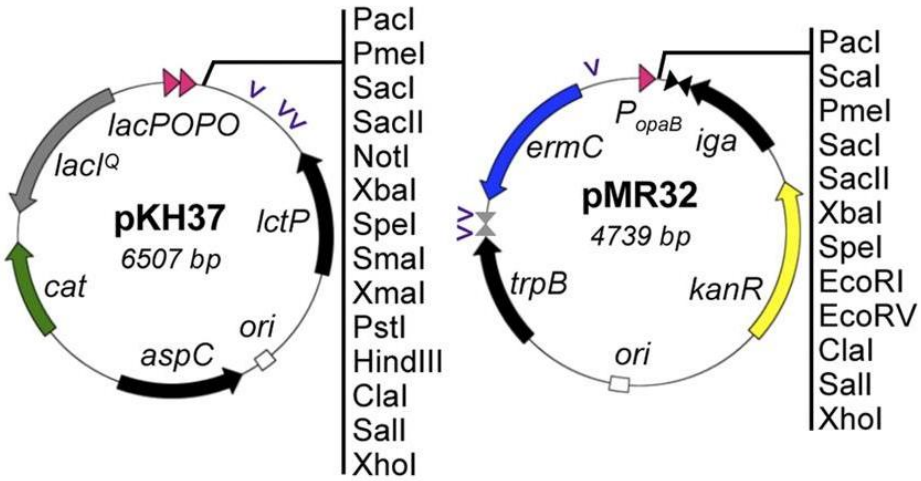

Figure 1.4: Plasmid maps of complementation constructs. Complementation constructs designed by Ramsey et al. show regions of homology with gonococcal chromosomes (black) and the pKH37 plasmid directs gene insertion between *lctP* and *aspC*, the pMR32 plasmid direct gene insertion between *trpB* and *iga*. The DUSs are shown by the purple arrows. All restriction sites are also shown. Image adapted from (Ramsey et al., 2012).

Engineered plasmids are typically not stably maintained in the gonococcus due to a large number of restriction enzyme endonucleases. However, a modification of the cryptic plasmid was the first incidence of an engineered plasmid being stably used to genetically manipulate *N. gonorrhoeae* without integration into the chromosome.

1.4.5 Genetic manipulation via plasmids

Christodoulides et al., created a hybrid shuttle vector for *N. gonorrhoeae* called pEG2, which was constructed using a pGFP plasmid containing the *gfp* gene from *Aequoria victoria*, and the gonococcal cryptic plasmid (Christodoulides et al., 2000). The *gfp* gene encodes for the green fluorescent protein (GFP) and they used this vector to make fluorescent strains of *N. gonorrhoeae* (Figure 1.5.a) that stably expressed the GFP protein indicating plasmid stability. Additionally, the shuttle-vector nature of the plasmid enables manipulation in *E. coli* prior to transformation into *N. gonorrhoeae*. The pEG2 plasmid contained multiple restriction sites, that can be used to alter the fluorescent protein, with the final version of the plasmid (pEG2) containing a red shift mutated GFP (*rs-gfp*) under the control of the *porA* promoter from *N. meningitidis*, an ampicillin resistance marker, EcoRI, BamHI, HindIII, KpnI restriction enzymes, and the linearised gonococcal cryptic plasmid ligated into the plasmid using a HindIII restriction site (Figure 1.5.b). Currently, this is the only literature that uses a plasmid that is not integrated into the chromosome for genetic manipulation of *N. gonorrhoeae*.

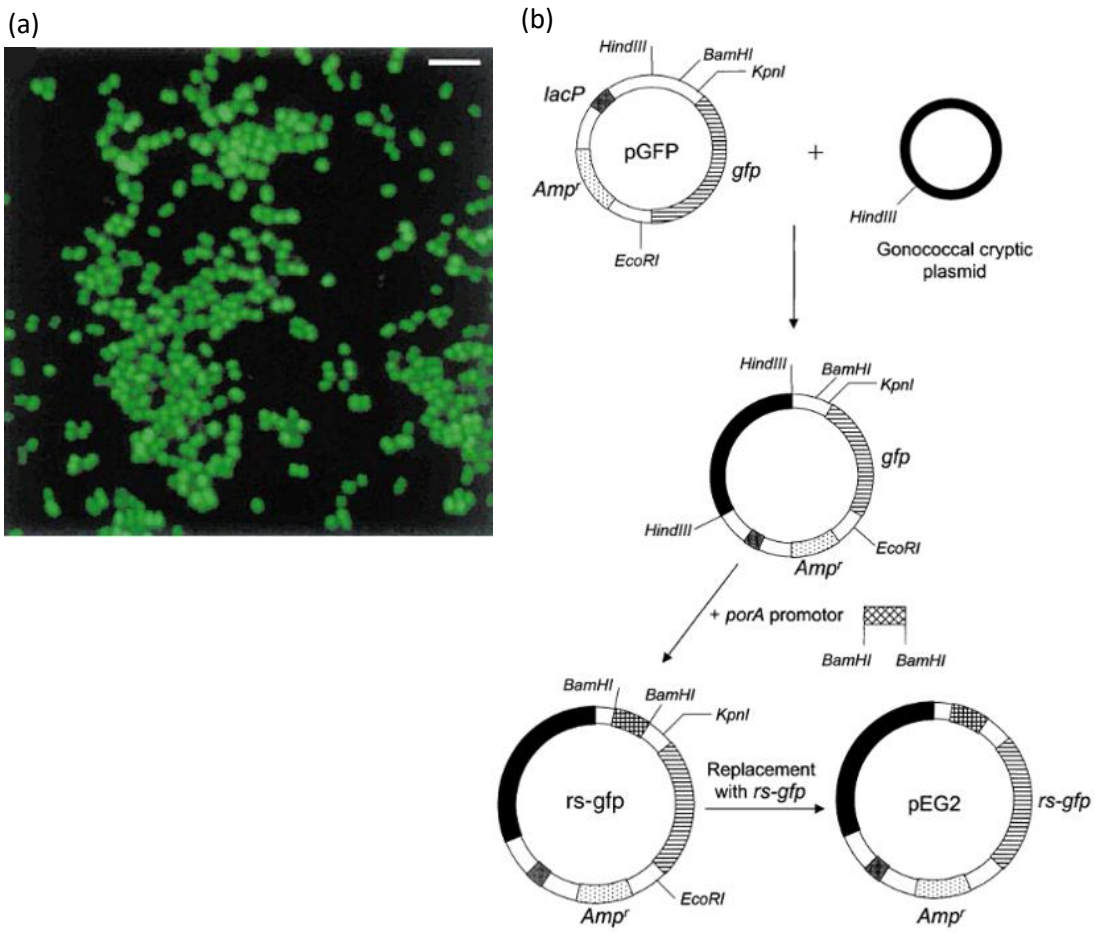

Figure 1.5: pEG2 plasmid details. The pEG2 plasmid was transformed into *N. gonorrhoeae*, resulting in a fluorescent strain that expressed the *gfp* gene (a). The scale bar represents 5 µm. A map of this plasmid details the contents (b), which contained a red shift mutated GFP (*rs-gfp*) under the control of the *porA* promoter from *N. meningitidis*, an ampicillin resistance marker, EcoRI, BamHI, HindIII, KpnI restriction enzyme sites, and the linearised gonococcal cryptic plasmid ligated into the plasmid using a HindIII restriction site. Images from: (Christodoulides et al., 2000).

Christodoulides et al. stably integrated pEG2 into *N. gonorrhoeae* and used this strain to infect primary human epithelial cells to demonstrate the importance of piliation and opacity-associated proteins (Opa) during gonococcal-host cell interactions. The pEG2 vector allowed for visualisation of primary human endometrial cells being infected with either Pili$^-$ Opa$^-$, Pili$^-$ Opa$^+$, Pili$^+$ Opa$^-$, and Pili$^+$ Opa$^+$ gonococci compared to uninfected endometrial cells after 7 hrs (Figure 1.6). The level of infection is visually comparable, panels E and F (Pili$^+$ Opa$^-$ and Pili$^+$ Opa$^+$) showing the highest adherence to the cells, and panel B (Pili$^-$ Opa$^+$) showing the lowest cell adherence compared to panel A (uninfected endometrial cells).

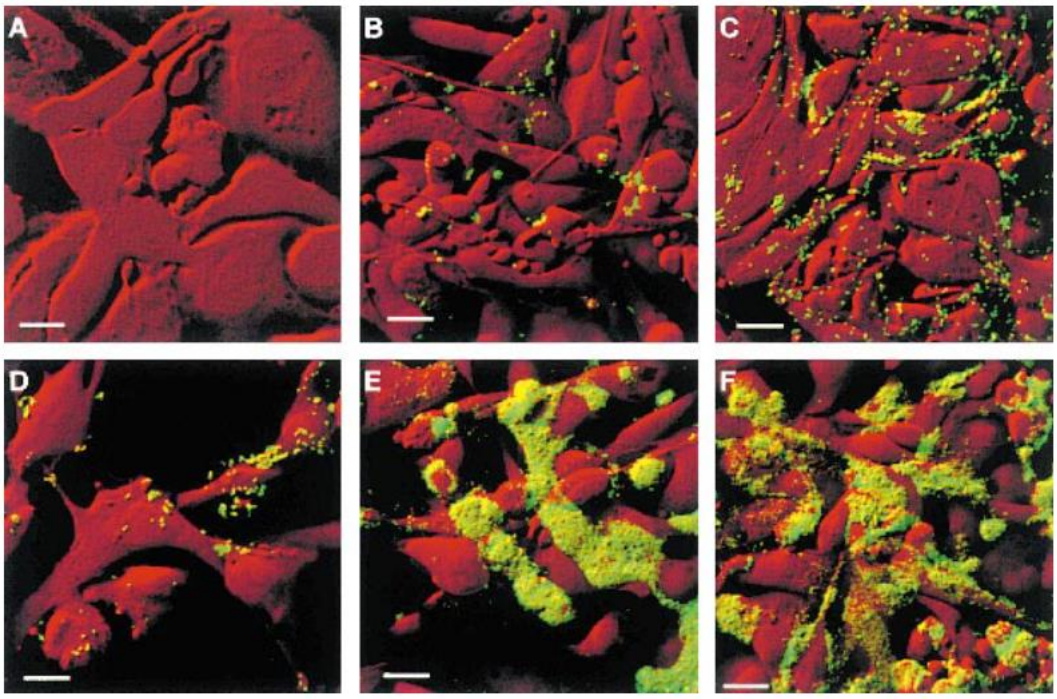

Figure 1.6: Primary human endometrial cells with gonococci infection. Confocal microscopy was used to observe primary human endometrial cells with *gfp* expressing gonococcal infection after 7 hrs. Gonococci were either Pili$^-$ Opa$^-$ (B), Pili$^-$ Opa$^+$ (C,D), Pili$^+$ Opa$^-$ (E), or Pili$^+$ Opa$^+$ (F). Infections were compared to uninfected endometrial cells (A). The scale bar represents 20 µm. Image from: (Christodoulides et al., 2000).

Complementation plasmids and the pEG2 plasmid have provided a path for the manipulation of *N. gonorrhoeae*, however a single plasmid system has limited flexibility and new tools for plasmid creation are now available.

1.5 Techniques for plasmid assembly: cloning

There are many different methods for plasmid assembly and cloning, including restriction enzyme cloning, isothermal DNA assembly, Gateway, and Golden Gate assembly. These methods have allowed researchers to easily manipulate DNA, allowing for the insertion of genes of interest into plasmids, each having its own advantage through cost, time, and materials used.

1.5.1 Restriction enzyme and ligation cloning

As discussed in Buckhout-White et al. (2018), restriction enzyme cloning relies on enzymes that are naturally found in bacteria and archaea, which cleave double stranded DNA (dsDNA) at particular sites in DNA sequences. This can result in fragments that have 5' or 3' overhangs (sticky ends) or flat edges (blunt ends), of which the 5' phosphates and 3' hydroxyl groups remain – allowing for simple ligation of new fragments as the ends are still prepped to bond to another piece of dsDNA (Buckhout-White et al., 2018). The results of this method can be easily visualised on an agarose gel, which will separate the fragments by size, showing samples that have successfully lost a fragment and which samples have gained sized due to the addition of a known sized fragment. Restriction enzyme cloning can be complicated when choosing an enzyme to work with. This is because the resulting cut in the fragment must be compatible with the ends of the fragment chosen to be inserted, and the cut site of the enzyme must not be found within the fragment of interest (Tóth et al., 2014). It is also important to know the methylation status of the fragment of interest as methylation can interfere with the enzymes ability to cut (Rand et al., 2013). However, the main advantage to restriction enzyme cloning is that there are hundreds of enzymes to choose from – many of which are low in cost – and most cloning plasmids contain common restriction enzyme sites. Although this method can take more time than others, it gives confidence in the results it produces due to enzyme ability to cut at specific target sequences of four to 13 bp (Buckhout-White et al., 2018).

1.5.2 Gateway cloning

As suggested by Reece-Hoyes & Walhout et al. (2018), Gateway cloning is similar in that it requires specific recombination sites either side of the DNA fragment of interest. However, instead of a short restriction site, it uses longer recombination sites of around 25 – 242 bp sequence, making for highly precise integration (Reece-Hoyes & Walhout, 2018). This method is based off recombination features of bacteriophage lambda and was designed for cloning of numerous DNA fragments at once with the same enzymes via a two-step process (Reece-Hoyes & Walhout, 2018). Firstly, a DNA fragment is modified to have the recombination sequences flanking the 5' and 3' by amplifying the DNA with particular Gateway attB1 and attB2 sites (Figure 1.7.a) (Soriano, 2017). This altered DNA fragment can now be cloned into a Gateway donor plasmid vector, which has been prepared with the matching attP sites. A Gateway BP Clonase™ II Enzyme Mix reaction takes place to switch out the current DNA between the attP sites with the DNA fragment of interest. The DNA now has flanking attL sites within the entry clone and is now set up for Gateway cloning. Gateway cloning allows for the DNA in this donor plasmid to be easily transferred into other compatible Gateway vectors that already have attR and attL sites via a Gateway™ LR Clonase™ Enzyme Mix reaction (Figure 1.7.b).

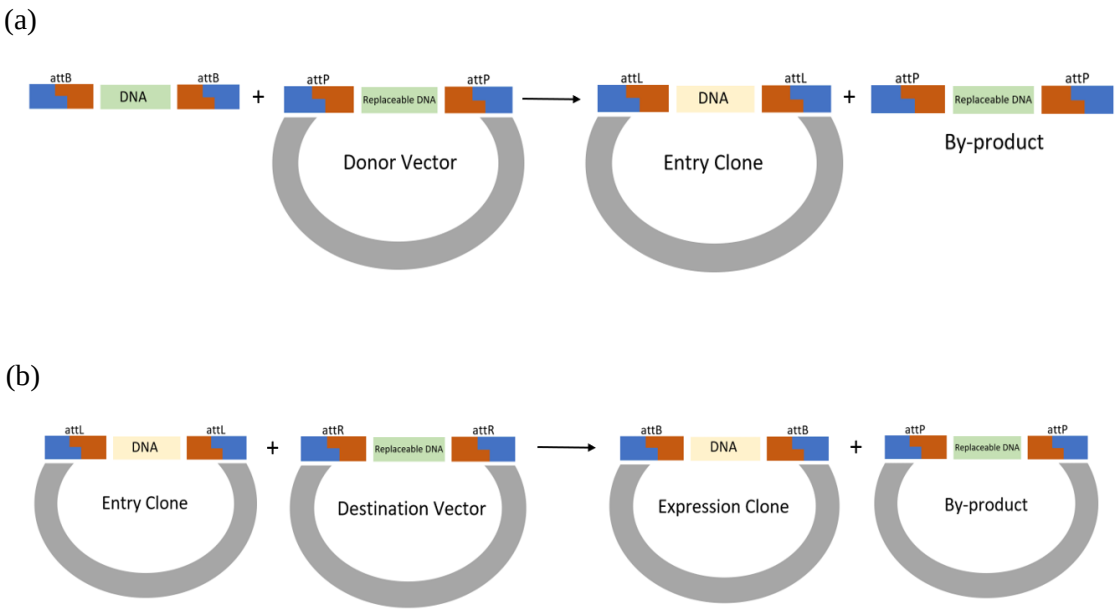

Figure 1.7: Gateway cloning reactions. Gateway cloning preparation reaction (a) requires a DNA fragment to be modified to contain the recombination sequences flanking the 5' and 3' by amplifying the DNA with particular Gateway attB1 and attB2 sites. This altered DNA fragment can be cloned into a Gateway donor plasmid vector, which has been prepared with the matching attP sites. A Gateway BP Clonase™ II Enzyme Mix reaction takes place to switch out the current DNA between the attP sites with the DNA fragment of interest. The DNA now has flanking attL sites within the entry clone. Gateway cloning reaction (b) allows for the DNA in the donor plasmid to be transferred into other compatible Gateway vectors that already have attR and attL sites via a Gateway™ LR Clonase™ Enzyme Mix reaction. Image adapted from (Invitrogen by life technologies, 2003).

This method has the advantage of having thousands of Gateway destination plasmids made already, which have a variety of genes, promotors, tags, and fluorescent proteins inside, allowing researchers to quickly move DNA into many different plasmid scenarios efficiently (Soriano, 2017). However, this method can be very expensive due to the cost of the recombination enzymes and Gateway vectors (Soriano, 2017). Although Gateway cloning allows for multiple varying DNA fragments to be cloned at once, it can be difficult to change to a different cloning method with the final Gateway products, due to the removal of parts such as restriction sites and stop codons (Reece-Hoyes & Walhout, 2018).

1.5.3 Gibson assembly

Gibson assembly, also known as isothermal cloning, uses similar techniques to overlap extension PCR (Chao et al., 2015). As described by Chao et at. (2015), in a microtube, PCR amplified DNA fragments that have 15 – 20 bp overlapping ends with both each other and with the ends of a vector, are added with the linearised vector (Figure 1.8.b). A Gibson assembly Master Mix is added and an isothermal reaction takes place as the components are incubated at 50 °C for 15 – 20 mins (Chao et al., 2015). The three enzymes in the Gibson assembly Master Mix are a 5' exonuclease, a DNA polymerase, and a DNA ligase (Pyhtila, 2016). The 5' exonuclease digests the 5' ends of the DNA fragments to produce overlaps, which the polymerase starts filling in the overhangs to prevent over digestion of DNA, and the DNA ligase sticks the two fragments together at the matching overhangs and with the vector, fusing them together (Figure 8.a) (Chao et al., 2015).

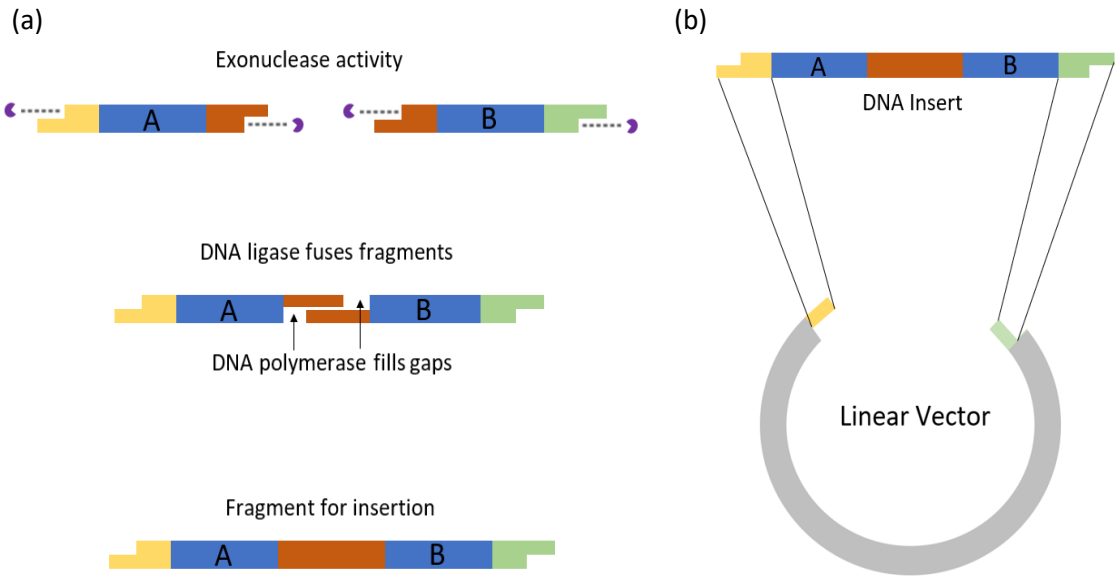

Figure 1.8: Gibson assembly workflow. PCR amplified DNA fragments that have 15 – 20 bp overlapping ends with both each other and with the ends of a vector, are added with the linearised vector. A Gibson assembly Master Mix is added, containing three enzymes: 5' exonuclease, DNA polymerase, and DNA ligase. The 5' exonuclease digests the 5' ends of the DNA fragments to produce overlaps, which the polymerase starts filling in the overhangs to prevent over digestion of DNA, and the DNA ligase sticks the two fragments together at the matching overhangs and to the vector, fusing them together. Components are incubated at 50 °C for 15 – 20 mins.

The advantage of this method is that it does not require extra sequences near the ends of the fragments for restriction enzyme digestion or Gateway recombination sites, and it can join multiple fragments in the order desired (Roth et al., 2014). Although Gibson assembly is fast and efficient, it only works efficiently when joining DNA fragments longer than 200 bp, otherwise the 5' exonuclease will digest too much of the sequence (Roth et al., 2014). However, recently there has been a production of Gibson assembly kits that are specifically designed for fragments smaller than 200 bp (SnapGene, 2022).

1.5.4 Golden Gate assembly

Golden Gate assembly is similar to restriction ligation cloning as it also relies on restriction enzymes to cut at specific points in DNA to create sticky ends for insertion of fragments. However, Golden Gate assembly uses type II restriction enzymes, such as BsaI, which creates a four nucleotide 3' recessed overhang next to its recognition site (Chao et al., 2015). Multiple fragments can be assembled at once using the same type II restriction enzyme to create specific sticky ends to join in a puzzle-like fashion (Figure 1.9). At the same time, the ends of ligated DNA fragments are joined to a backbone (vector) that has matching sticky ends. This is an efficiently quick way to join DNA fragments in a one-step reaction that ensures no further digestion can occur as the recognition site is lost. Software such as Geneious Prime can perform an in-silico reaction to confirm all the DNA fragments can ligate successfully and in the preferred order. Once ligation has completed, the assembled construct can be transformed into a recipient strain (such as *E. coli* DH5-α) and selection based off a resistance or fluorescent maker can help confirm the colonies have successfully transformed (Bird et al., 2022). Sequencing can then confirm if the construct has ligated properly or running the DNA on an agarose gel can find samples of expected size.

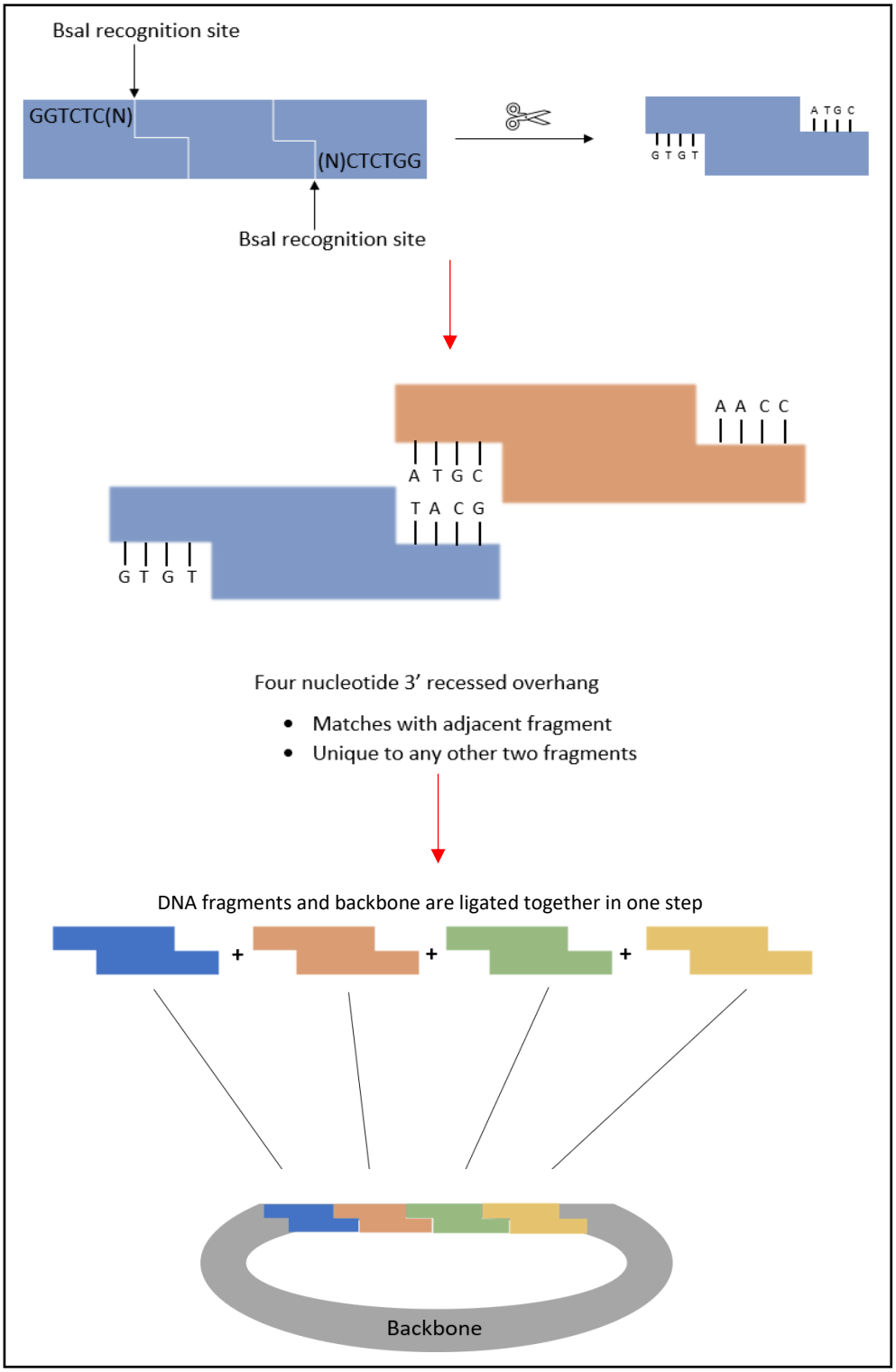

Figure 1.9: Golden Gate assembly workflow. The DNA fragments are designed with BsaI restriction enzyme cut sites which cut downstream from the recognition site, resulting in a unique four nucleotide 3'recessed overhang for specific ligation arrangement. In a 1-step reaction, T4DNA ligase and BsaI work tighter to perform this cut and fragments are ligated together to the backbone (vector) in the specific order of the design, creating a circularised plasmid.

Golden Gate assembly can join large amount of DNA fragments, recently reported to have 35 fragments successfully ligate together in one reaction (Pryor et al., 2020). However, this can cause issues when designing overhangs, as the more overhangs are required, the more unique combinations have to be found. Furthermore, the more overhangs used in one ligation reaction, the higher the chances of mismatch ligations, making this method less reliable as the fragment number rises (Pryor et al., 2020).

1.6 Research objectives

The aim of this research was to generate a modular plasmid system that is small, efficient, and stable for gene expression in both *E. coli* and *N. gonorrhoeae*. A system like this will provide researchers with better tools for understanding the nature of *N. gonorrhoeae* with the aim to find reliable treatment and preventative options. The following objectives were set to reach this:

Objective one:

To isolate and characterise the pEG2 plasmid.

Objective two:

To design a modular cloning system for the genetic manipulation of *N. gonorrhoeae* using Golden Gate assembly techniques.

Chapter Two

Materials and Methods

2.1 Preparation of stocks and bacterial growth media

2.1.1 Preparation of 50x and 1x Tris Acetate agarose (TAE) Buffer

In a 1 L Schott bottle, 242 g of Tris Base (MW = 121.14), 100 mL of 0.5 M EDTA (pH 8.0), and 57.1 mL of glacial acetate were reconstituted to 1 L with ddH_2O in a fume hood. This solution was left to mix overnight using a magnetic stir bar and stored at room temperature. To make 1x TAE for gel electrophoresis, the 50x buffer was diluted by mixing 20 mL 50x TAE with 980 mL ddH_2O.

2.1.2 Preparation of 20% and 50% glucose for glycerol stocks

In a 250 mL Schott bottle, 20 g glucose was dissolved in 80 mL of ddH_2O to a final volume of 100 mL (20% w/v) or 50 g of glucose was dissolved in 50 mL of ddH_2O to a final volume of 100 mL (50% w/v). Bottles were autoclaved and stored at room temperature.

2.1.3 Preparation of LB broth

In a 1 L Schott bottle, 10 g bacto-peptone, 5 g yeast extract, and 10 g NaCl were reconstituted to 1 L with ddH_2O. The media was pH adjusted to 7.0 with 1 M NaOH, autoclaved, and stored at room temperature.

2.1.4 Preparation of LB agar plates

In a 1 L Schott bottle, 10 g bacto-peptone, 5 g yeast extract, 10 g NaCl, and 15 g Bacto-agar were reconstituted to 1 L with ddH_2O. The pH was adjusted to 7.0 with 1 M NaOH, autoclaved, and stored at 50 °C in an incubator. Plates were cast by spreading 10 – 15 µL of liquid LB agar into 100 mm petri dishes and stored at 4 °C once set.

Erythromycin antibiotic plates were made at 100 µg/mL during preparation. For kanamycin or ampicillin antibiotic plates, 50 µg/mL of antibiotics were added.

2.1.5 Preparation of SOC media

In a 1 L Schott bottle, 20 g tryptone, 5 g yeast extract, 585 mg NaCl, 186 mg KCl, 2.46 g $MgSO_4 7H_2O$, and 2.03 g $MgCl_2 6H_2O$ were reconstituted to 1 L with ddH_2O. This solution was autoclaved and once cooled, sterile glucose was added to 20mM.

2.1.6 Preparation of GCB agar plates

In a 1 L acid-washed Schott bottle, 36.25 g of GC Medium Base and 1.25 g Bacto-agar were reconstituted to 1 L with ddH_2O. This solution was autoclaved and stored in a 50 °C incubator. When ready to pour plates, GCB agar was prepared by adding 11.2 mL of Kellogg's supplements (see below) immediately before pouring. GCB plates were made by pipetting 10 – 15 mL of the GCB + Kellogg's supplement agar into the centre of the dish, swirling to spread over the plate, and stored at 4 °C once set.

2.1.7 Preparation of GCBL media

In a 1 L acid-washed Schott bottle, 15 g proteose peptone, 4 g K_2HPO_4, 1 g KH_2PO_4, and 1 g NaCl were reconstituted to 1 L with ddH_2O. The pH was adjusted to 7.2 with HCl and autoclaved before storage at 4 °C.

2.1.8 Preparation of Kellogg's supplements

This recipe is from Dillard (2011) for the growth of *N. gonorrhoeae* and is made in two parts.

Part one: 400 g glucose, 10 g glutamine, and 20 mg cocarboxylase were dissolved in 1 L ddH_2O. The supplement solution was sterile filtered through a 0.2 µm filter, separated into 11 mL aliquots in 15 mL Falcon tubes, before storage at -20 °C.

Part two: 50 mg $Fe(NO_3)_3 9H_2O$ was dissolved in 100 mL H_2O. The supplement solution was sterile filtered through a 0.2 µm filter, separated into 1.2 mL aliquots in sterile 1.5 mL microcentrifuge tubes, and stored at -20 °C.

A volume of 11 mL from Part one was mixed with 1.2 mL Part two in a 15 mL Falcon tube (11.2 mL total) and stored at -20 °C.

2.2 Molecular Biology Techniques

2.2.1 Restriction enzyme digests

Restriction enzyme digests were performed for analysis of plasmids. In a 1.5 mL tube, 10x CutSmart buffer, one unit of restriction enzyme per μg of DNA, 1 μg of plasmid DNA, and Nuclease-Free H_2O up to 50 μL was added. Reactions were shaken at 300 RPM at 37 °C for 2 – 8 hrs.

2.2.2 Agarose gel electrophoresis

Agarose gels were made by determining the percentage required for the expected fragment size. Commonly, a 1% (w/v) agarose gel was used. This was prepared by adding 0.6 g HydraGene LE Agarose to 60 mL of 1x TAE buffer (see section 2.1.1), microwaved for 10 – 30 second periods until all agarose was dissolved. When cooled to handling temperature, 6 μL of thiazole orange dye (10,000x stock) was added for DNA visualization. This was poured into a small caster and a 10 - 18 well comb was inserted, left to set at room temperature for ~30 mins. When set, 5 – 8 μL of Intron Biotechnology SiZer 1000 bp plus DNA ladder was added to the first well. After sample loading, gels were run in an OWL electrophoresis tank (ThermoFisher 37 Scientific) containing 1x TAE with a LighteningVolt OSP-250L electrophoresis machine (Biolab scientific) at 90 – 100 V for 40 – 50 mins. Gels were visualized using the iBright FL1000 (Invitrogen).

2.2.3 DNA purification from agarose gel extraction

Selected DNA bands were cut from an agarose gel using a scalpel and transferred to pre-weighed 1.5 mL tubes. The weight of the gel was determined, and Buffer QG was added at a ratio of 3:1 (w:w) then incubated in a shaking heat block at 55 °C for 20 mins at 600 RPM to dissolve the gel. Isopropanol was mixed in at a ratio of 1:1 (v:v), transferred to a silica spin column (BioLabs Inc. Monarch DNA Cleanup Columns, 5 μg), and centrifuged at maximum speed for one min in an Eppendorf 5425 benchtop centrifuge. The supernatant was discarded, and the DNA was washed with 600 μL of PE buffer twice (centrifuged at maximum speed for one min, supernatant discarded each time). The column was centrifuged at maximum speed for one min to dry and 30 μL of pre-warmed UltraPure™ DNase/RNase-Free Distilled Water was added to the column. The tube was left to stand for one min before being centrifuged for 1 min at maximum

speed (~13000 RPM) DNA yield was analysed at 260 nm on a DeNovix DS-11 FX Spectrophotometer before storage at -20 °C.

2.2.4 Sequencing pEG2 via the MinION Nanopore

MinION Nanopore sequencing was carried out following the manufacturer's protocol for the Rapid Sequencing gDNA (SQK-RAD004) and the Flow Cell Priming kits (EXP-FLP002). These kits work together to tagment the DNA, a process that attaches sequencing adapters to the DNA ends, and subsequently prime the flow cell for DNA loading. Tagmentation via a transposome complex cleaves the DNA and adds transposase adapters to the ends, sequence adapters then bind to these transposase adapters, and this is loaded into the primed flow cell for analysis (Figure 2.1).

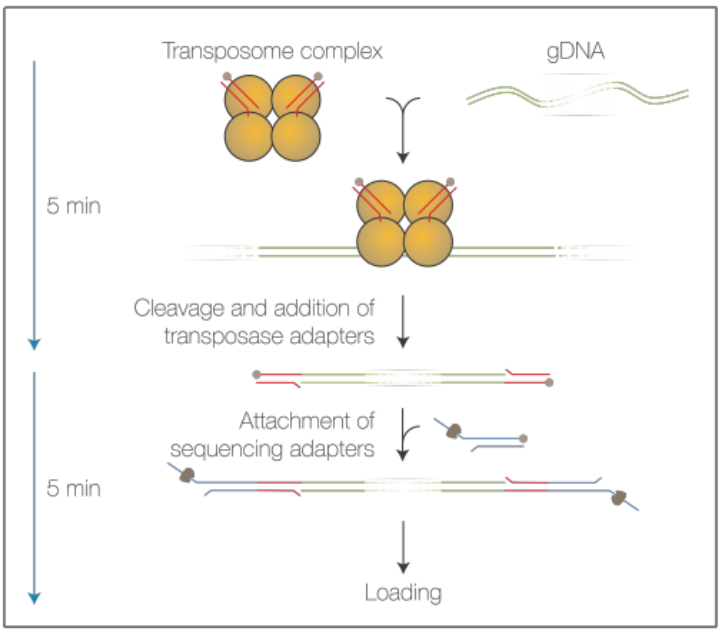

Figure 2.1: Workflow of the transposome complex tagmenting DNA. The transposome complex cleaves DNA and attaches transposase adapters to either end. Sequence adapters bind to the transposase adapters, preparing the DNA for flow cell loading (*Rapid Sequencing gDNA (SQK-RAD004)*, n.d.).

2.2.4.1 Library preparation

All kit components were thawed, briefly centrifuged, and kept on ice until used. In the library, ~400 ng of DNA was added to a DNA LoBind tube, along with 6.85 µL of nuclease-free H_2O and mixed gently to prevent DNA shearing. In a PCR tube, 10 µL of the prepared DNA was mixed with 2.5 µL of the Fragmentation Mix from the SQK-RAD004 kit, gently mixed and centrifuged. The tube was incubated for one min at 30 °C, then for one min at 80 °C, and put on ice. A volume of 1 µL of Rapid Adapter was added to the PCR tube, mixed gently, incubated at room temperature for five mins, and stored on ice.

2.2.4.2 Priming the SpotON Flow Cell

Components of the EXP-FLP002 kit were thawed at room temperature and the Sequencing Buffer, Flush Tether, and Flush Buffer tubes were vortexed and centrifuged. The priming port was opened on the MinION Nanopore and any bubbles under the cover were removed, using a 1000 µL pipette to draw back 10 – 30 µL of buffer liquid that sits in the port. To prepare the flow cell priming solution, 30 µL of Flush Tether was added to the tube of Flush Buffer, vortexed to mix and centrifuged. Being careful not to add air bubbles into the flow cell, 800 µL of the priming solution was pipetted into the priming port and left for 5 min.

Meanwhile, in a separate microtube, 34 µL of Sequencing Buffer, 4.5 µL of nuclease-free H_2O, 25.5 µL of Loading Beads (vortexed immediately before use), and 11 µL of DNA library were added together.

2.2.4.3 Loading the flow cell

The SpotON sample port was lifted before adding 200 µL of the priming solution to the priming port, with care taken not to introduce air bubbles. In the SpotON sample port, 75 µL of DNA library was added dropwise. Both the SpotON sample port and priming port covers were closed, and the MinION Nanopore lid was replaced.

2.2.4.4 MinION Nanopore data analysis

The raw reads from the Nanopore were analysed using Guppy high-accuracy base calling software (*Guppy Protocol*, n.d.). Base called reads were imported in to Geneious software and de novo assembled into contiguous sequences. Plasmid features were annotated using the same software.

2.2.5 Primer design, analysis, and preparation.

Primers were designed using Geneious Prime 2023.1.1 and analysed using the OligoAnalyzer™ Tool (Integrated DNA Technologies). Primers met the parameters of a Tm between 53 – 60 for optimal annealing (with the exception of Primer 2 for self-dimerisation reasons), having at least 50% G – C content for binding strength, and a length of at least 18 bp to ensure binding specificity (Table 2.1). A number of other preexisting primers were used in addition to those specifically designed for this project, including: LIT110, LIT111, LIT112, and LIT113 from Dr Will Kelton. Primers Neo-F and mCherryqpcr were from Jolyn Pan and the standard M13 forward and M13 reverse primers were used. Primers were ordered or had been previously ordered from Integrated DNA Technologies, Inc and made to 10 µM with UltraPure™ DNase/RNase-Free Distilled Water. Primers were stored at -20 °C.

Table 2.1: Primers for PCR and sequencing

Primer Label	Melting Temperature (°C)	G – C Content (%)	Sequence (5' to 3')
Primer 1	57.1	60	CCT TCA CCC TCT CCA CTG AC
Primer 2	61.4	65	GCT CTT ACG CTG CCG CCA TC
Primer 3	58.4	54.5	GGC TCA TCG GAA TAG TTT GCG G
Primer 4	60.7	61.9	GTC TCT GTG AAC ATC CGC CGC
Primer 5	59.7	50	CGC TTT TGC TTC AAT GCC TCG TTG
Primer 6	59.7	57.1	GTG CTT CCA CAT TGC CCA ACG
Primer 9	57.2	47.8	GCA AGA TTT CCG ATT TGG CGA AG
Neo – F	54.8	50	CGT TGG CTA CCC GTG ATA TT
mCherryqpcr	54.9	45.5	CAA TTC ATG TAC GGC AGC AAA G
LIT10	69.5	58.3	TAG GTA CCA GGT CTC ACT GCA AGC TTG GAG CGC AGC
LIT11	66.5	51.4	TAT GGA TCC GGT CTC AAT GTA GCT TTA CCG CTT CGC C
LIT12	61.2	58.3	GCA TGG CTG ATA GTG ACC TAC GGG
LIT13	61.2	58.3	CCG TAG GTC ACT ATC AGC CAT GCG
LIT14	55.3	55	GAA CCC GAT ATA ATC CGC CC
LIT16	56.8	55	CAT CCG CTT GAA CGA ACA CG
M13 Fwd	56	55	CCC AGT CAC GAC GTT AAA CG
M13 Rev	55.7	43.5	AGC GGA TAA CAA TTT CAC ACA GG

2.2.6 Polymerase Chain Reaction (PCR) of bacterial colonies

Colony PCR (cPCR) was used to screen colonies of bacteria, usually following a transformation step to verify that the desired genetic construct is present. For the amplification of a portion of a construct of interest, template DNA was included in the place of a colony. Table 2.2 was used as a composition guide for both single reactions and for the creation of master mixes (MM) for multiple reactions.

Table 2.2: PCR reaction components for amplification of construct DNA or screening of bacteria

Component	1x MM (µL)	10x MM (µL)
5x HOTFIREPOL® Master Mix	4	40
10 µM Fwd Primer	0.6	6
10 µM Rev Primer	0.6	6
Nuclease-free H_2O	14.8	148
Total Volume (µL)	20	200

For a cPCR, a 10 µL pipette tip was used to scrape a colony of interest from an agar plate streaked onto an agar plate for future recovery of the clone. The tip was then transferred into the corresponding PCR tube that contained 20 µl of the PCR MM. A negative control was made by leaving one PCR tube free of a colony. For template DNA PCRs, 2 – 5 µl of DNA template was added to the respective PCR tube that contained 20 µl of PCR MM. Tubes were briefly centrifuged before transfer to a BIO RAD T100™ Thermal Cycler. Table 2.3 and Table 2.4 show the PCR conditions used in the thermo cycler (all PCR reactions follow PCR conditions protocol #1 unless specified).

Table 2.3: PCR cycling conditions (protocol #1)

Cycle Step	Temperature (°C)	Time (min)	
Initial Denaturation	95	5	
Denaturation	95	0.5	Repeat 30x
Annealing	48 – 55*	2	
Amplification	72	2 – 4**	
Enzyme Deactivation	72	10	
Hold	12	∞	

*Time dependent on amplicon length.

**Temperature dependent on primer Tm.

Table 2.4: PCR cycling conditions (protocol #2)

Cycle Step	Temperature (°C)	Time (min)	
Initial Denaturation	94	10	
Denaturation	94	0.5	Repeat 25x
Annealing	53	0.5	
Amplification	68	6	
Enzyme Deactivation	68	10	
Hold	8	∞	

PCR products were purified using a QIAGEN DNA purification kit according to manufacturer's instructions.

2.2.7 Sanger sequencing

Preparation of plasmid DNA for sequencing was carried out using Table 2.5 as a composition guide. For primer design see section 2.2.5.

Table 2.5: Composition of Sanger sequencing reactions for plasmid DNA

Plasmid DNA Quantity	Primer Quantity	Final Volume (ddH_2O adjusted)
250 – 625 ng	0.4 µL	20 µL if adding own primers*

*19 µL if using Massey primers

2.3 Culturing of *E. coli*

2.3.1 Transformation of chemically competent *E. coli*

A 100 µL frozen stock of chemically competent *E. coli* cells was thawed on ice and 1 – 10 µL of plasmid DNA or ligation reaction was added. This was incubated for 30 mins on ice and transferred to 42 °C for 90 sec to heat shock the bacteria. The cells were then incubated on ice for two mins and 450 µL of pre-warmed (37 °C) SOC media (see section 2.1.5) was added, and cells were incubated at 37 °C for 60 mins. On LB agar plates (see section 2.1.4) (containing appropriate antibiotic for screening), 200 µL of transformation mix was pipetted between two plates and the remainder pelleted using an Eppendorf 5425 benchtop centrifuge at maximum speed for one min. All but 100 µL of supernatant was removed and cells were resuspended by gently flicking the tube. This was plated onto LB agar plates (with appropriate antibiotic) and incubated overnight at 37 °C. For GMO approval number see Appendices.

2.3.2 Preparation of *E. coli* liquid cultures

Using a 10 µL pipette tip, single colonies were selected off an agar plate and the tip was dropped into a 14 mL culture tube containing 3 mL LB broth (see section 2.1.3). Additionally, 3 µL of kanamycin or 6 µL of erythromycin was added and the cultures were incubated overnight at 37 °C with shaking at 180 RPM.

2.3.3 Preparation of glycerol stocks for *E. coli*

A volume of 500 µL was removed from each of the overnight liquid cultures and added to a 2 mL cryovial with 500 µL of 50% glycerol (see section 2.1.2). This was stored at -80 °C.

2.3.4 Plasmid DNA extraction from overnight liquid culture

Plasmid DNA was extracted from 3 mL overnight liquid culture and purified via the QIAGEN QIAprep Spin Miniprep Kit as follows:

Liquid cultures were pelleted at 4600 x *g* for five min at room temperature. Pellets were resuspended in 250 µL Buffer P1 and transferred to 1.5 mL tubes. A volume of 250 µL Buffer P2 was added, and tubes were inverted five times or until the liquid became clear. This reaction was left to sit for at least 3 mins but no longer than 5 mins. Buffer N3 was then added at a volume of 350 µL, immediately inverting the tubes five times to mix. Tubes were centrifuged for 10 mins at 13,000 RPM in a benchtop centrifuge. Of the supernatant, 800 µL was taken and transferred into QIAprep 2.0 spin columns and centrifuged for 1 min at 13,000 RPM, and the supernatant was discarded. Columns were washed with 500 µL Buffer PB, centrifuged at 13,000 RPM, and supernatant discarded. The columns were then washed with 750 µL Buffer PE, centrifuged at 13,000 RPM, and supernatant discarded. The columns were centrifuged for 1 min at 13,000 RPM to pull down any residual wash buffers. Columns were then placed into a clean 1.5 mL tube and 30 µL of UltraPure™ DNase/RNase-Free Distilled Water was added to the centre of the column. Tubes rested for one min before being centrifuged at 13,000 RPM for one min. Columns were discarded and DNA yield was analysed at 260 nm on a DeNovix DS-11 FX Spectrophotometer before storage at -20 °C.

2.3.5 Culturing *E. coli* for microscopy

On the day prior to microscopy analysis, glycerol stocks of *E. coli* DH5-α strains containing plasmid constructs were streaked onto LB agar plates (with appropriate antibiotic) and incubated overnight with at 37 °C. A volume of 20 µL 3.7% paraformaldehyde PBS solution was added to a labelled 1.5 mL tube with one loop of corresponding colonies from the pre-prepared plates to fix cells. Tubes were mixed via pipetting up and down for an even spread of cells and 20 µL of liquid was pipetted onto the centre of a glass slide. A coverslip was added, using a clear coat nail polish to seal, and left to dry at room temperature for 30 – 45 mins.

2.3.6 Microscopy analysis of *E. coli*

Fluorescence in *E. coli* strains was observed using a Zeiss compound microscope, using the green filter set for GFP observations. The excitation range for this set is 546/12, dichroic (beam splitter): 580 and LP (long pass) emission 590. The lens was set to 4x objective to observe cells and gradually increased to a 100x objective oil lens. Scalebars were added post processing.

2.4 Transformation of Neisseria gonorrhoeae

2.4.1 Spot transformation into *N. gonorrhoeae*

Methods for transformation were adapted from that of the Dillard paper. For insertion-duplication mutagenesis of a plasmid into *N. gonorrhoeae*, the plasmids were left circularized as opposed to linearized. A recipient *N. gonorrhoeae* MS11 strain was streaked out from a frozen stock onto a plain GCB agar plate (see section 2.1.6) one day prior to transformation and incubated at 37 °C overnight with 5% CO_2 (~18 hrs). On the underside of a prewarmed GCB agar plate, four circles were drawn, where 2 – 20 µL of purified pDNA was spotted into three circles to give a final concentration of 250 ng, 500 ng, and 1000 ng and the fourth left as a negative control. pDNA concentration did not exceed 10 µg to prevent overgrowth. pDNA was left to dry on the plate for 10 – 15 mins then one piliated colony off the MS11 recipient plate was selected and streaked through each circle. The plate was then incubated overnight at 37 °C with 5% CO_2. A single colony from each circle was then streaked onto a separate agar plate (prewarmed

to 37 °C) containing antibiotic (dependant on the pDNA marker) and incubated overnight at 37 °C with 5% CO_2. Depending on the antibiotic, screening of the colonies was performed 24 – 48 hrs after streaking. Erythromycin selection typically takes around 48 hrs whereas kanamycin selection typically takes around 24 hrs. For GMO approval number see Appendices.

2.4.2 Preparation of the pEG2 plasmid for *N. gonorrhoeae* transformation via demethylation

The pEG2 plasmid was methylated via the HaeIII methyltransferase enzyme. In a 1.5 mL tube, 2.8 μL of the pEG2 plasmid (711 ng/μL) was added to 15 μL of UltraPure™ DNase/RNase-Free Distilled Water and 2 μL of 1x HaeIII methyltransferase reaction buffer. Additionally, 1 μL of HaeIII enzyme and 0.2 μL of 400x S-adenosylmethionine (160 μM) was added and incubated for 1 hr at 37 °C followed by 65 °C for 15 mins.

2.4.3 Preparation of *N. gonorrhoeae* lawn plates

Using a sterile swab, eight piliated Opa^+ colonies were scraped off a 24-hr streak plate made one day previous. Piliated colonies were identified using a stereo microscope to select colonies that had a dark ring surrounding it, and picked colonies that were opaque/darker in colour for Opa^+ selection.

The swab was then used to draw a line down the centre of a plain GCB agar plate to spread the bacteria. Then using the same swab, lines were drawn horizontally back and forth across the plate, covering its entirety with cells. Plates were incubated with 5% CO_2 at 37 °C for 16 hrs.

When it came to harvesting the lawn plates, two different methods were used. The first method used sterile swabs to collect cells by dragging the swab back and forth across the entire plate, ensuring to collect from all edges, and washing the swab off in GCBL media (see section 2.1.7) via multiple rotations against the walls of the tube.

In method two, 1 mL GCBL media was pipetted onto the centre of the lawn plate, swirled around by hand to ensure the plate was fully covered by the liquid. Having the plate tilted to form a small pool at the bottom edge, cells were scraped down into the pool using a sterile cell scraper, scraping at least twice to ensure all cells have been washed into the GCBL media. The liquid was then pipetted into a 5 mL tube.

All experiments used method one unless stated otherwise. Method one was found to be less efficient than method two therefore was discontinued after its discovery.

2.4.4 Liquid transformation into *N. gonorrhoeae*

Methods for liquid transformation were adapted from that of Dillard 2011. A recipient strain of *N. gonorrhoeae* MS11 was streaked onto a GCB plate from a frozen stock one day previous to the transformation and incubated overnight at 37 °C for ~24 hrs with 5% CO_2. Lawn plates (two per strain) were prepared as per section 2.4.3. Incubation did not exceed 18 hrs to ensure bacteria retained their piliation. No more than 20 µL of DNA was added to 200 µL of pre-warmed (37 °C) GCBL medium containing 5 mM $MgSO_4$ in a six-well plate and warmed to 37 °C for ~15 mins. For the suspensions of *N. gonorrhoeae* cells, half of a lawn plate (up to two full plates if low growth) were collected using a swab into a 1.5 mL tube containing pre-warmed GCBL + 5 mM $MgSO_4$ (37 °C). Tubes were vortexed vigorously for 2 mins to break up colonies. A volume of 20 µL of the recipient cells was added to the pre-warmed DNA suspension and incubated for 30 mins at 37 °C with 5 % CO_2. To recover the cells, 2 mL of pre-warmed GCBL media containing freshly added Kellogg's supplement (see section 2.1.8) was added into each well and incubated for 2 hrs (37 °C, 5 % CO_2). A check for microcolony formation was carried out using a stereo microscope as this is a sign of piliated colonies for efficient transformations. A 1 mL pipette tip was used to vigorously scrape the cells off the surface of the wells and two lots of 100 µL of the transformation liquid was plated onto GCB plates containing the appropriate antibiotic for screen selection. Of the remaining transformation liquid, 1 mL was pelleted using an Eppendorf 5425 benchtop centrifuge at max speed for 2 mins and resuspended in 100 µL of GCBL for plating onto a third GCB plate (with appropriate antibiotic). Plates were incubated until colonies were observed (24 - 48 hrs). Colonies were selected off the plates for glycerol stocks (see below).

2.4.5 Preparation of glycerol stocks for *N. gonorrhoeae*

Using a sterile swab, bacteria was scraped off a lawn plate grown one day prior and resuspended in 1 mL GCBL media. The tube was vortexed for 2 mins and 200 – 500 µL was added to a 2 mL cryovial, depending on the confluency the lawn plate. The volume in the cryovial was made up to 1 mL with 20% glycerol and stored at -80 °C.

2.4.6 Culturing *N. gonorrhoeae* for microscopy

On the day prior to microscopy analysis, glycerol stocks of *N. gonorrhoeae* MS11 and *N. gonorrhoeae* strains containing plasmid constructs were streaked onto GCB agar plates (with appropriate antibiotic) and incubated overnight with 5% CO_2 at 37 °C. A volume of 20 µL 3.7% paraformaldehyde PBS solution was added to a labelled 1.5 mL tube with one loop of corresponding colonies from the pre-prepared plates to fix cells. Tubes were vortexed to break up microcolonies for an even spread of cells and 20 µL of liquid was pipetted onto the centre of a glass slide. A coverslip was added, using a clear coat nail polish to seal, and left to dry at room temperature for 30 – 45 mins.

2.4.7 Confocal microscopy analysis of *N. gonorrhoeae*

Fluorescence in *E. coli* and *N. gonorrhoeae* strains was observed using a confocal microscope, using the 488 laser and the 561 laser. For GFP observations the microscope was set to the GFP channel with excitation at 480 nm and emission at 510 nm. For mCherry observation the microscope was set to the Alexa Fluor 568 channel with excitation at 579 nm and emission at 603 nm. The gain and offset settings were optimised to minimise background fluorescence. Scalebars were added post processing by Dr Joanna Hicks.

2.4.8 Monitoring of *N. gonorrhoea* growth in culture via colony forming units

At least 70 GCB agar plates were prepared per strain being tested. Each plate had between five and eight sterile 5 mm glass beads added (except for six plates used for streak and lawn preparations), stored at -4 °C upside down so that the beads rested on the lid. Approximately 80 1.5 mL tubes per strain were autoclaved and prepared with 900 µL GCBL media and stored at -20 °C.

Exactly two days prior to starting, two plates were streaked from glycerol stocks per strain, incubated with 5% CO_2 at 37 °C for ~24 hrs. Prior to starting the growth curve, four lawn plates per strain were grown using lawn method one (see section 2.4.3) for the first growth curve, and lawn method two for the following growth curves. The 1.5 mL tubes with GCBL and the bead-prepared plates were placed at room temperature.

The 1.5 mL tubes were set up in a rack in rows of five, labelled one to five (since there are three wells per strain in each plate, tubes were grouped by 15).

On the day of the growth curve, 550 µL of Kellogg's supplements were added to 50 mL GCBL in a 50 mL Falcon tube for each strain. For the strains containing plasmid with kanamycin selection, 50 µL kanamycin was also added to the 50 mL Falcon tube to a final concentration of 50 µg/mL. In a 5 mL tube, 2.5 mL GCBL media was added, and lawns were scraped using a sterile swab and added to the GCBL media. All four plates were collectively washed into the tube. The 5 mL tubes were vortexed for 3 mins. In a sterile cuvette, 900 µL GCBL was added and 100 µL of the vortexed 5 mL tube contents were mixed for an OD_{600} reading. This value was multiplied by 10 to get an OD_{600} for the whole 5 mL tube. Using this value and in a separate 50 mL Falcon tube, the 5 mL resuspension tube was diluted to 0.05 OD_{600} with the prepared GCBL + Kellogg's supplements to a total volume of 35 mL. In the 12 well plates, 1.2 mL of the 0.05 OD_{600} dilution was added to three wells per strain/per plate, filling any empty wells with plain GCBL media. Plates were incubated with 5% CO_2 at 37 °C until taken out at each time point (T). The time was noted as T0.

For T0, the 0.05 OD_{600} preparation was serially diluted via five prepared 900 mL GCBL tubes. For this, 100 µL of the OD_{600} 0.05 dilution was added to a prepared 900 µL GCBL 1.5 mL tube and vortexed for 30 sec. This was repeated until tube five, which was plated onto two labelled T0 plates using the beads to spread the liquid, and incubated with 5% CO_2 at 37 °C for 48 hrs.

At each following time point (every 1.5 hours), one 12 well plate was removed and observed under a stereo microscope to monitor growth and microcolony formation. The wells were then vigorously scraped using a 1 mL pipette tip, repeatedly scraping the bottom and walls of the well to remove gonococci that adhered to the well surface. All liquid was pipetted from the well into a sterile 1.5 mL tube and vortexed for 3 mins. The well's contents were serially diluted by pipetting 100 µL into a 900 µL GCBL tube, vortexed for 30 sec, and repeated until tube five. Tube five was vortexed for 30 sec and plated onto two labelled plates, incubated with 5% CO_2 at 37 °C for 48 hrs. This equated to two plates per well, therefore six plates per strain per time point.

The six plates from each time point were observed under a stereo microscope counted using a handheld tally counter, the six plates were averaged, and multiplied by 10^6 to get the CFU/mL of the original 12 well plate before dilutions.

Data collected during a growth curve was recorded in an excel spreadsheet, organised by time point and by strain. Each time point was averaged and multiplied by 10^6 to take the serial dilutions into account for colony forming units (CFUs) per mL (Appendix x). Standard deviation and standard error were calculated using Excel functions.

2.4.8.1 Normalisation of growth curve data

Normalisation of the CFU/mL data collected in the methods above was undertaken to make T0 was the same for all strains. The OpaGK strain data was scaled up by a factor of 2.48 (average T0 of WT divided by average T0 of OpaGK). Data was then presented in a line graph to visualise results.

2.4.9 Measuring growth of *N. gonorrhoeae* using optical density

During each time point of the growth curve, when the well contents had been pipetted into a 1.5 mL tube, vortexed, and 100 µL taken out, an OD_{600} reading was taken using the left over well contents tube; 100 µL was taken and added to a sterile cuvette containing 900 µL GCBL media. The OD_{600} reading was multiplied by 10 to give the reading for the whole tube. As there were three wells per time point, the time point OD_{600} was averaged to give a single OD_{600} per time point for each strain.

2.4.10 Measuring fluorescence and cell count of *N. gonorrhoeae* during growth curves

Fluorescence and cell count of the *N. gonorrhoeae* strains were measured using the ThermoFisher Countess 3FL cell counter at each 1.5 hr time point of the growth curves. A volume of 10 µl was taken from the left-over contents of the 12 well plates, vortexed before withdrawal, and pipetted onto a disposable slide to be inserted into the cell counter. A fluorescence percentage and cell count number was recorded, and the side was discarded.

2.4.11 Optimisation of inoculum Optical Density (OD) for growth curves

N. gonorrhoeae strains were streaked onto plain GCB agar plates two days prior to optimisation, incubated at 5% CO_2 at 37 °C for 24 hrs. A day prior, four lawn plates per strain were made using the second lawn method (see section 2.4.3), incubated at 5% CO_2 at 37 °C for 16 hrs. Lawns resuspensions were vortexed for 2 mins and an OD_{600} was measured. From this reading, three separate OD_{600} 2.0 were made in 2.5 mL GCBL media per strain and vortexed for 2 mins. An OD_{600} measurement was taken again for each OD_{600} 2.0 as the exact reading was used in a $C_1 \times V_1 = C_2 \times V_2$ calculation to determine the volume of OD_{600} 2.0 needed to create three inoculum samples of OD_{600} 0.05, 0.075, and 0.1 per OD_{600} 2.0 tube per strain. Tubes were vortexed for ~2 mins and diluted down to 10^{-5} for plating. The inoculum OD_{600} that gives 50 – 100 colonies on one plate is the ideal starting OD_{600} for growth curves.

2.5 Modular plasmid cloning system

2.5.1 Golden Gate assembly design

Golden Gate constructs (shuttle vectors) were designed using Geneious Prime. Sequences for the Opa promoter, NptII promoter, and the erythromycin resistance gene were obtained from Dr Joanna Hicks. The kanamycin resistance gene, origin of replication (ColE1), and sfGFP gene sequences were all provided by Dr William Kelton and Kyrin Hanning. Finally, the mCherry sequence was sourced from Jolyn Pan. All fragments were ordered as gene fragments from Twist Biosciences.

Lyophilised fragments were reconstituted to 10 ng/ µL with UltraPure™ DNase/RNase-Free Distilled Water. Golden Gate assemblies were performed using a prepared Master Mix containing both the type II restriction enzyme BsaI-HFv2 and T4 ligase according to Table 2.6. Each assembly was incubated at 16 °C overnight in a thermocycler before transformation into chemically competent *E. coli* cells, plating, and overnight incubation at 37 °C (see section 2.3.1).

Table 2.6: Reaction composition for Golden Gate assembly ligation

Component	Volume (µL)
Combined Plasmid/DNA Fragments	12
T4 DNA Ligase Buffer	2.5
T4 DNA Ligase	0.5
BsaI-HFv2	1.5
Nuclease-free H2O	8.5
Total	25

2.5.2 Preparation of Golden Gate assembled constructs for subsequent cryptic region ligation

Successfully assembled constructs presented as green or pink to the eye when transformed into *E. coli*, depending on the fluorescent marker gene used. Colonies were selected off the plates based off this colouring and cultured in liquid overnight at 37 °C in 3 mL LB broth with 50 µg/mL kanamycin, 50 µg/mL ampicillin, or 100 µg/mL erythromycin, depending on the construct make up. Each culture was prepped via the QIAGEN QIAprep Spin Miniprep Kit and analysed via the DeNovix^{R} DS-11 FX Spectrophotometer.

The constructs were linearised via a HindIII restriction enzyme digest, and to minimise self-ligation in later steps, constructs underwent a dephosphorylation step. For this, 1

µL of Quick CIP was added to the digest and the mixture was incubated for 10 mins at 37 °C. Constructs were incubated at 80 °C for 2 mins to deactivate the enzyme and purified by DNA cleanup (see below).

2.5.2.1 Cleanup of plasmid DNA

Buffer PB from the QIAGEN QIAprep Spin Miniprep Kit was added to the plasmid DNA at a ratio of 5:1 (v/v) and mixed. The liquid was transferred to a QIAprep 2.0 spin column and centrifuged for 1 min at 13,000 RPM. The supernatant was discarded. The DNA was then washed with 750 µL of Buffer PE and centrifuged for 1 min at 13,000 RPM, supernatant discarded. The QIAprep 2.0 spin column was centrifuged for 1 additional minute to dry the column before placing the column into a sterile 1.5 mL microtube. A volume of 30 µL of UltraPure™ DNase/RNase-Free Distilled Water was added to the centre of the column and the microtube rested for 2 mins before being centrifuged at 13,000 RPM for 1 min. Columns were discarded and DNA yield was analysed at 260 nm on a DeNovix DS-11 FX Spectrophotometer before storage at -20 °C.

2.5.3 Extraction of the cryptic region from pEG2

For the uptake and maintenance of the constructs in *N. gonorrhoeae,* the cryptic region was extracted from the pEG2 plasmid and purified for insertion into the Golden Gate Assemblies.

The pEG2 plasmid was HindIII restriction enzyme digested for 2 – 4 hrs at 37 °C . The digestion was run on a 1% agarose gel for 45 mins at 100 V and excised for spin column purification (see section 2.2.3). After quantification of the DNA concentration using the DeNovix DS-11 FX Spectrophotometer, the product was stored at -20°C.

2.5.4 Ligation of cryptic region into Golden Gate assembly constructs

The cryptic region was ligated into the construct plasmids using a prepared Master Mix containing T4 DNA ligase according to Table 2.7. Each assembly added to a PCR tube and incubated at 16 °C overnight in a thermocycler before transformation

into chemically competent *E. coli* cells. The resulting cells were plated onto antibiotic plates, containing either kanamycin or erythromycin and grown overnight at 37 °C.

Table 2.7: Ligation reaction components

Component	Sample volume (µL)	Control volume (µL)
Vector	0.05 – 0.56*	0.05 – 0.56*
Insert	0.5 – 2.5**	0**
T4 DNA ligase buffer	1	1
T4 DNA ligase	0.5	0.5
H_2O	Up to 10 µL	Up to 10 µL
Total	10	10

*Vector volume dependent on

**Insert volume dependent on insert size and volume of vector required.

2.5.5 Golden Gate assembly version 2.0

For the second-generation shuttle vector designs, all DNA fragments were ordered via Twist Bioscience (USA). Lyophilised DNA was resuspended in ddH_2O to a final concentration of 10 ng/µL. For long term storage and to improve Golden Gate cloning efficiency, each fragment was digested with BamHI and KpnI restriction enzymes and inserted into the pLIT100 storage plasmid.

2.5.6 Ligation of fragments into pLIT100 storage plasmids

The fragments were ligated into the pLIT100 plasmid using a prepared Master Mix containing T4 DNA ligase according to Table 2.7. Each assembly was incubated at 16 °C overnight in a thermocycler before transformation into chemically competent *E. coli* cells. The resulting cells were plated onto antibiotic plates containing 50 µg/mL ampicillin and grown overnight at 37 °C. For modified pLIT100 ligations, the insert and vector concentrations were doubled, and the H_2O volume adjusted.

Chapter Three

Results and Discussion

3.1 Isolation and characterisation of pEG2 plasmid

A sample of the pEG2 plasmid referred to by Christodoulides et al., (2000) was obtained from Dr Fiona Radcliff's lab at the University of Auckland.

3.1.1 Transformation of pEG2 into *N. gonorrhoeae*

Initially, there was an attempt to perform a spot transformation (see section 2.4.1) into wild type *N. gonorrhoeae* MS11 (known as WT from here) using pEG2, however, multiple transformation attempts were unsuccessful. In an attempt to improve efficiency of pEG2 transformation, the plasmid was demethylated by exposure to the HaeIII methyltransferase (see section 2.4.2). The HaeIII methyltransferase enzyme originates from an *E. coli* strain that has the cloned HaeIII modification gene from *Haemophilus aegyptius* (ATCC 11116) and adapts the internal cytosine residue of the GGCC sequence (Cohen et al., 2004). Demethylation of the plasmid DNA is proposed to increase transformation efficiency by removing any *E. coli* methylation patterns that enable the gonococcus to recognise the DNA as foreign and subsequently destroy via restriction endonucleases. However, this did not appear to improve efficiency as there were still no colonies on the transformation plate. This method was therefore not continued in future transformations.

A liquid transformation of pEG2 into *N. gonorrhoeae* was instead carried out (see section 2.4.4), yielding one successful colony. A glycerol stock was subsequently made and stored at -80 °C. The transformant was verified by growth on an antibiotic plate

containing 10 ng/µL erythromycin and GFP expression visualised by confocal microscopy (Figure 3.1).

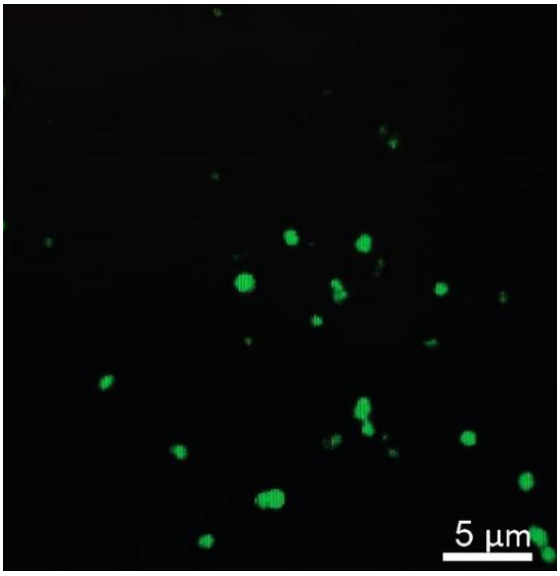

Figure 3.1: Expression of GFP from the pEG2 plasmid in *N. gonorrhoeae*. The pEG2 plasmid was transformed into *N. gonorrhoeae* via liquid transformation. GFP expression was observed via confocal microscopy, under a 60x objective lens, as shown by fluorescent round gonococci.

Due to difficulties transforming the pEG2 plasmid and lack of multiple transformants, the sequence of the pEG2 plasmid was questioned, as Christodoulides et al., (2000) suggested that pEG2 was highly transformable. It was decided that further characterisation of the pEG2 plasmid was necessary to determine why this plasmid was not as easily transformable as first thought.

3.1.2 Restriction enzyme digest of the pEG2 plasmid

The pEG2 plasmid was isolated by transformation into *E. coli* DH5-α cells (see section 2.2.1) and the pEG2 DNA extracted by mini-prep (see section 2.2.3). The characterisation of pEG2 began with a restriction enzyme digest (see 2.2.1) using BamHI, HindIII, KpnI, and EcoRI (Figure 3.2) to compare to the plasmid map in Christodoulides et al., (2000).

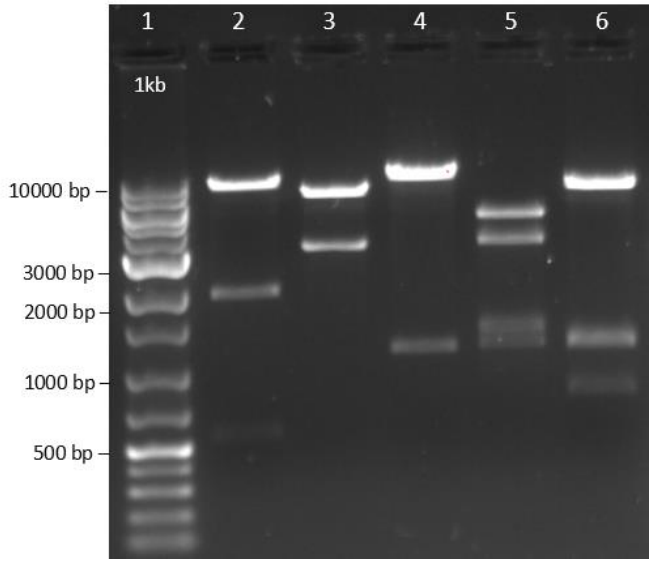

Figure 3.2: Restriction enzyme digest analysis of the pEG2 plasmid. A restriction enzyme digest of the pEG2 plasmid was carried out to compare to Christodoulides et al., 2000 plasmid map. Lane 1: 1kb ladder. Lane 2: BamHI. Lane 3: KpnI. Lane 4: EcoRI. Lane 5: HindIII. Lane 6: EcoRI/KpnI. The digest was run on a 1% agarose gel at 100 V for 45 mins.

The BamHI digest of the pEG2 plasmid (lane 2) showed the expected two bands, one large at 10,000^{+} bp and one small at ~2300 bp, suggesting two BamHI cut sites were present in pEG2 as suggest by Christodoulides et al., 2000. There were two cut sites observed upon the pEG2 plasmid digestion with KpnI (lane 3), with one large band at ~ 9000 bp, and a smaller band ~4000 bp, suggesting an extra cut site than anticipated. EcoRI was expected to cut once (lane 4), however, the gel suggested two cuts sites, with one large band at 10,000^{+} bp and a smaller band at ~1300 bp. As for the HindIII digestion of the pEG2 plasmid (lane 5), there were two similar sized larger bands at ~6000 bp and ~4000 bp, and two similar sized smaller bands clustered around 1500 bp. However, according to Christodoulides et al., 2000, only two cut sites for HindIII were expected. Next, KpnI and EcoRI were combined to excise *rsGFP* as the plasmid map (see Figure 1.5) suggested a small fragment of unknown size containing rsGFP should be present alongside a larger fragment of unknown size (lane 6). However, the agarose gel showed bands at 10,000^{+} bp, ~1300 bp, and ~800 bp.

Overall, the analysis of the pEG2 plasmid via restriction enzyme digests provided information on plasmid size and reliability. Collectively, the pEG2 plasmid has multiple unexpected cut sites that could make future plasmid manipulation difficult.

3.1.3 Sequencing the pEG2 plasmid

To further characterise pEG2, sequencing was carried out using a MinION Nanopore (see section 2.2.4). From a brief sequencing run, 1325 reads were obtained, of which 696 were viable for the creation of an assembled sequence (Figure 3.3). The high-performance Guppy base caller was used to process the raw Nanopore reads before assembling the reads in Geneious Prime to produce 20 contigs, which were assembled using the MIRA alignment function (Chevreux, B., Wetter, T. and Suhai, S., 1999). This sequence acted as a reference sequence for any further sequencing.

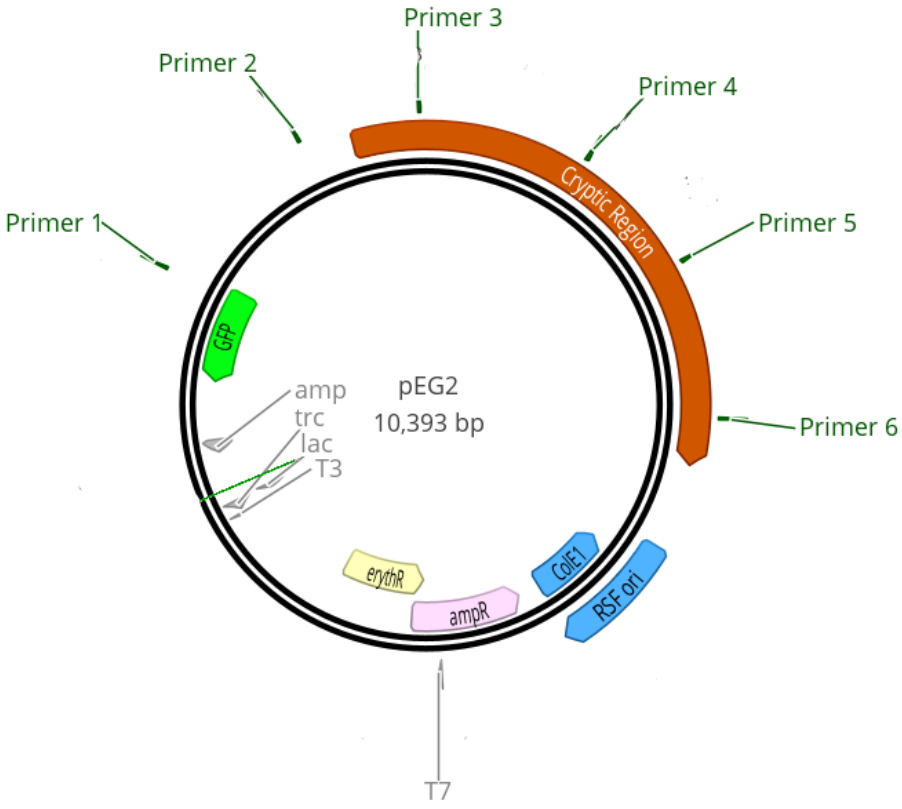

Figure 3.3: The sequenced pEG2 plasmid. Assembled sequence of pEG2 after sequencing via the MinION Nanopore, generated using Geneious Prime. The sequence presents a cryptic region (dark orange), *gfp* gene (green), erythromycin and ampicillin resistance genes (yellow), ampicillin resistance (pink), ColE1 and RSF origin of replication (blue) for propagation in *E. coli*. The sequence is 10,393 bp long and was used as a reference sequence for any further pEG2 sequencing.

The plasmid sequencing implied pEG2 is around 10,400 bp and provided information of the contents of pEG2, which did not match the pEG2 plasmid map. Sequencing suggested there was an RSF Ori, ColE1, ampicillin resistance gene, erythromycin resistance gene, trc, lac T3, T7, a GFP gene, and a large region of ~ 4000 bp that contained 10 repeat regions. This large region was the cryptic region that contained the DNA uptake sequence (DUS) that was essential for the maintenance of the plasmid in *N. gonorrhoeae.* It was important that there was high confidence in the sequence of this region, however, the repeat regions it contained could potentially interfere with sequencing results. Therefore, primers were designed for further cryptic region sequencing (Green annotations in Figure 3.3).

3.1.4 Sanger sequencing of pEG2

To build a high confidence sequence of pEG2, Sanger sequencing was carried out for the cryptic region (see section 2.2.7). To ensure full coverage of the cryptic region, primers were designed using sequence obtained by Nanopore, with each aiming to cover approximately 1000 bp of sequence.

A total of seven primers were designed (see section 2.2.5) and sufficient for full coverage of the cryptic region by Sanger sequencing (Primers 1 to Primer 6 and Primer 9 in Table 2.1). All but Primer 4 gave high quality results. The quality of sequencing is defined by a log transformed QV (quality value) score from one to 50, where 50 has a less than 0.001% chance of an incorrect base call. These values are plotted above each base in the sequencing traces (Figure 3.4) and have high confidence when they exceed QV 25 (a height of 50%). Primer 4 appeared not to bind in the expected area, leaving a gap in the sequence and instead covering where Primer 5 had bound. Instead, a new primer was designed, Primer 9, to cover the region between Primer 3 and Primer 5. The final sequenced product came to 3994 bp.

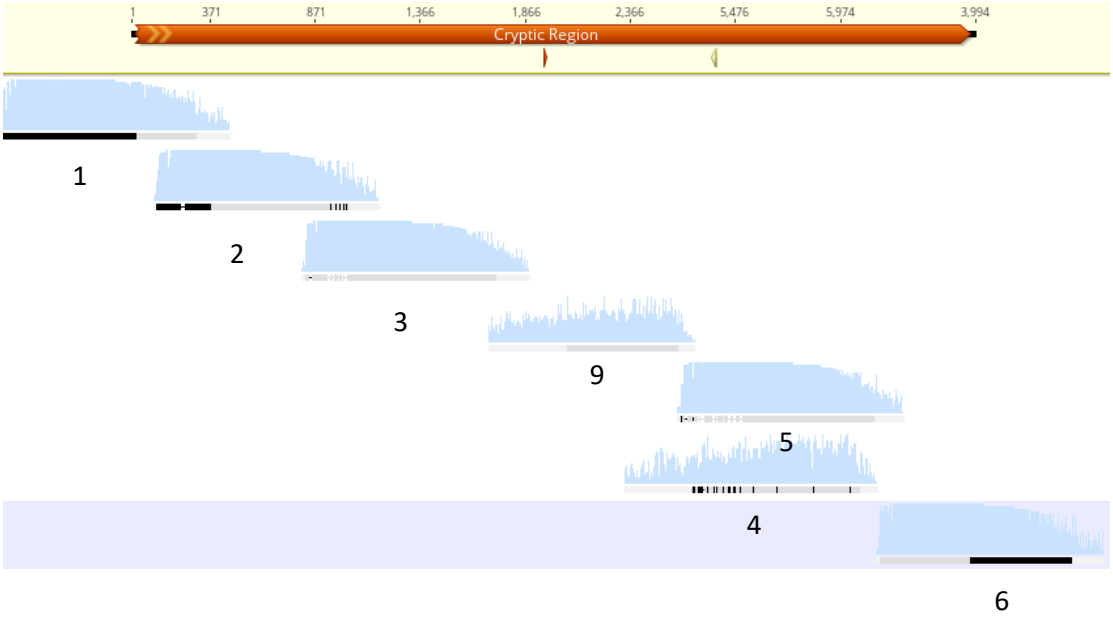

Figure 3.4: Sequencing of the cryptic region from pEG2. Sequence coverage by the seven primers designed in Geneious Primer for in-depth coverage of the cryptic region. The cryptic region (dark orange) is fully covered by the primer sequences below. Primers are represented by grey/black bars, labelled by a corresponding number. Sitting above the primers are blue QV scores that give an indication of base call confidence.

The Sanger sequencing results were combined with the Nanopore data to create a final plasmid map of pEG2. Quality score profiles (Figure 3.5, for example) were compared between the two datasets and the bases called with the highest confidence were used at any uncertain positions. The exception was the Sanger sequencing for Primer 9, which did not return high confidence base calling. However, the Nanopore sequencing was base called with high confidence in this region.

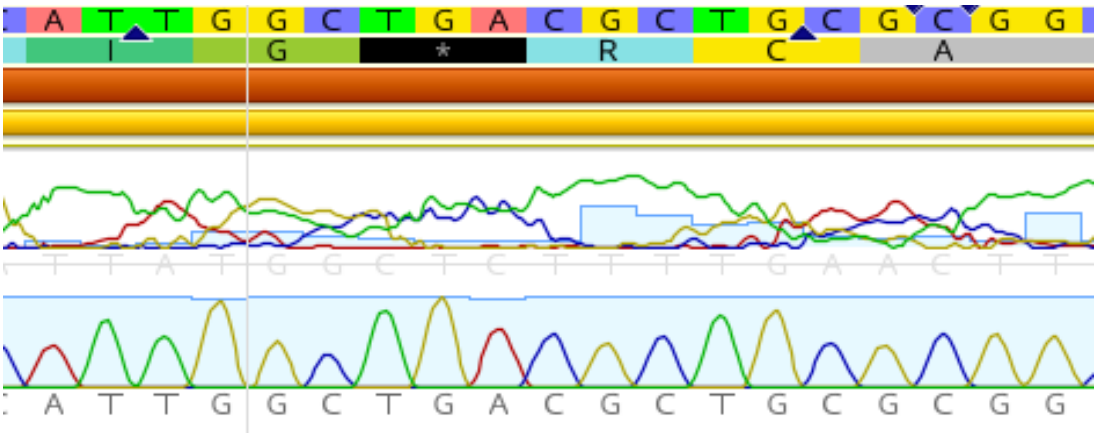

Figure 3.5: Quality score profiles of sequencing. Quality score represented by an overlaying blue graph – the taller the graph, the higher the confidence of the base calling. Here, two graphs are displayed: the top graph represents low confidence base calls; the bottom graph represents high confidence base calls.

The final pEG2 sequencing results made it clear that the pEG2 plasmid was not reliable; having unexpected elements that were not shown on the plasmid map, such as overlapping genes and promoters facing the wrong way. Furthermore, pEG2 was not easy to manipulate given the odd promoter arrangements, making cloning and replacement of genes through genetic manipulation difficult. Therefore, designing a new plasmid expression construct from synthetically made DNA fragments and joining them via Golden Gate assembly was proposed as an alternative. This design would include the cryptic region from pEG2; however, it was unclear what the function and identity of its components were. Therefore, an analysis of the cryptic region was undertaken.

3.1.5 Analysis of the cryptic region

The pEG2 plasmid from Christodoulides et al., (2000) was constructed to include the gonococcal cryptic plasmid to confer plasmid stability in the gonococcus. The pJD1 cryptic plasmid from the gonococcus was linearised by digestion with the HindIII restriction enzyme and inserted using the HindIII site into pGFP.

The pJD1 plasmid discussed in Korch et al. (1985) is 4207 bp in length and said to be found in 96% of gonococci naturally (Figure 3.6.a). The plasmid contains seven open reading frames (ORFs) and three genes: *cppA*, *cppB*, and *cppC* (Korch et al., 1985). This paper provided a sequence for the pJD1 plasmid of which a BLAST search

revealed a sequence called *N. gonorrhoeae* strain 10771 plasmid pJD1. This sequence was downloaded into Geneious Prime for analysis. The sequence was annotated, containing two hypothetical proteins, cryptic plasmid proteins A and B, endonuclease *vapD*, DUF5397 domain-containing protein, helix-turn-helix domain-containing protein, replication initiation protein, mobC family plasmid mobilisation relaxosome protein, and relaxase/mobilisation nuclease domain-containing protein (Figure 3.6.b). The structure of the two plasmids are identical, with the exception of the orf6/HP annotation orientation. The pJD1 sequences were pairwise aligned in Geneious Prime, showing a 99.6% identity.

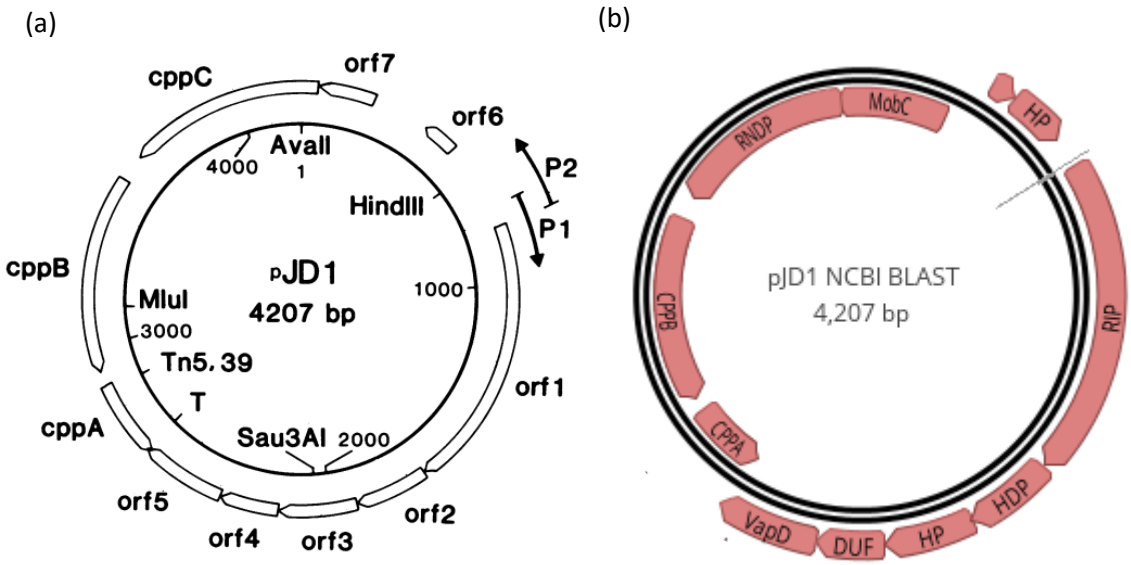

Figure 3.6: The pJD1 plasmids found in literature and using a BLAST search. The first plasmid (a) was found in literature by Korch et al., (1985). It was 4207 bp in size and contained seven ORFs and three genes: *cppA*, *cppB*, and *cppC*. A BLAST search of this plasmid sequence presented with pJD1 from a *N. gonorrhoeae* strain 10771 (b). This plasmid contained two hypothetical proteins, cryptic plasmid proteins A and B, endonuclease *vapD*, DUF5397 domain-containing protein, helix-turn-helix domain-containing protein, replication initiation protein, mobC family plasmid mobilisation relaxosome protein, and relaxase/mobilisation nuclease domain-containing protein. Sequences were downloaded into Geneious Prime to compare to the cryptic region of the pEG2 plasmid.

Both sequences were separately aligned to the cryptic region sequence in Geneious Prime. The pJD1 sequence from Korch et al. (1985) aligned with 92.6% identity, presenting a 250 bp gap in the cryptic region sequence that aligns with ORF1 in pJD1.

There was also a 23 bp gap within this alignment where Primer 4 was expected to bind, potentially explaining the issues during Sanger sequencing. When aligning the cryptic region with the pJD1 BLAST sequence, a 92.9% identity was reported, having the same gaps near Primer 4 and within the replication initiation protein (same area as ORF1).

These alignment results confirm the cryptic region is in fact a cryptic plasmid commonly found naturally in gonococci and contains ORFs that code for the same genes found in *N. gonorrhoeae* strain 10771 plasmid pJD1, and the sequence of this region/plasmid has not been altered significantly. The annotations were transferred onto the cryptic region sequence (Figure 3.7). If the cryptic region does in fact contain a functional *vapD* gene, this explains why the pEG2 plasmid is said to be so stable during transformation. Obtaining these functional annotations gives higher confidence in the use of the cryptic region sequence isolated from pEG2 for Golden Gate assembly.

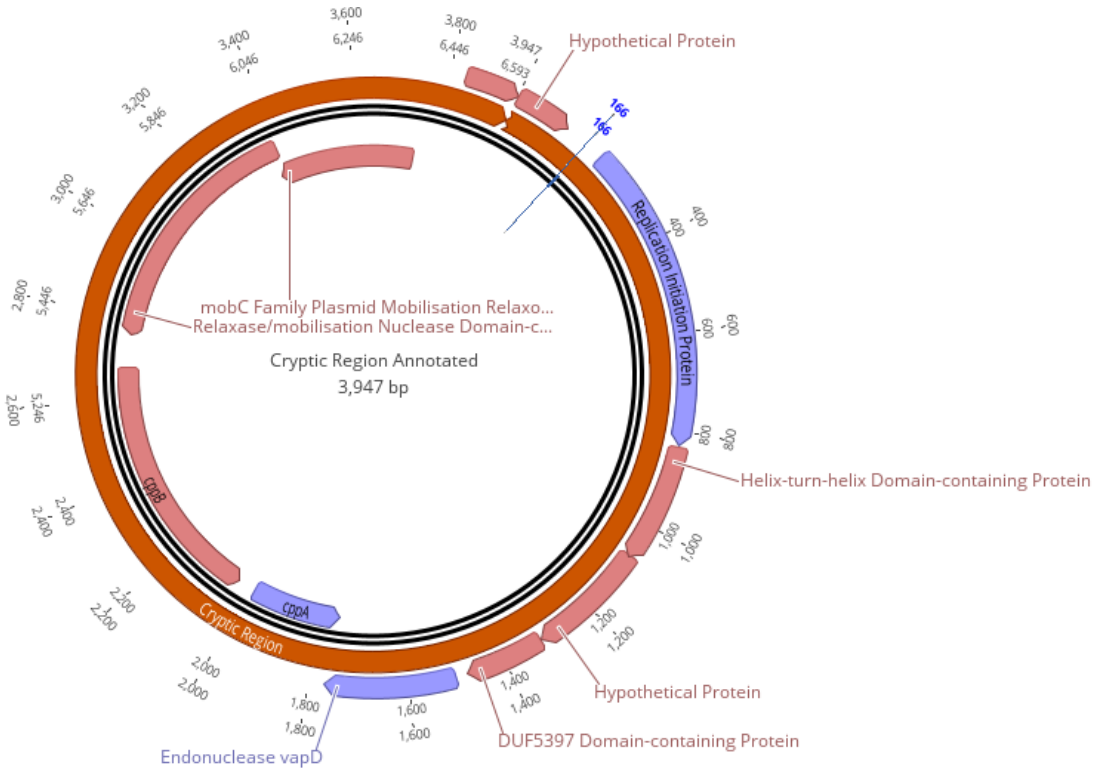

Figure 3.7: Annotated cryptic region after pairwise alignment with pJD1 strains. The cryptic region isolated from the pEG2 plasmid was pairwise aligned in Geneious Prime with two pJD1 gonococcal cryptic plasmids. The pairwise identities of ~93% indicated that the annotations of the pJD1 plasmids could be transferred to the cryptic region. Annotations in pink represent near 100% pairwise identity to the cryptic region and annotations in purple represent near 90% pairwise identity.

3.2 Golden Gate assembly: building the cloning system

3.2.1 DNA Fragment design

Due to the inability to genetically manipulate *N. gonorrhoeae* easily using the pEG2 plasmid, based on nanopore sequencing, a new plasmid system was created for expression of genes in *N. gonorrhoeae*. The aim of the new design was to make a simpler, more modular, shuttle vector than pEG2 that can be transformed into both *E. coli* and *N. gonorrhoeae*. The design (see section 2.5.1) consisted of five main parts: a promoter, an antibiotic resistance marker, a fluorescent protein, an origin of replication, and the cryptic region from pEG2. The promoter, resistance markers, and fluorescent protein parts each had two variants: Opa or NptII, kanamycin resistance marker or erythromycin resistance marker, and GFP or mCherry respectively (Table 3.1). To ensure stable fluorescence, a super fold GFP variant (*sfGFP*) was chosen for the new design.

Table 3.1: DNA fragment options showing restriction enzyme effects and DUS locations. Golden Gate DNA fragmnets were designed in Genious Prime to have BsaI digested sticky ends for ligation, except for the 3' end of the promoters and the 5' end of the ColE1 as these ends join with the cryptic region fragment that was HindIII *restriction enzyme digested (RE) from pEG2. The reporter proteins (fluorophores) and ColE1 were designed with a DUS for plasmid maintanance in *N. gonorrhoeae*. Fragments are displayed as a result of restriction enzyme digestion, not as complete fragments as ordered.

DNA Fragment	Option One	Option Two
Promoter		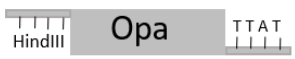
Resistance Marker		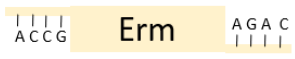
Reporter Protein		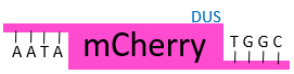
Origin of Replication		
Cryptic Region (RE)*		

To each fragment, high fidelity Golden Gate assembly overhangs were selected from those described as part of standard modular cloning (MoClo) parts (Weber et al., 2011). The exception to this rule was at the 5' end of the promoter fragments and the 3' end of the ColE1 origin fragment where the overhangs were designed for compatibility with the HindIII restriction enzyme to allow incorporation of the cryptic gonococcus origin derived from pEG2. BsaI type IIs restriction enzyme sites were then added to the 5' and 3' ends of each sequence (Figure 3.8) to mediate the formation of these Golden Gate overhangs upon cleavage.

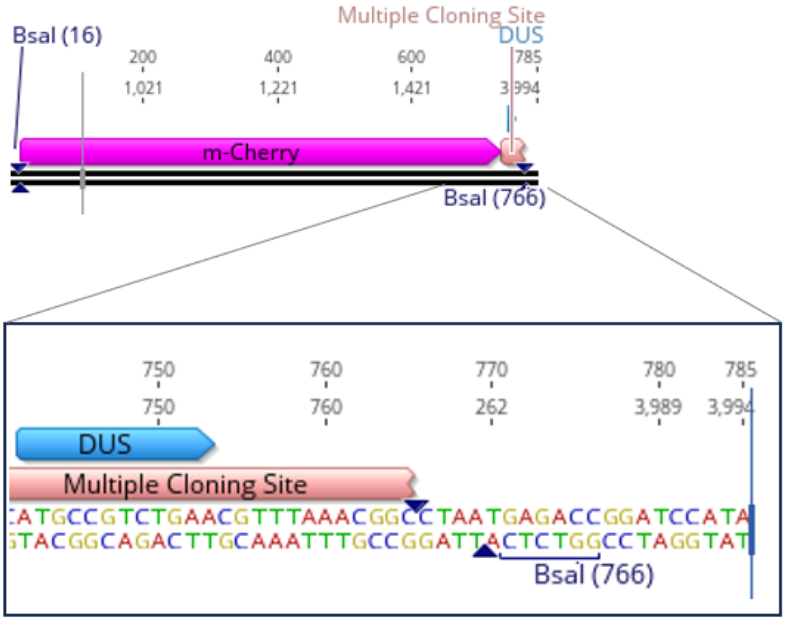

Figure 3.8: The mCherry fragment close up of the BsaI cut site. The type IIs restriction enzyme was added to each end of the majority of DNA fragments for the Golden Gate assembly. The recognition site for the enzyme (dark blue triangles) sits before the cut site (dark blue line), allowing the design to include a variety of sticky ends for a specific order of fragment ligation.

As the assembled operon was designed to be driven from a single promoter, ribosome binding sites were additionally included before the fluorophore and antibiotic resistance genes. Likewise, short linking regions were designed between each of the expressed genes to incorporate additional features in the future. Gonococcal DUS sequences were appended to the 5' ends of the fluorophore and ColE1 fragments to promote uptake during transformation. Similarly, a commonly used strong terminator sequence was also included from the chloroplast *TpsbA* (*Pinus sp.*) gene following the resistance fragments.

Upon Golden Gate assembly, the fragments were designed to seamlessly form a functional plasmid capable of replication in *E. coli*, ready for HindIII-based incorporation of the cryptic region required for plasmid replication in *N. gonorrhoeae*.

Fragments were ligated in four different combinations (Figure 3.9), creating a variety of constructs without the cryptic region to first demonstrate replicative ability in *E. coli.* An example of a fully ligated construct is shown in Figure 3.9.

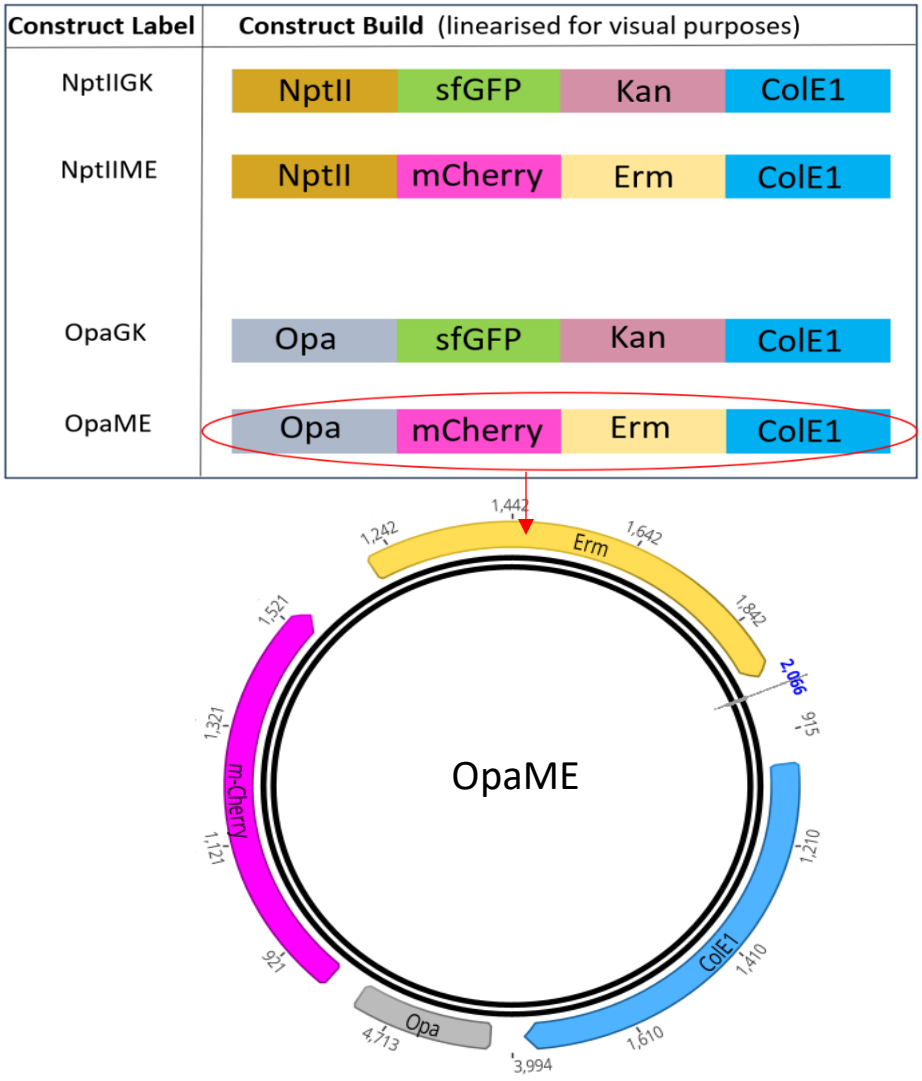

Figure 3.9: The four combinations of Golden Gate assembly constructs. The Golden Gate assembly design involved four different combinations of constructs, two with the NptII promoter and two with the Opa promoter. Each set of Opa and NptII constructs had either a sfGFP and kanamycin combination or a mCherry and erythromycin combination. All constructs had a ColE1 fragment for regulation in *E. coli*. The OpaME construct has been circularised to show what the construct looks like as a plasmid.

3.2.2 Transformation of Golden Gate constructs into *E. coli*

The constructs were transformed into *E. coli*, using a negative control ligation with no insert to compare the level of self-ligating colonies.

The OpaGK, NptIIGK, OpaME, and NptIIME construct plates had high numbers of transformants. All *sfGFP* constructs fluoresced green under an Invitrogen Safe Imager™ (Figure 3.10) and the *sfGFP* fluorescence appeared brighter than the GFP in pEG2. However, the mCherry constructs required different excitation wavelengths and were only visualised using a confocal microscope (section 3.3.1). However, a pink colouring could be observed in some of the mCherry construct colonies without fluorescence excitation. Colonies that presented with this fluorescence/colouring were selected off the plates for DNA extraction, purification, and glycerol stocks were made and stored at -80 °C (see section 2.3.3).

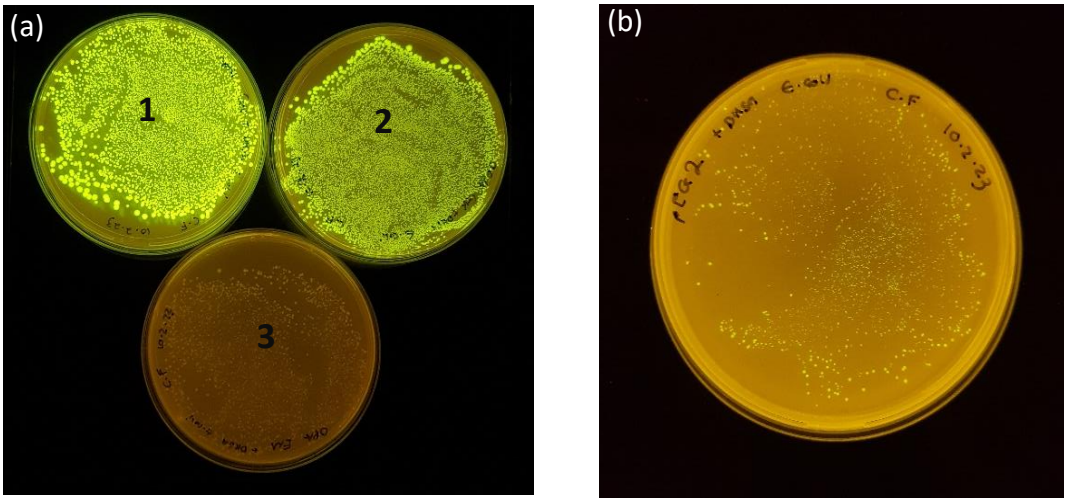

Figure 3.10: Colony GFP fluorescence under blue light. GFP fluorescence was observed for the NptIIGK (a.1) and OpaGK (a.2) *E. coli* constructs when viewed under the Invitrogen Safe Imager™. This was compared to no fluorescence under blue light in OpaME (a.3) and fluorescence in the pEG2 plasmid (b). The fluorescence expression in the OpaGK and NptIIGK colonies is more intense than pEG2.

3.2.3 Cryptic region addition into the Golden Gate constructs

After determining the feasibility of Golden Gate assembly in *E. coli*, the addition of the cryptic region from pEG2 was necessary for plasmid maintenance in *N. gonorrhoeae*. The cryptic region was excised from pEG2 (see section 2.5.3) using the HindIII restriction enzyme and treated as the fifth DNA fragment option for Golden Gate constructs (Figure 3.11).

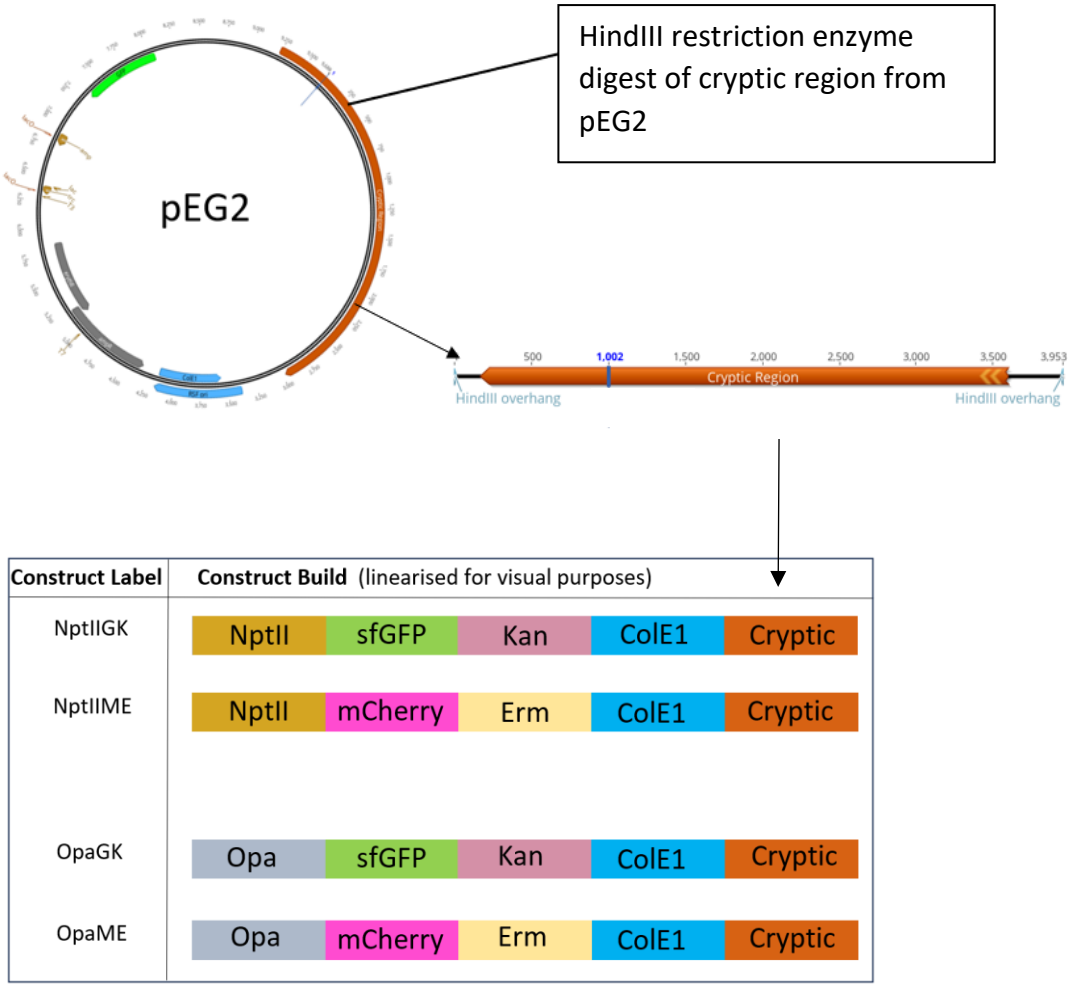

Figure 3.11: Digestion of the cryptic region from pEG2 to create shuttle vector constructs. A HindIII restriction enzyme digest of pEG2 dropped out the cryptic region so that it could be added to the four combinations of fragments of the Golden Gate assembly design to create shuttle vector plasmids.

The digest resulted in four DNA bands when run on an agarose gel (Figure 3.12). As the Sanger sequencing results suggested the cryptic region was around 4000 bp, the largest DNA band was excised, and DNA purified for ligation into the plasmid constructs.

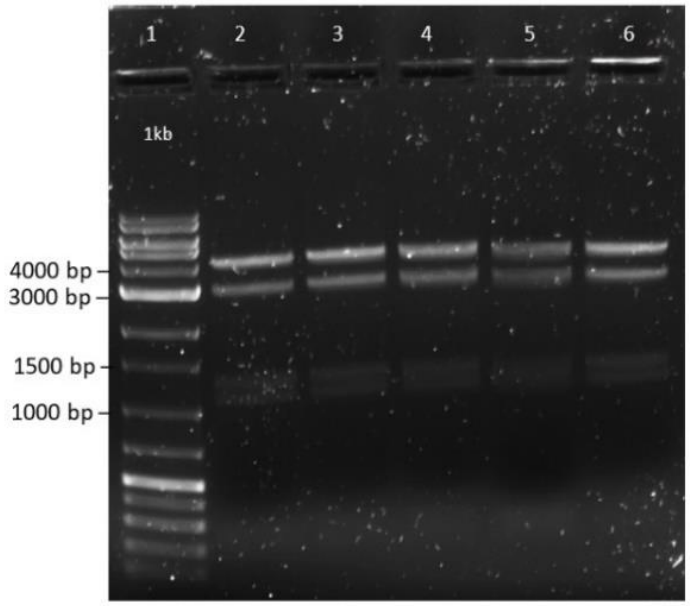

Figure 3.12: HindIII enzyme digest of pEG2. The pEG2 plasmid was HindIII digested to separate out the cryptic region (~4000 bp). Lane 1: 1kb DNA ladder. Lanes 2 to 6: HindIII digest. The digest was run on a 1% agarose gel at 100 V for 45 mins and visualized using the iBright FL1000 (Invitrogen).

In parallel, each of the four constructs were also digested with HindIII and dephosphorylated to prevent self-ligation in downstream cloning (see section 2.5.2). The cryptic region was ligated into each of the four plasmid constructs in two parts to complete the full builds: first the NptII constructs, then Opa constructs, as per section 2.5.4 and ligation conditions in Table 2.7. Ligations were transformed in *E. coli* and grown on respective antibiotic plates for screening. A negative control ligation was included, which excluded the Cryptic Region fragment to evaluate background growth of self-ligating constructs. Few colonies were observed on the control plates and therefore colonies off the ligation plates were selected for amplification and purification.

For the NptII construct ligations, nine colonies from the NptIIME construct plate and four colonies from the NptIIGK construct plate were selected for DNA extraction and

purification. To analyse which colonies had successful cryptic region integration, a HindIII restriction enzyme digest was carried out, producing two DNA bands when run on an agarose gel if successful. There was one successful integration for NptIIME (Figure 3.13.a) and two successful integrations for NptIIGK (Figure 3.13.b).

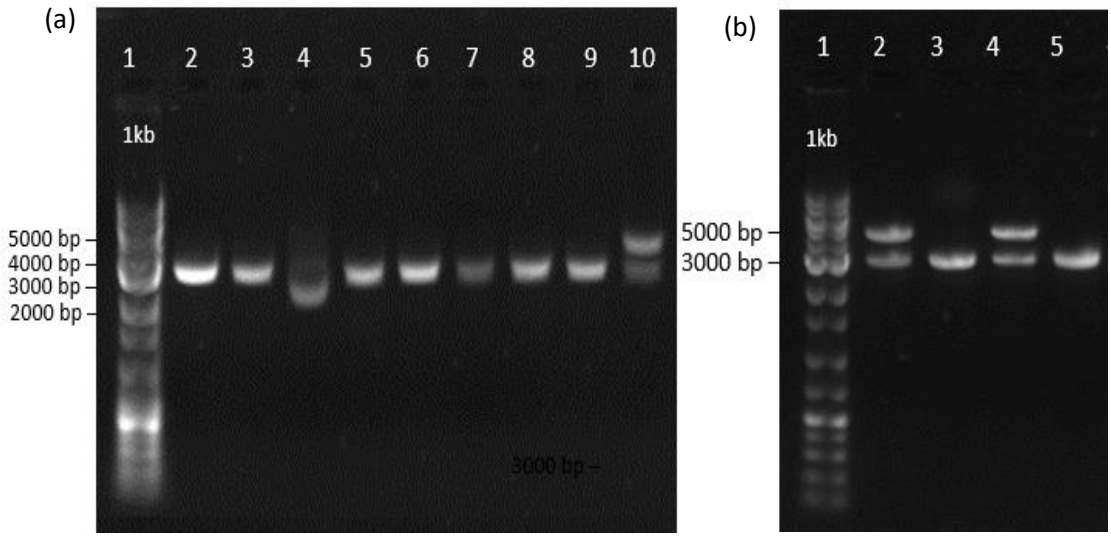

Figure 3.13: Analysis of cryptic region ligation into constructs via HindIII digestion. Ligations underwent a HindIII digestion to show which ligations contained two DNA fragments, confirming cryptic region integration. (a) Lane 1: 1kb DNA ladder. Lanes 2 – 9: unsuccessful integrations. Lane 10: two DNA bands indicating successful integration. (b) Lane 1: 1kb DNA ladder. Lanes 2 and 4: successful ligations. Lanes 3 and 5: unsuccessful ligations. The digests were run on a 1% agarose gels at 100 V for 45 mins and was visualized using the iBright FL1000 (Invitrogen).

For the Opa construct ligations, 14 colonies from the OpaME construct plate and 14 colonies from the OpaGK construct plate were selected for DNA extraction and purification. To analyse which colonies had successful cryptic region integration, PCR was carried out (see section 2.2.6) using Primer 6, Neo-F, and mCherryqpcr. This was run on an agarose gel to confirm which samples contained the cryptic region, due to the primer design to amplify from the resistance gene into the cryptic region. (Figure 3.14). The OpaGK construct had four DNA bands appear around the expected DNA band size of 1459 bp and the OpaME construct had one DNA band appear around the expected PCR product size of 2644 bp. The DNA bands appearing at ~500 bp are non-specific binding of the primers.

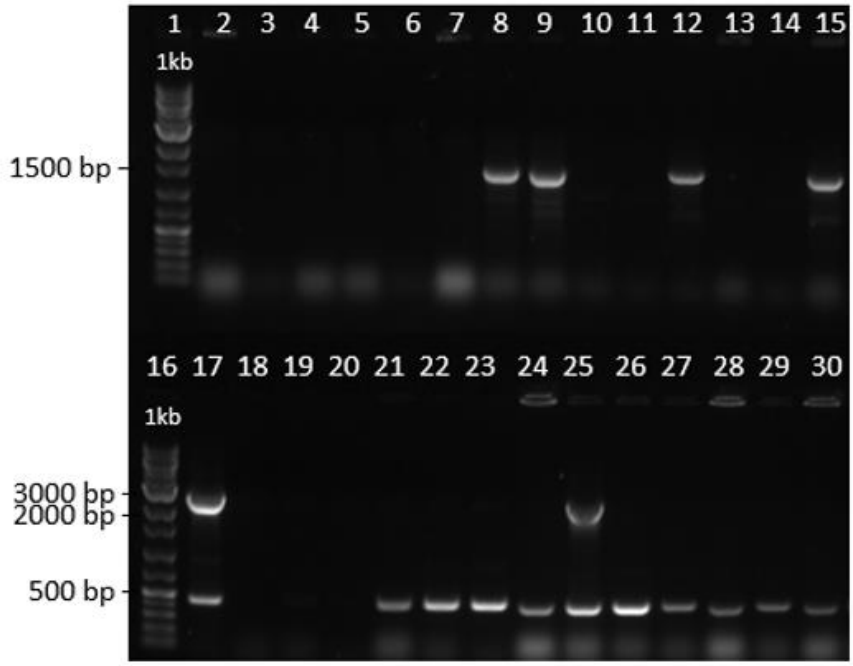

Figure 3.14: Agarose gel of PCR for OpaGK and OpaME ligations. Lanes 1 and 20: 1kb DNA ladders. Lanes 2 to 15: OpaGK ligations, of which lanes 8, 9, 12, and 15 were successful. Lanes 17 to 30: OpaME ligations, of which lane 21 was successful. The PCR was run following Table 2.3 conditions, the digest was run on a 1% agarose gel at 100 V for 45 mins and was visualized using the iBright FL1000 (Invitrogen).

3.3 Analysis of the Golden Gate assembled constructs

3.3.1 Microscopy analysis of Golden Gate constructs

To validate that the constructs successfully express fluorescent proteins in *E. coli* before transforming into *N. gonorrhoeae*, microscopy was used to visualise fluorescence. First, GFP expression was observed in the NptIIGK construct in *E. coli* (Figure 3.15.b) using a Zeiss compound microscope (see sections 2.3.5 and 2.3.6). Upon discovering this microscope could only visualise GFP fluorescent emission, only the NptIIGK construct in *E. coli* was analysed on this instrument and confocal microscopy was used to visualise the remainder of the constructs.

Confocal microscopy was subsequently used via an Olympus IX81 confocal microscope to visualise both mCherry and GFP fluorescence in *E. coli* (see section 2.4.7). Both OpaME and NptIIME constructs were tested as well as OpaGK and WT *E. coli*. The WT negative control presented with no fluorescence (Figure 3.15.a). Fluorescence was

observed in OpaGK (Figure 3.15.c), and NptIIME (Figure 3.15.d), but not in OpaME. Collectively this suggests that both promoters work in the *E. coli* constructs, however, no fluorescence was observed for mCherry under the control of the Opa promoter.

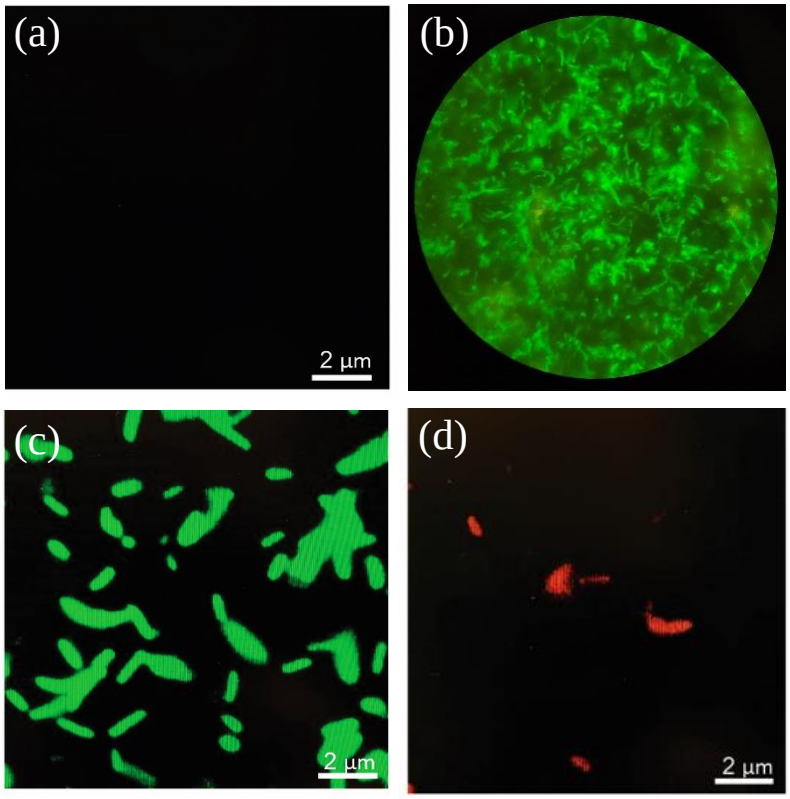

Figure 3.15: Microscopy analysis of *E. coli* OpaGK, OpaME, and NptIIGK strains compared to wild type. Under the confocal microscope WT *E. coli* presented with no fluorescence (a). Under the Zeiss compound microscope NptIIGK in *E. coli* presented with green fluorescence (b). Under the confocal microscope OpaGK in *E. coli* presented with green fluorescence (c). Under the confocal microscope NptIIME in *E. coli* presented with red fluorescence (d).

3.3.2 Transformation of Golden Gate assembly constructs into *N. gonorrhoeae*

To validate the Golden gate assembly shuttle vectors, the constructs were transformed into *N. gonorrhoeae*. Constructs OpaGK, OpaME, NptIIGK, and NptIIME were transformed into *N. gonorrhoeae* via a liquid transformation (see section 2.4.4).

As there was distinct growth observed on the antibiotic plates after transformation, this validated that the constructs were successfully taken up by the gonococcal cells.

Additionally, a cPCR was carried out to confirm that the transformants had successfully taken up the plasmid DNA and this was run on an agarose gel (Figure 3.16). Primer 6 and Neo-F were used for OpaGK (lane 6) and NptIIGK (lane 5) samples, and Primer 6 and mCherryqpcr were used for OpaME (lanes 3 and 4) and NptIIME (lane 1) samples. The PCR products for both OpaME and NptIIME should be 2644 bp and the OpaGK and NptIIGK PCR products should be 1459 bp. The DNA bands on the agarose gel match these predictions, therefore all the selected transformations were successful. However, the NptIIME and NptIIGK constructs had less than eight colonies grow, compared to ~25 colonies on both the OpaGK and OpaME plates. This suggested that the NptII promoter is not as efficient in *N. gonorrhoeae* as the Opa promoter.

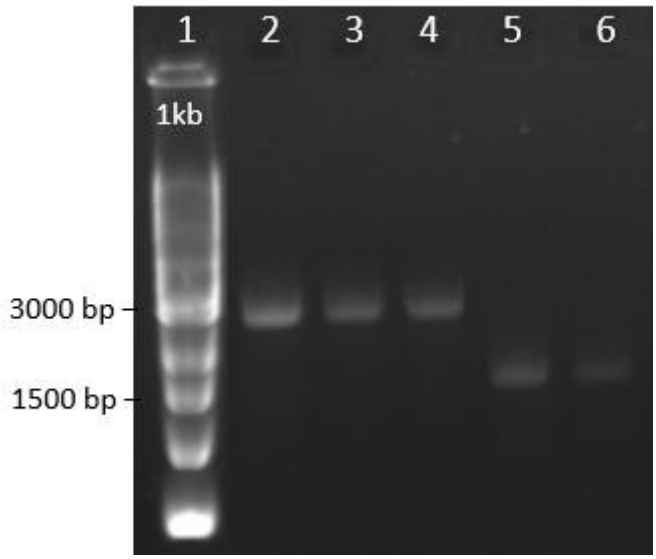

Figure 3.16: Agarose gel of *N. gonorrhoeae* transformants. The OpaGK, OpaME, NptIIGK, and NptIIME constructs were transformed into *N. gonorrhoeae* and a cPCR was carried out to confirm transformation success. Lane 1: 1kb DNA ladder (Zymo Research 1kb DNA Marker), lane 2: NptIIME, lane 3: OpaME, lane 4: OpaME, lane 5: NptIIGK, and lane 6: OpaGK. The PCR was run following Table 2.3 conditions, the digest was run on a 1% agarose gel at 100 V for 45 mins and was visualized using the iBright FL1000 (Invitrogen).

To visualise expression of fluorescent proteins, confocal microscopy was used (see sections 2.4.6 and 2.4.7) to view the *N. gonorrhoeae* OpaGK (Figure 3.17.a), NptIIGK, OpaME, and NptIIME plasmids compared to pEG2 (Figure 3.17.b) and WT *N. gonorrhoeae* (Figure 3.17.c).

Of the four plasmid constructs tested, only the GFP expressing OpaGK and pEG2 exhibited fluorescence in *N. gonorrhoeae.* This suggested that fluorescence is not observed under the control of the NptII promoter in *N. gonorrhoeae* and that the OpaME construct again did not present with fluorescence under the control of the Opa promoter in *N. gonorrhoeae*. This data also suggested that WT *N. gonorrhoeae* does not exhibit background fluorescence and that OpaGK is comparable to pEG2 in *N. gonorrhoeae*.

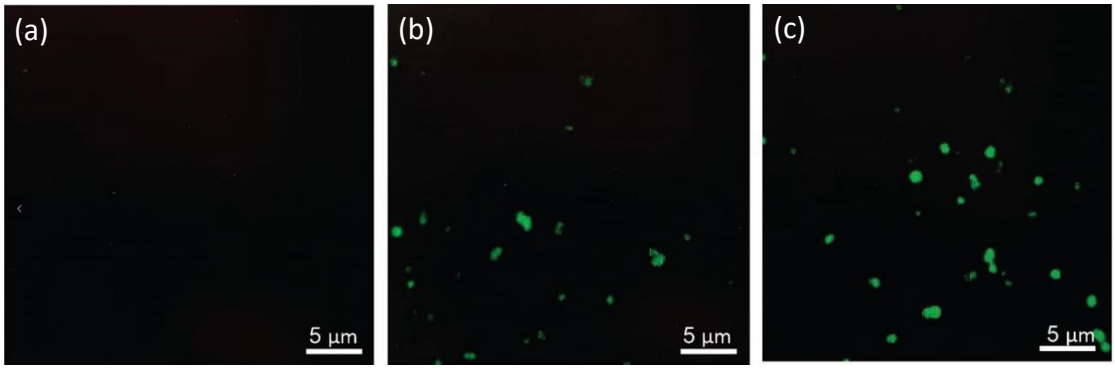

Figure 3.17: Confocal microscopy of fluorescence in *N. gonorrhoeae* plasmid strains. (a) WT *N. gonorrhoeae* presented with no fluorescence at 60x objective. (b) OpaGK *N. gonorrhoeae* strain with green fluorescing cells at 60x objective. (c) pEG2 with green fluorescing cells at 60x objective.

As for the mCherry constructs (OpaME and NptIIME), there were issues with fluorescence signal in *E. coli* and no expression in *N. gonorrhoeae*. Therefore, an investigation as to why the mCherry constructs were not fluorescing was undertaken using Sanger sequencing.

3.3.3 Sequencing *mCherry* in selected constructs

As both the mCherry and antibiotic resistance genes are driven from the same promoter (with the antibiotic resistance placed second), an antibiotic resistant phenotype in a colony should indicate the promoter, antibiotic resistance, and cryptic region fragments

are functional. Therefore, instead of sequencing the entire constructs, focus was placed on sequencing the *mCherry* gene specifically.

Sequencing primers were designed (see section 2.2.5) to cover the *mCherry* gene to investigate why mCherry constructs that were transformed into *E. coli* and *N. gonorrhoeae* were not fluorescing as expected. LIT114 covered mCherry by beginning in the Opa promoter, and the LIT116 primer covered mCherry by starting in erythromycin and going in the reverse direction for constructs with the NptII promoter (Figure 3.18).

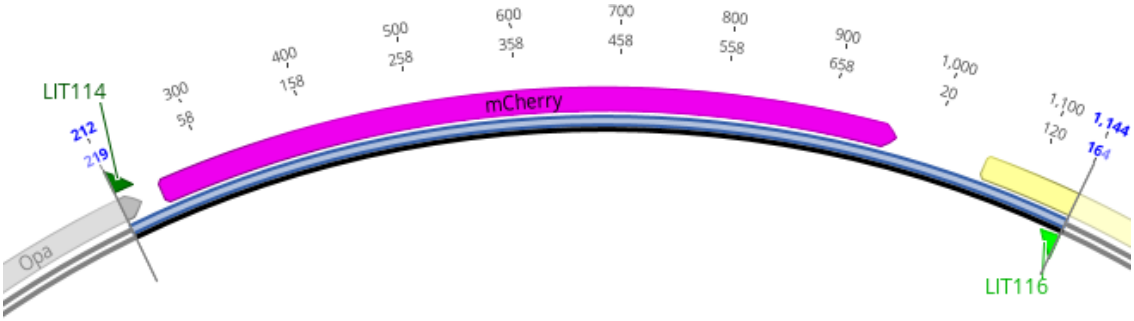

Figure 3.18: LIT114 and LIT116 primers designed for mCherry sequencing. LIT114 (left) was designed to fully cover the mCherry region in a forward direction for mCherry-containing constructs that had the Opa promoter. LIT116 (right) was designed to cover the mCherry region in a reverse direction for mCherry-containing constructs that had the NptII promoter and erythromycin. Primers were designed using Geneious Prime.

The OpaME and NptIIME *E. coli* construct that were used in the transformation experiments were sequenced via Sanger sequencing. The LLT114 primer was used for the OpaME construct and the LIT116 primer was used for the NptIIGK construct. Sequencing data was analysed using Geneious Prime. The sequences were aligned to the original mCherry Twist fragment sequence as the reference sequence, using the Map to Reference tool. This allowed for the identification of mutations potentially affecting protein expression and fluorescent signal.

The OpaME construct Sanger sequencing was mapped to the reference sequence with a pairwise identity of 97.7%. There were single bp mutations throughout and a 9 bp gap in the OpaME construct sequence where the reference had base pairs present (Figure 3.19). This gap might suggest a small section of the OpaME *mCherry* gene is missing, resulting in fluorescence expression issues.

Figure 3.19: Pairwise alignment of OpaME *mCherry* and reference *mCherry* sequences. The Sanger sequence for OpaME *mCherry* was pairwise aligned to the original mCherry sequence ordered from Twist Biosciences to see any mutational differences. A nine bp gap was observed in the OpaME *mCherry* sequence (close up image). Sequences were analysed using Geneious Prime.

Unfortunately, the LIT116 primer was designed in the incorrect direction, resulting in a sequence that pairwise aligned elsewhere in the NptIIME sequence instead of covering the *mCherry* gene. It would have been expected to see 100% identity in the pairwise alignment as this was the sample used in the *E. coli* transformation that presented with red fluorescence under the confocal microscope. However, it would have been useful to compare this sequence to the OpaME *mCherry* to see if the differences were the same. A new primer will have to be designed to get sequence data on the NptIIME *mCherry* gene.

It could be possible that there are mutations elsewhere in the construct such as in the Opa or NptII promoters, affecting expression of the *mCherry* gene, which arose after transformation into *N. gonorrhoeae*. This is less likely due to the antibiotic resistance and ColE1 (plasmid replication) working in the constructs. In the future, sequencing of the *N. gonorrhoeae* construct *mCherry* genes could be done to compare to the *E. coli* results. A distinct possibility is that the NptII promoter is non-functional in *N. gonorrhoeae* transformations despite prior evidence showing function in a broad range of species (Schlechter et al., 2018).

3.3.4 Analysis of OpaGK in *N. gonorrhoeae*

3.3.4.1 Growth curve

To analyse the effect (if any) of GFP expression from OpaGK on *N. gonorrhoeae* growth, growth curves were performed to monitor the growth of the OpaGK *N. gonorrhoeae* strain compared to WT *N. gonorrhoeae* (see section 2.4.8). It was important to make sure the insertion of the OpaGK construct did not affect growth, as when using this strain for a comparison of fluorescence against a variable of interest, there needs to be confidence that data collected are not skewed by the construct itself.

Growth curve time points were taken every 1.5 hrs. At each time point, the culture was observed under a stereo microscope with a 40x objective lens to monitor microcolony formation and samples were taken for plating CFUs.

Microcolony formation was expected throughout the experiment as this suggested the colonies were still piliated. Before 6 hrs, microcolony formation was not observed (Figure 3.20.a). Signs of microcolony formation started at 6 hrs (Figure 3.20.b) and cell numbers and microcolony formation expanded at 10. 5 hrs (Figure 3.20.c). Microcolony formation peaked at 12 hrs (Figure 3.20.d) and was maintained through to 13 hrs. Both OpaGK and WT had similar microcolony formation numbers, however it was observed that OpaGK had more free flowing cells around the clustered formations than WT. This is likely due to the WT stock used being slightly more piliated than the OpaGK stock, but this was not seen to affect the growth curve in any way.

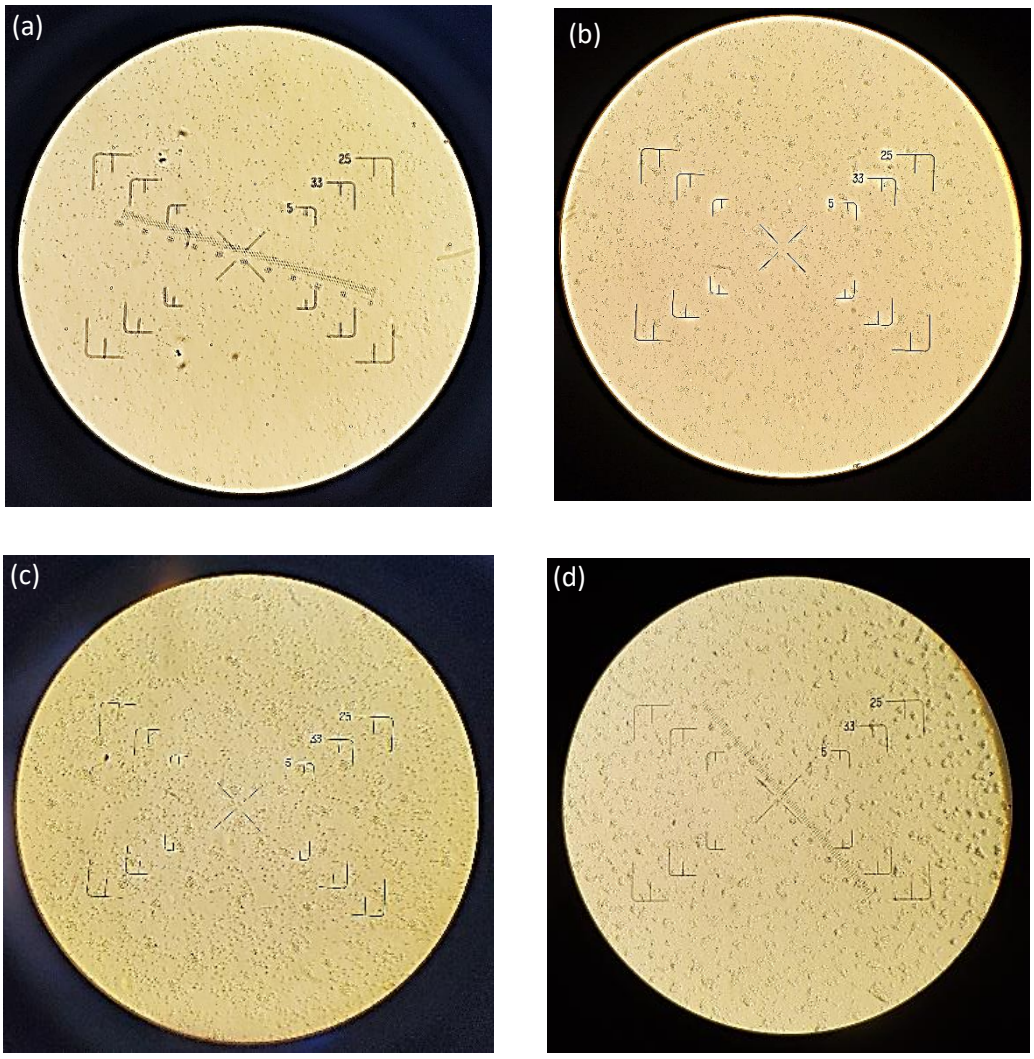

Figure 3.20: *N. gonorrhoeae* microcolony formation during growth. (a) no microcolony formation in OpaGK *N. gonorrhoeae* cells after 4.5 hrs of growth (40x objective lens). (b) WT *N. gonorrhoea* cells after 6 hrs of growth beginning to form microcolonies (40x objective lens). (c) OpaGK *N. gonorrhoeae* cells after 10.5 hrs of growth, forming few dense microcolonies (40x objective lens). (d) WT *N. gonorrhoeae* cells after 12 hrs of growth, forming numerous dense microcolonies. All cells were grown in 1.2 mL GCBL + Kellogg's supplement media in 12 well plates at 37 °C with 5% CO_2.

The six plates from each time point were observed under a stereoscope to count CFU using a handheld tally counter and the six plates were averaged. The data from all the time points (Appendices A) were normalised (see section 2.4.8.1) and overlapped to show the difference in growth between WT and OpaGK *N. gonorrhoeae* (Figure 3.21).

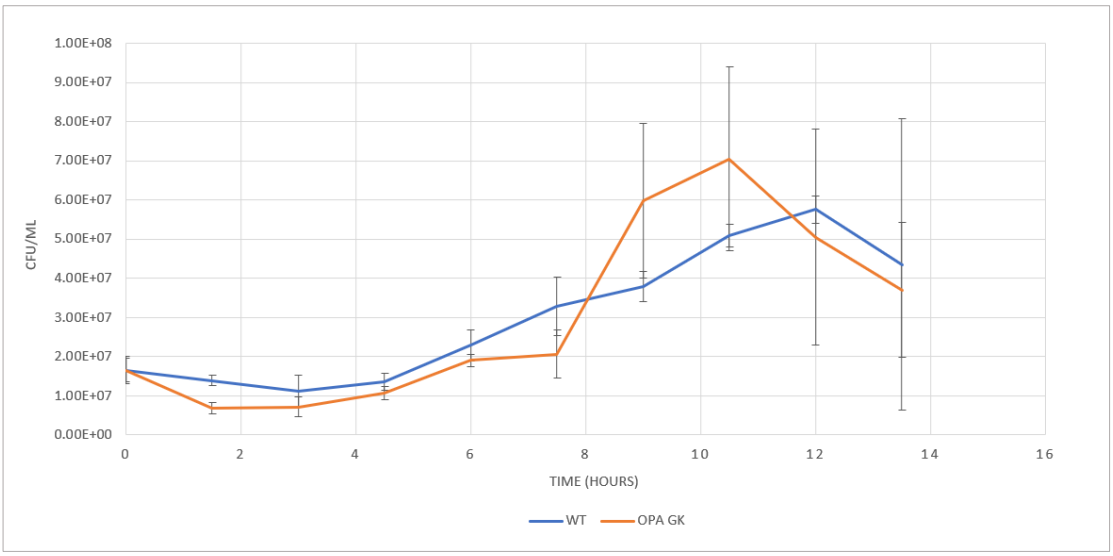

Figure 3.21: Growth curve of *N. gonorrhoeae* WT and OpaGK strains. Growth of WT and OpaGK strains of *N. gonorrhoeae* were compared over 10 lots of 1.5 hr time points (13.5 hours total) to observe if the addition of the OpaGK shuttle vector plasmid into *N. gonorrhoeae* effects its growth. Growth was measured by counting the CFU that present on agar plates 48 hrs after each time point, multiplying this number by 10^6 to account for dilutions, to get a final CFU/mL over time. All cells were grown in 1.2 mL GCBL + Kellogg's supplement media in 12 well plates at 37 °C with 5% CO_2. All data points are averages with standard errors (error bars) from six technical replicates (except T0 which had two replicates).

The growth curve showed no significant difference between *N. gonorrhoeae* WT and OpaGK strains. This confirmed that the OpaGK construct can be used in further experimentation with no effect on gonococcal growth and overall, the Golden Gate assembly cloning design can successfully generate a modular system that allows for interchangeable features for genetic manipulation of gonococci.

3.3.4.2 OD_{600} measurements during growth curve

The OD_{600} of *N. gonorrhoeae* was measured during each 1.5 hr time point of the growth curves (see section 2.4.9) (Appendices A). Monitoring OD is an easy way to estimate culture growth and works by measuring the amount of light scattered by bacterial cells in solution; more cells result in more light scattered and a higher OD. However, using OD to measure viable growth of gonococci can be misleading. This is because when *N. gonorrhoeae* reaches a decline growth phase, cells start to die, leading to a higher OD

as the cells are still affecting light scatter. This means it is still important to compare OD to CFU/mL or comparing OD to live cell count data.

The OD_{600} data for the *N. gonorrhoeae* WT and OpaGK strains (Figure 3.22) suggested that there is no significant difference in growth between the strains, due to how closely the data points in Figure 3.22 follow each other. When compared to the CFU/mL data, the cell density was increasing even when CFU was decreasing. This is logical as CFU measures alive cells and OD measures both alive and dead cells.

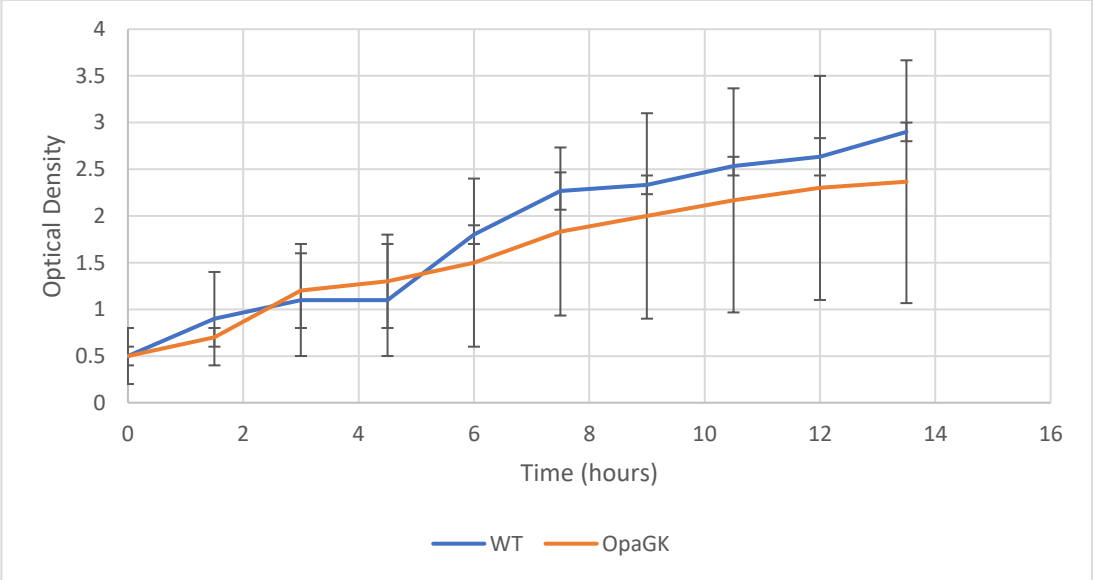

Figure 3.22: OD_{600} readings during WT and OpaGK *N. gonorrhoeae* strains growth curve. During the growth curve, OD_{600} measurements were taken at every 1.5 hrs. All OD_{600} measurements were similar over time between the two strain samples, suggesting no adverse growth differences between the *N. gonorrhoeae* WT and the OpaGK strains. All data points are averages with standard errors (error bars) from three technical replicates (except T0, T1, T2, and T3 which had one replicate).

3.3.4.3 Growth curve repetition

When repeating the growth curves for *N. gonorrhoeae* strains, OD_{600}, fluorescence, and cell count were all measured at each time point to see if the fluorescence was maintained during growth and if the OD_{600} was comparable to the cell count. An OpaGK strain was also tested without kanamycin antibiotic (-kan) in the growth media to see how stable the construct plasmid is within the gonococci cells by measuring fluorescence.

However, the incubator available for the experiment malfunctioned, resulting in large negative effects on the growth and culturing of cells laboratory wide.

As growth on streak and lawn plates appeared normal and Opa^+ or piliated colonies were still in high numbers, the problem was thought to be within the incubator. Upon investigation, a CO_2 leak was found. Until the issues had been discovered and the machine replaced, growth curve analysis resulted in unusual data (Figure 3.23) (Appendices B).

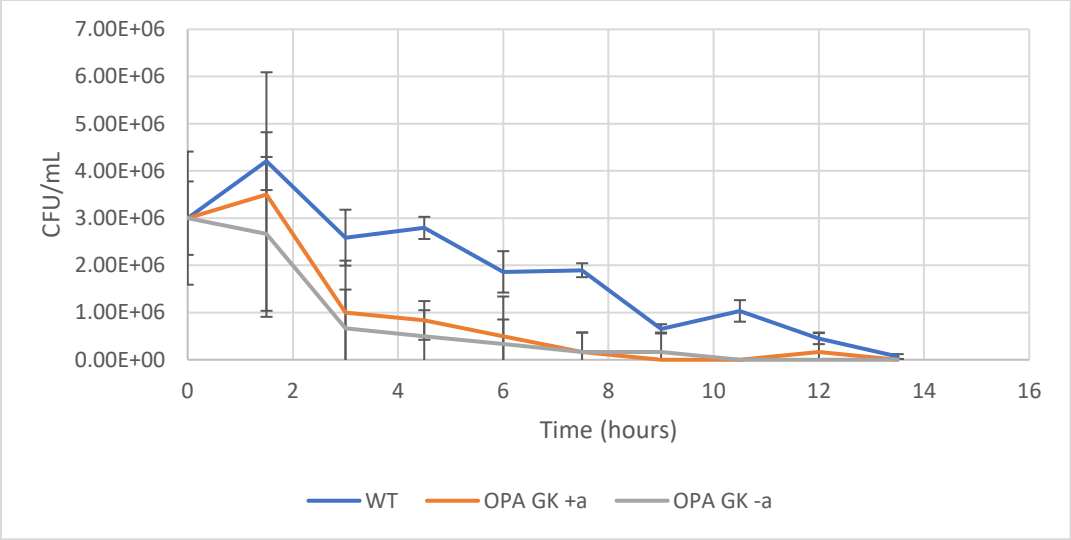

Figure 3.23: Subsequent growth curve data for WT and OpaGK *N. gonorrhoeae* strains. Growth of WT and OpaGK strains of *N. gonorrhoeae* were compared over 10 lots of 1.5 hr time points (13.5 hours total) to observe if the addition of the OpaGK shuttle vector plasmid into *N. gonorrhoeae* effects its growth. However, due to technical difficulties, the data was heavily affected. Data was measured and collected in the same method as the previous growth curve. All data points are averages with standard errors (error bars) from six technical replicates (except T0 which had two replicates).

Although the data does not represent a normal growth curve, there appears to be a rise and fall pattern observed between all samples as growth declined. Due to the similarity in growth, this suggests that the plasmid does not require antibiotic in the media to maintain stability. The growth of both the *N. gonorrhoeae* WT and OpaGK strains declined gradually over time until no CFUs were detected on the plates. This was likely due to the low availability of CO_2 in the failing incubator.

3.3.4.4 Fluorescence monitoring of *N. gonorrhoeae* during growth curves

Fluorescence in *N. gonorrhoeae* cells was recorded at each 1.5 hr time point of the growth curves (see section 2.4.10) (Appendices B). Fluorescence was monitored using a ThermoFisher Countess 3FL cell counter to observe how the level of GFP expression changed over time, indicating how well gonococci retain and maintain the plasmid construct. Fluorescence was expected to be maintained at a constant level throughout the growth curve time points as this would mean the plasmid was stably held within the cells. Alternatively, it was expected the percentage of fluorescence would increase in proportion to cell count, as the higher the number of cells, the more fluorescence was available to be measured.

Although the growth curves were affected by the malfunctioning incubator, producing impacted fluorescence readings, it can be seen that as the hours increase, both OpaGK samples follow a similar pattern of fluorescence (Figure 3.24). In contrast, the WT strain shows very little background fluorescence. The first few time points are less reliable as the number of detectable cells are low, but as cell count increased over time, fluorescence appears to be very similar between the two samples. Therefore, this data suggests plasmid stability in the absence of antibiotic. These experiments will need to be repeated to confirm findings.

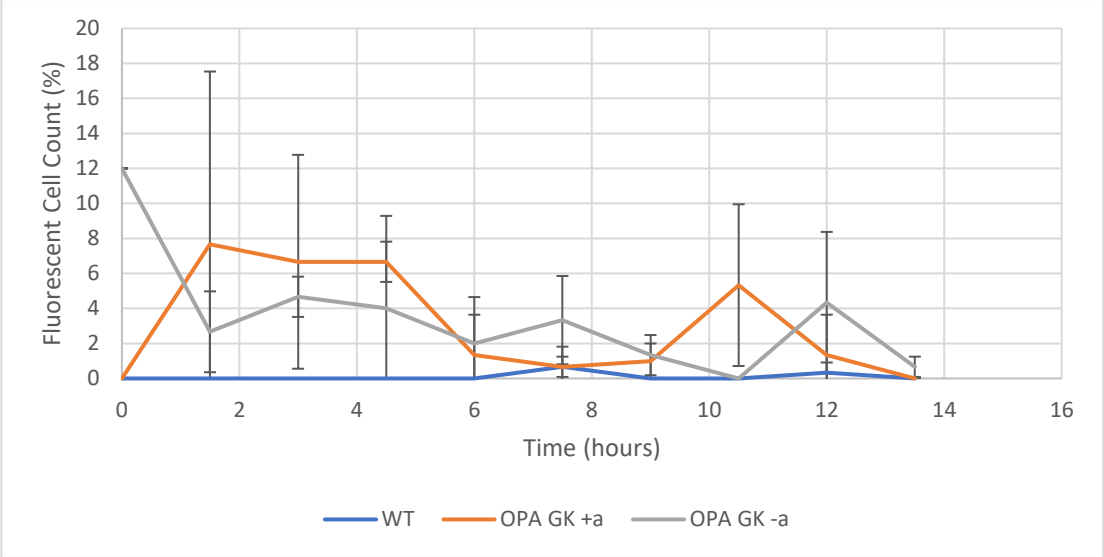

Figure 3.24: Fluorescence in WT and OpaGK *N. gonorrhoeae* strains. The fluorescence observed from the *sfGFP* gene in the OpaGK samples is compared to see if the OpaGK plasmid is stable over time without antibiotic. Due to lab equipment difficulties, the data was impacted. However, it can be observed that OpaGK samples follow a similar pattern after 2.5 hours (when cell numbers may have increased enough for reliable fluorescence detection), and the WT strain has minor background fluorescence which is observed at 7.5 hours. All data points are averages with standard errors (error bars) from three technical replicates (except T0 which had one replicate).

3.3.4.5 Cell counting of *N. gonorrhoeae* strains during growth curve experiments

Cell count of *N. gonorrhoeae* WT and OpaGK strains were recorded at each 1.5 hr time point of the growth curves (see section 2.4.10) (Appendices B) using a ThermoFisher Countess 3FL cell counter. The cell count was measured to compare to an OD_{600} reading as OD readings will measure all cells in a given solution, whereas the cell counter can measure just the living cells. Therefore, cell counting will help determine what percentage of the OD_{600} are living cells and should correlate with CFU/mL data at each growth phase.

However, due to the malfunctioning incubator, the cell count presented impacted results. According to the CFU data, the cell viability consistently decreased over time, however the cell count data fluctuates on an overall incline (Figure 3.25).

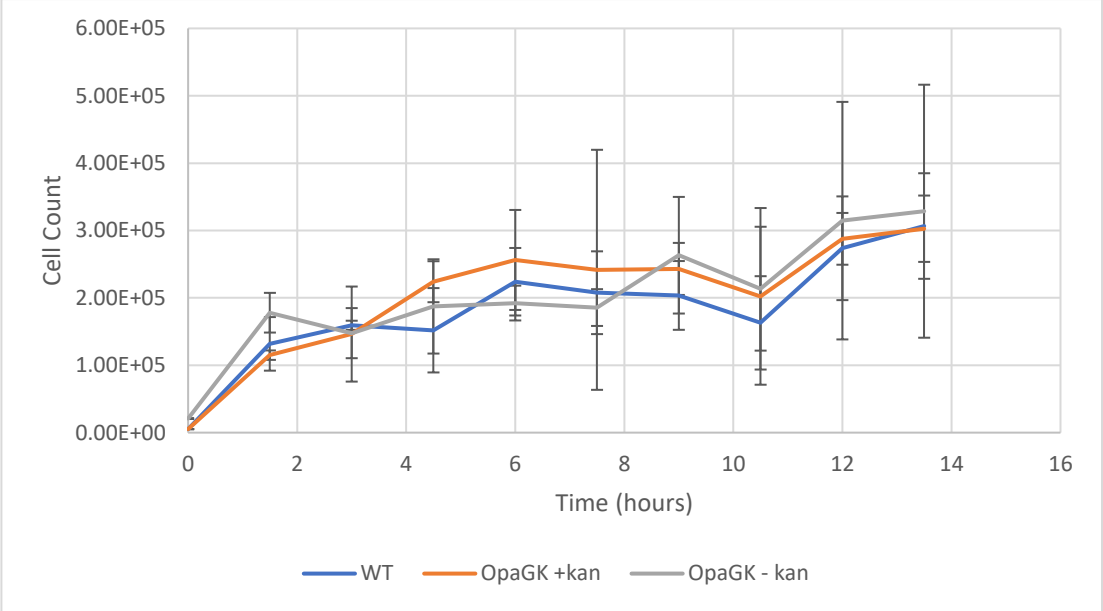

Figure 3.25: Cell count for WT and OpaGK *N. gonorrhoeae* strains. Cell count was measured during each time point of the growth curves via a ThermoFisher Countess 3FL cell counter. Results were impacted due to an incubator malfunction A pattern can be seen in the data that possibly reflects the CO_2 fluctuations in the failing incubator. All three strains follow the same pattern, indicating OpaGK has no adverse effects on growth and the plasmid is stable without antibiotic. All data points are averages with standard errors (error bars) from three technical replicates (except T0 which had one replicate).

Normally, there would be an expected plateau in cell count as cells reach a death phase after ~10 hrs, however, the cell count data does not reach this plateau. This is possibly due to the malfunctioning incubator causing a lag in the growth phases due to the lack of required CO_2 for growth, leading to data that only captured early stages of a growth cycle that does not reach a stationary or death phase. Despite this, all three strains closely follow the same incline in growth pattern. Furthermore, the plasmid does not appear to be affecting cell count and the antibiotic does not appear to be an advantage to the plasmid stability. If the gonococci were rejecting the plasmid, it would be expected that the antibiotic sample would have noticeably less cells as some would die off as a result of the plasmid DNA loss. In the future, this experiment would be redone to validate findings with normal levels of CO_2.

3.3.4.6 Optical density monitoring of *N. gonorrhoeae*

The OD_{600} of *N. gonorrhoeae* was measured during each 1.5 hr time point of the repeated growth curves (Appendices B), however the growth curves were affected by the malfunctioning incubator, producing impacted OD_{600} results. It was expected that the OD_{600} follows a similar pattern to the CFU/mL over time; increasing as hours increase. Furthermore, there should be a point in where the OD_{600} reading keeps increasing where live cell count and CFU/mL decrease during a death phase. The OD_{600} data does follow this initial incline, however, the OD_{600} unexpectedly plateaus after seven hours, showing a decrease in cell density as the cells stopped surviving after a certain point (Figure 3.26). This is likely due to the cells dying in the suboptimal conditions of the incubator.

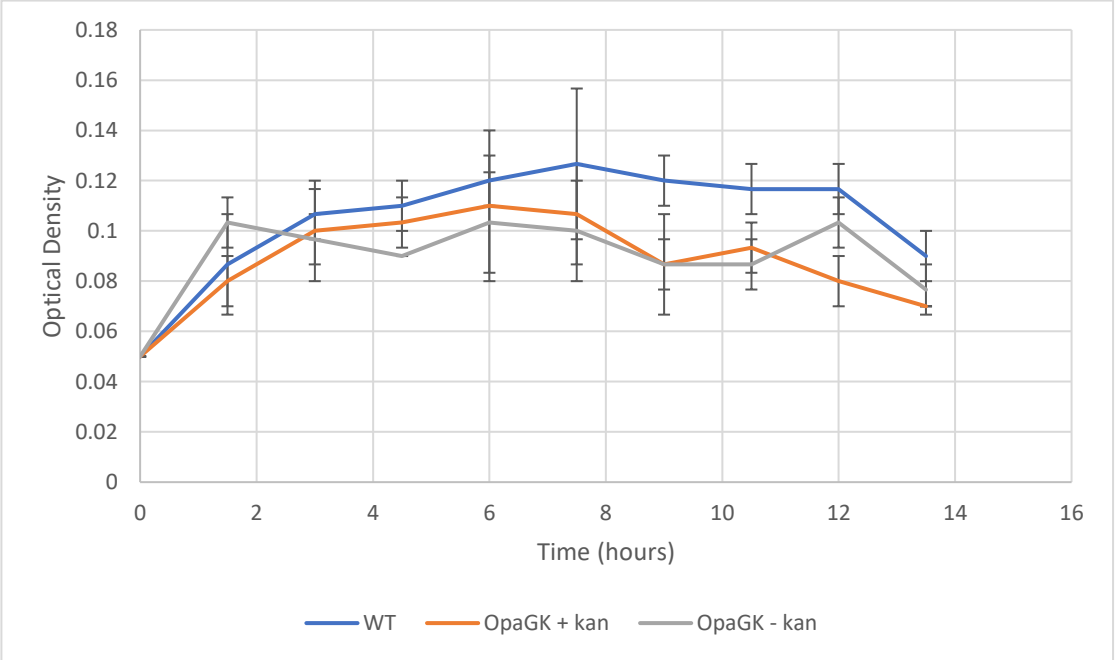

Figure 3.26: OD_{600} readings during WT and OpaGK *N. gonorrhoeae* strains repeated growth curves. During growth curves, OD_{600} measurements were taken at every 1.5 hrs for six replicates of each strain. All OD_{600} readings were similar over time between the three strain samples, however the data is impacted due to lab equipment difficulties. The effect can be observed in the peak OD_{600} readings, as none reach the expected OD_{600} of 3.0. All data points are averages with standard errors (error bars) from three technical replicates (except T0 which had one replicate).

What does not correlate however, is that the cell count data kept increasing while the OD_{600} plateaued. A second explanation (to the forementioned in 3.3.4.5) is that dead cells are known to produce autofluorescence (Kozlova et al., 2020) and this is potentially causing the cell counter to read dead cells as living cells, causing a constant incline in data.

Normally, it would be expected that the OD_{600} reading peaks between 2.0 and 3.0 for each sample but the WT data only peaked at 1.12, the OpaGK with antibiotic peaked at 1.1, and the OpaGK without antibiotic peaked at 1.03. Therefore, the OD_{600} data needs to be recollected in future growth curves for a more reliable representation of the *N. gonorrhoeae* WT and OpaGK strains growth. Nonetheless, all three strains follow a similar OD_{600} pattern, suggesting no adverse effects on growth from OpaGK in *N. gonorrhoeae*.

Until a new incubator was installed, optimisation of starting inoculum was carried out, reassuring that the CFU count at T0 was optimal for each individual strain before starting the next growth curve.

3.3.4.7 Optimisation of inoculum OD_{600} for growth curves

The starting inoculum for growth curves ideally results in 50,000,000 – 100,000,000 CFU/mL or 50 – 100 colonies on the T0 plate. To make sure future growth curves with *N. gonorrhoeae* strains had an optimal start, analysis of which OD_{600} value results in the ideal starting inoculum took place (see section 2.4.11) (Appendices C).

There were three inoculum OD_{600} dilutions tested per strain for *N. gonorrhoeae* WT, OpaME, and OpaGK strains: 0.05, 0.075, and 0.1 (Figure 3.27). Previously, 0.05 was used, however after testing the three different inoculum OD_{600} dilutions, it was found *N. gonorrhoeae* WT OD_{600} of 0.075 gave an average of 67,500,000 CFU/mL. For OpaME, an OD_{600} of 0.1 gave an average of 48,500,000 CFU/mL. For OpaGK, all results averaged to ~10,000,000 CFU/mL, suggesting none of the OD_{600} dilutions were appropriate. Therefore, in future growth curves, the inoculum OD_{600} values should be 0.75 for WT, 0.1 for OpaME, and OpaGK requires further testing of higher OD_{600} inoculums. The sub optimal starting inoculums used in this project may have been a contributing factor to the low growth observed and therefore all future growth curve experiments will use these new OD_{600} inoculums.

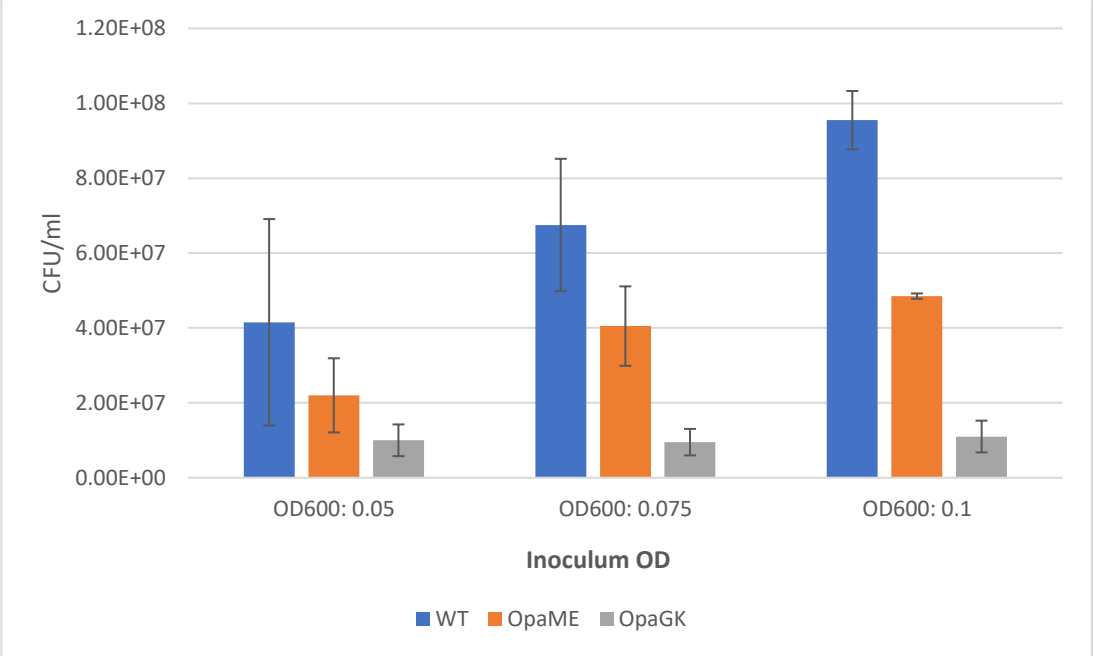

Figure 3.27: Inoculum dilutions for *N. gonorrhoeae* strains. CFU/mL for different OD_{600} inoculum dilutions for WT, OpaME, and OpaGK *N. gonorrhoeae* strains to determine which inoculum OD_{600} would give an ideal count of 50 – 100 colonies. The average OD_{600} that gave closest to 75,000,000 CFU/mL would be the ideal starting inoculum OD_{600}. For WT, OD600 0.075 gave an average of 67,500,000 CFU/mL. For OpaME, OD_{600} 0.1 gave an average of 48,500,000 CFU/mL. For OpaGK, all results averaged to ~10,000,000 CFU/mL, suggesting neither inoculum OD. All data points are averages with standard errors (error bars) from two technical replicates.

After validation that the Golden Gate cloning system works in both *E. coli* and *N. gonorrhoeae*, optimisation of the Golden Gate design took place.

3.4 Golden Gate assembly version 2.0

3.4.1 New modular cloning system design

To further improve the Golden Gate assembly system, a second generation of fragment designs were created (see section 2.5.5) to refine the ease of use and enable new features such as fluorescence induction from a pTet + TetR pMR68 Integron promoter. The key goals were to include the cryptic region as a Golden Gate fragment, standardise the storage of fragments in holding plasmids, and further improve the fragment overhang designs following MoClo rules for high efficiency assembly. The updated designs also included extra fragments such as sfGFP with a terminator, kanamycin with a promoter

and terminator, and an erythromycin for knock out (KO) constructs that has a promoter and terminator (Table 3.2). As the NptII promoter was not successful in producing transformants in *N. gonorrhoeae*, this was not carried through to version 2.0 of shuttle vector design.

Table 3.2: Golden Gate assembly version 2.0 DNA fragment options. The Golden Gate assembly version 2.0 included the addition of a pTet + TetR pMR68 Integron promoter, kanamycin with a promoter and terminator (P/T), erythromycin with a promoter and terminator (P/T), sfGFP with a terminator (T), and the cryptic region. The NptII promoter was not included. All fragments had altered flanks for the ligation into the pLIT100 plasmid and DUS labelled fragments also contained the gonococcal DUS for plasmid uptake and maintenance. Fragments were designed using Geneious Prime and ordered as gene blocks from Twist Biosciences.

DNA Fragment	Option One	Option Two	Option Three	Option Four
Promoter	ACAT Opa TTAT	ACAT pTet + TTAT		
Resistance Marker	CTAA Kan CACT	DUS CTAA Kan P/T CACT	CTAA Erm CACT	CTAA Erm P/T CACT
Reporter Protein	DUS ATTA sfGFP GATT	DUS ATTA sfGFP T GATT	DUS ATTA mCherry GATT	
Origin of Replication	DUS GTGA ColE1 GACG			
Cryptic Region	DUS CTGC Cryptic TGTA			

Fragments for the Golden Gate assembly version 2.0 were designed to have BamHI and KpnI restriction cut sites each side of the fragments (Figure 3.28) to allow for insertion of the fragment into the pLIT100 holding plasmid (A pUC19 derivative). This allowed for easy storage of each individual fragment so that when a construct was being built, a selection of pLIT100 plasmids (rather than linear fragments) could be combined in a single step Golden Gate reaction.

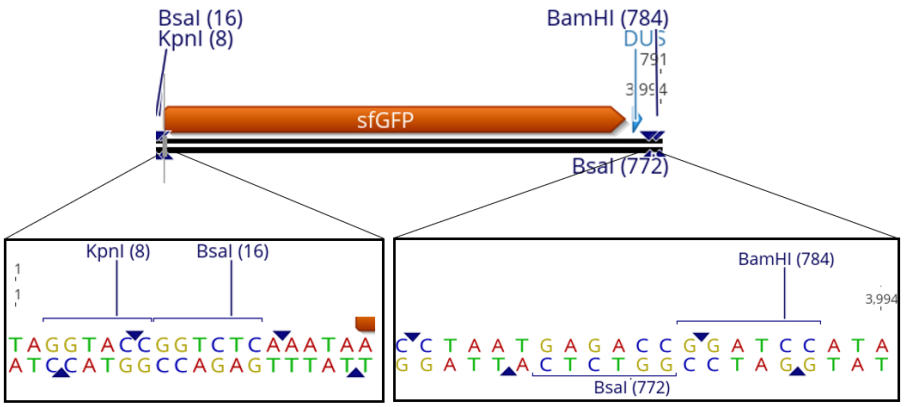

Figure 3.28: Example of the restriction enzyme cut site placement in a DNA fragment. The Golden Gate assembly version 2.0 design included the type IIs restriction enzyme BsaI cut site on each end of all DNA fragments. It also included a KpnI cut site and BamHI cute site per fragment for ligation into the pLIT100 cloning plasmid. Fragments were designed using Geneious Prime.

3.4.1.1 Cryptic Region addition to the new modular cloning system

Subsequently, the cryptic region sequence was analysed for internal BsaI cut sites to ensure compatibility with the Golden Gate system. A single BsaI was identified and confirmed by BsaI digest which resulted in a singular band at ~2000 bp (Figure 3.29). This band pattern is indicative of two fragments that together added to ~4200 bp.

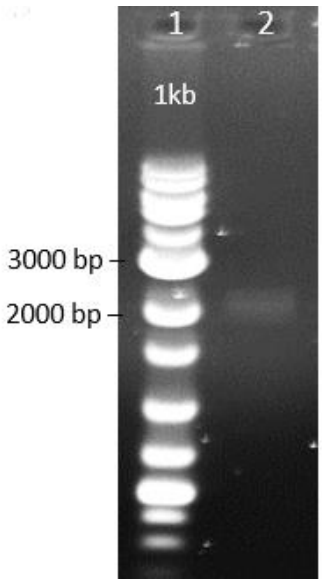

Figure 3.29: Agarose gel of a BsaI digest of the cryptic region. The cryptic region sequence was analysed for internal BsaI cut sites to ensure compatibility with the Golden Gate system. Lane 1: 1kb DNA ladder. Lane 2: BsaI digest resulting in a singular band at ~2000 bp. This band pattern is indicative of two fragments that together added to ~4200 bp. The digest was run on a 1% agarose gel at 100 V for 45 mins and was visualized using the iBright FL1000 (Invitrogen).

Due to the high number of repeat regions in the cryptic region, the sequence was perceived as being incompatible with gene synthesis approaches. Therefore, there was an attempt to mutate the BsaI restriction site via a two-step PCR reaction (Figure 3.30) called 'overlap extension mutagenesis' adapted from methods used in Hilgarth and Lanigan (2020) (Hilgarth & Lanigan, 2020). PCR reactions followed PCR protocol #1 (see section 2.2.6). The four primers LIT110, LIT111, LIT112, and LIT113 (Table 2.1) were designed to amplify the cryptic region into two fragments that contained a T>A mutation to disrupt the BsaI cut site. A combination of the two fragments in a second PCR reaction would result in the mutation being included in the final product.

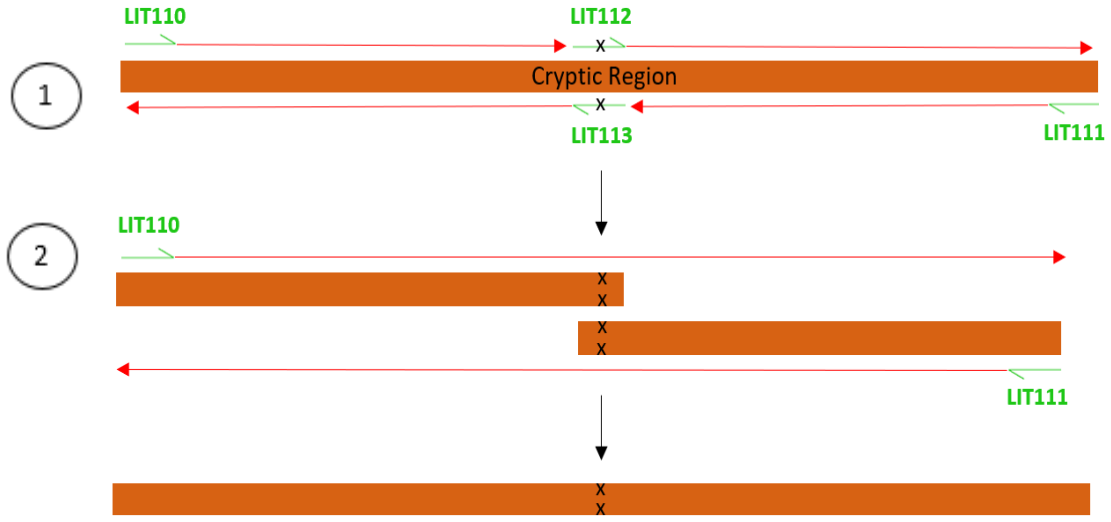

Figure 3.30: Cryptic region T>A mutation via two-step PCR reaction. In step one, the primers LIT110, LIT111, LIT112, and LIT113 work together to amplify the cryptic region into two sections, each new section now containing the single base pair mutation (x). The primers LIT110 and LIT111 work together in step two to amplify both strands at once, resulting as one single strand that has the single base pair mutation.

Step one was successful, producing correctly sized DNA bands (~2200 bp) for both PCR steps (Figure 3.31.a). These were extracted and gel purified for step two. However, step two of the PCR proved challenging, every attempt resulted in agarose gel DNA bands ~350 bp instead of the expected full fragment of ~4200 bp (Figure 3.31.b).

This may have resulted due to the large number of repeat elements in the cryptic region which could have prevented efficient amplification. Therefore, it was necessary to order the modified cryptic region as a synthesised fragment through Twist Biosciences.

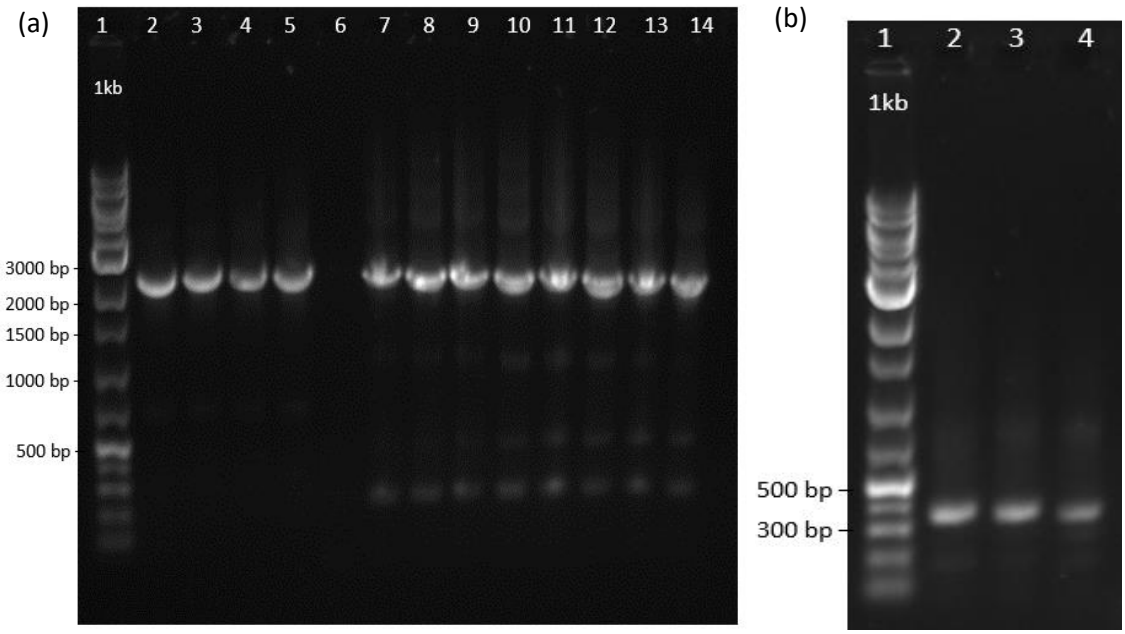

Figure 3.31: Agarose gels of the two-step PCR reaction for cryptic region mutagenesis. Step one of the two-step PCR reaction produced DNA bands just higher than 2000 bp (a), the expected size of half the cryptic region plus mutation-containing DNA template. Lane 1: 1kb ladder. Lanes 2 – 5 and 7 – 14: PCR step one product. Lane 6: empty. Step two of the two-step PCR reaction produced DNA bands of ~ 350 bp rather than the expected ~4000 bp (b). Lane 1: 1kb DNA ladder. Lanes 2 to 4: PCR product of step two. The PCR was run following Table 2.3 conditions, the digest was run on a 1% agarose gel at 100 V for 45 mins and was visualized using the iBright FL1000 (Invitrogen).

3.4.1.1.1 Single nucleotide mutation of the cryptic region fragment to remove BsaI site

Due to the cryptic region sequence in Geneious Prime containing a BsaI cut site sequence (GGTCTC) in the centre, the cryptic region sequence had to be modified via the singular base pair mutation T>A before sending the sequence for synthesis (Figure 3.32) so that it would not interfere with the Golden Gate assembly. According to the annotated cryptic region sequence, this mutation falls within the cppA. The effects of this mutation will need to be investigated in the future to determine if the mutation effects gene function.

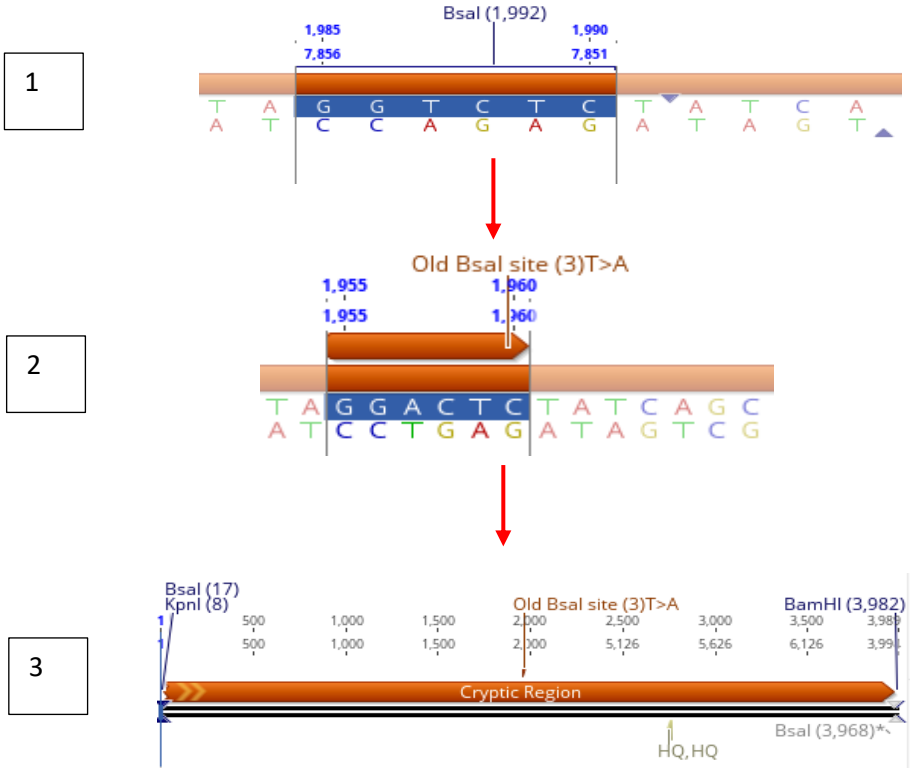

Figure 3.32: In silico BsaI cut site mutagenesis. The cryptic region sequence GGTCTC (1) was edited in Geneious Prime to change the third bp of the BsaI cut site from a T to an A (2). The sequence was then edited to include the same restriction enzyme cut sites on its flanks (3) and ordered as a DNA fragment through Twist Biosciences.

The sequence flanks were modified in Geneious Prime to include the restriction enzyme sites KpnI and BsaI on the 5' and BamHI and BsaI on the 3' end. This ensured that the fragment could be used directly in Golden Gate reactions alongside all the other fragments or could be cloned into the pLIT100 storage vector for consistency via a BamHI/KpnI digestion. This sequence was ordered via Twist Biosciences and arrived sequence verified in a pTwist Amp vector.

3.4.2 Golden Gate Fragment Storage

In unpublished work, researchers in our group have observed higher Golden Gate efficiencies using plasmids as compared to fragments. All second-generation fragments were KpnI/BamHI restriction enzyme digested for ligation into the pLIT100 storage plasmid. Fragments were ligated as per section 2.5.6, transformed into *E. coli*, and grown on antibiotic plates (ampicillin). Each plate had between 40 and 120 colonies

whilst the control plate had 0 colonies. As the constructs were grown on antibiotic plates and the control (self-ligation) plate had no growth, this gave confidence that there was low levels of self-ligation of pLIT100. Colonies were selected off the plates (two per fragment type), overnight cultures were made for DNA extraction and purification, and glycerol stocks were made.

To confirm that the fragments had ligated successfully, Sanger sequencing via Massey Genome Services was used. The pLIT100 plasmid was designed with M13 forward and M13 reverse primers (see Table 2.1) either side of the region where the inserted fragments ligated, producing full cover of any fragment. Therefore, sequencing results were pairwise aligned in Geneious Prime with the ordered fragment sequences from Twist Biosciences to confirm which ligations have the correct insert.

The pairwise alignments showed most of the ligations were successful. However, the Opa promoter, pTet + TetR pMR68 Integron promoter, and mCherry, had unsuccessful ligations. A pairwise identity percentage was given for each alignment (Table 3.3). The Opa promoter, pTet + TetR promoter, and mCherry sequences could not map to the Twist Biosciences sequences, suggesting the pLIT100 ligation did not work. These three fragment sequences were then pairwise aligned to the pLIT100 plasmid, of which Opa shared 95.8% identity, the pTet + TetR promoter shared a 95.3% identity, and mCherry shared 93.8% identity. This confirmed that the ligations were not successful.

Table 3.3: Pairwise alignments of pLIT100 and DNA fragments.

Fragment	Pairwise Identity %	Inserted into pLIT100
Opa Promoter	-	NO
pTet + TetR Promoter	-	NO
mCherry	-	NO
sfGFP	100	YES
sfGFP Terminated	99.9	YES
Kanamycin Resistance	100	YES
Erythromycin Resistance	99.8	YES
Kan GC	99.4	YES
Erythromycin - KO	99.6	YES
ColE1	100	YES

The fragments in pLIT100 storage were deemed fit for use if 100% identity was observed. This included sfGFP, kanamycin resistance, and ColE1. All other fragments that had less than 100% identity will have on going sequencing to resolve point mutation changes. The three fragments that were not confirmed to have successful ligations into pLIT100 were repeated with modified methods.

3.4.2.1 Modified ligation for Golden Gate assembly version 2.0

Fragments were ligated as per section 2.5.4 and Table 2.7. To confirm successful ligations, up to 10 colonies were selected off the plates for cPCR (PCR protocol # 2) (see section 2.2.6), using primers M13 forward and M13 reverse (Table 2.1). The cPCR products were run on a 1% agarose gel, showing the mCherry pLIT100 ligation was successful for six colonies, having the expected DNA band size of ~976 bp (Figure 3.33.a) and the pTet + TetR promoter ligation was successful for four colonies with the expected DNA band size of ~1367 bp (Figure 3.33.b). Due to the size of the Opa promoter being the same as the fragment that drops out of pLIT100 during a Golden Gate reaction, PCR was not used for analysis.

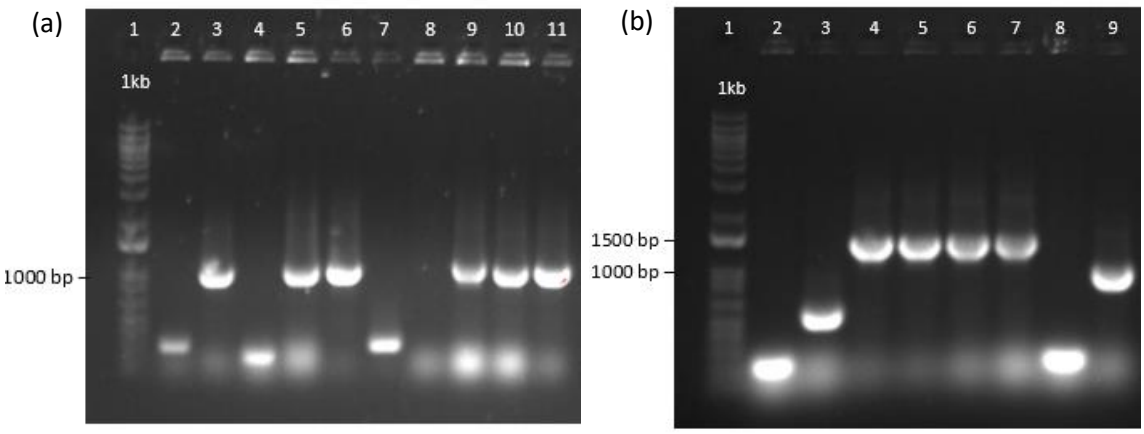

Figure 3.33: Agarose gels of cPCR products for pLIT100 ligations. The mCherry/pLIT100 PCR (a) lane 1: 1kb DNA ladder. Lanes 3, 5, 6, 9, 10, and 11 show the correct PCR product of around 976 bp. The pTet + TetR promoter/pLIT100 PCR (b) lane 1: 1kb DNA ladder. Lanes 4, 5, 6, and 7 show the correct PCR product of around 1367 bp. The PCR was run following Table 2.4 conditions, the digest was run on a 1% agarose gel at 100 V for 45 mins and was visualized using the iBright FL1000 (Invitrogen).

Successful ligations and selected Opa colonies went through DNA extraction and purification. Of the successful colonies, two mCherry and two pTet samples were selected for Sanger sequencing, along with the Opa colonies. Sequencing results confirmed the two colonies for mCherry and pTet had ligated successfully, however the Opa colonies were confirmed to have not ligated successfully (Table 3.4).

Table 3.4: Pairwise alignments of pLIT100 and DNA fragments 2.0

Fragment	Pairwise Identity %	Inserted into pLIT100
Opa Promoter	-	NO
pTet + TetR Promoter	99.6, 99.8	YES
mCherry	100, 100	YES

It was unclear why the Opa promoter was not ligating into the pLIT100 plasmid although it was suspected that the constitutive nature of the promoter could be disrupting maintenance functions of the plasmid. An option to correct this issue would be to incorporate a strong terminator in the Opa fragment sequence that is outside the BsaI flanking restriction enzyme sites (and therefore would not be incorporated during Golden Gate assembly). To continue with the Golden Gate assembly version 2.0, a final ligation of the pLIT100 stored fragments and the linear Opa promoter fragment took place.

3.4.3 Modular cloning system model construct

While there still needs to be verification of the fidelity of some of the cloned fragments, it was nonetheless desired to confirm that the second-generation Golden Gate assembly works using those parts with 100% sequence identity. Therefore, a model construct was built by via a one-step ligation reaction and transformed into *E. coli* (see section 2.5.6). The pLIT100 cloning plasmids chosen contained the fragments: *sfGFP*, kanamycin resistance, ColE1, and the cryptic region. The Opa promoter DNA fragment was added directly from the ordered tubes from Twist Biosciences and all components were mixed together with T4 DNA ligase and BsaI to create a successful ligation made by the Golden Gate assembly version 2.0 (Figure 3.34).

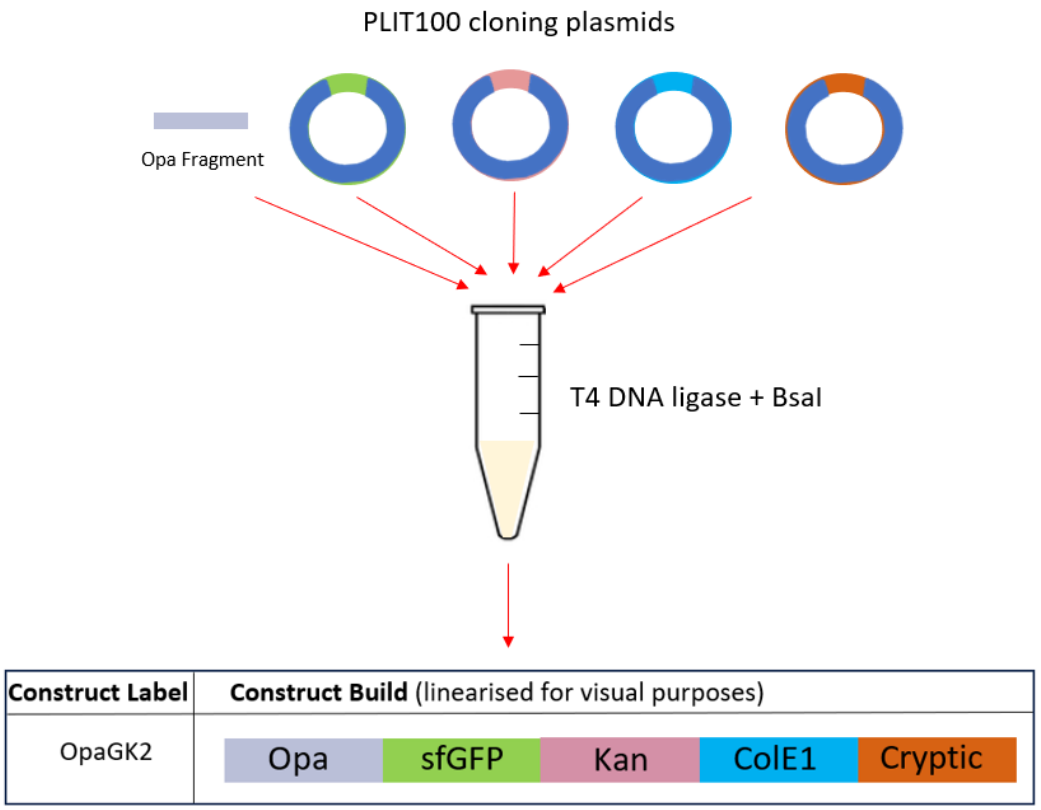

Figure 3.34: Golden Gate assembly of five DNA fragments from pLIT100 cloning plasmids. DNA fragments were BsaI digested out of pLIT100 storage plasmids via the type IIS restriction enzyme BsaI and ligated together via a T4 DNA ligase. This generated the OpaGK2 construct that can be used for gene expression in both *E. coli* and potentially *N. gonorrhoeae*.

This construct was successfully transformed into *E. coli* which gave rise to kanamycin resistant and GFP expressing colonies. Fluorescence was observed when looking at the liquid culture under an Invitrogen Safe Imager™ (Figure 3.35.a). This suggested that the Opa promoter, kanamycin resistance marker, GFP and ColE1 are all functional within the construct. To confirm the construct contains the cryptic region, a HindIII and NotI restriction enzyme digest was carried out (Figure 3.35.b). The construct size is 2707 bp without the cryptic region and is 6669 bp with all fragments integrated.

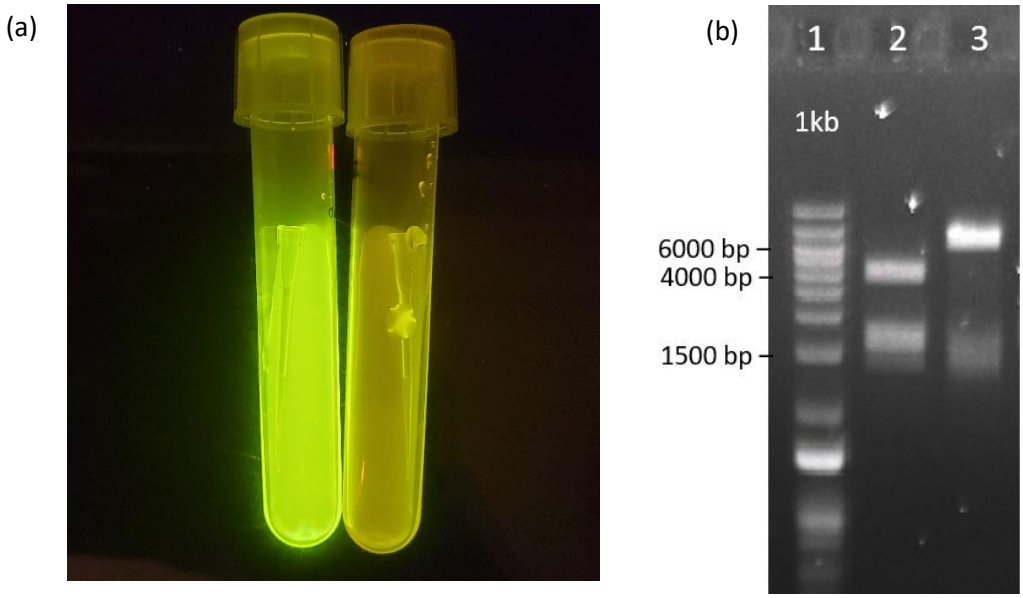

Figure 3.35: Final ligation fluorescence and size confirmation. The liquid culture of a successful ligation was viewed under an Invitrogen Safe Imager™ to observe GFP expression (a; left tube) compared to a construct that did not ligate successfully (a; right tube). A HindIII restriction enzyme digest (b; lane 2) and NotI restriction enzyme digest (b; lane 3) of a Golden Gate ligation of five fragments shows the correct DNA band sizes of around 6669 bp when combined. Lane 1: 1kb DNA ladder. The digests were run on a 1% agarose gel at 100 V for 45 mins and were visualized using the iBright FL1000 (Invitrogen).

The HindIII digest (lane 2) produced DNA bands just above 4000 bp and just above 1500 bp. The NotI digest (lane 3) produced a DNA band just above 6000 bp, therefore suggesting the Golden Gate assembly version 2.0 design is functional in *E. coli*. However, there appears to be slight contamination in the gel around 1500 bp, possibly RNase from DNA extraction, therefore this gel will need to be repeated for further validation of these results.

A transformation into *N. gonorrhoeae* using this new construct will further confirm the viability of the Golden Gate assembly version 2.0 shuttle vector system. This design has consequently created a shuttle vector plasmid that is significantly smaller, more efficient, and easier to transform than the pEG2 plasmid for gene expression in both *E. coli* and (futuristically) *N. gonorrhoeae.*

Chapter Four

Conclusions and Future Directions

Neisseria gonorrhoeae is the pathogen responsible for the STI, gonorrhoea. Increasing rates of gonorrhoea infection is the rise of antibiotic resistant *N. gonorrhoeae* strains that have reduced treatment options. There is no current vaccine for gonorrhoea, and *N. gonorrhoeae* has become resistant to all antibiotics used for its treatment, gaining the 'superbug' status. The natural abilities of *N. gonorrhoeae* has quickly led to the spread antibiotic resistance. Research and development is urgently required for new antimicrobials and vaccines against *N. gonorrhoeae*. To support these efforts, a new generation of recombinant DNA tools specific for modification of *N. gonorrhoeae* would be of high value.

To date, several genetic manipulation tools have been described for *N. gonorrhoeae* that allow researchers to insert or delete genes, create fluorescent strains, or fuse proteins of interest to various reporter tags. There are general considerations for genetic manipulation of *N. gonorrhoeae*. For example, it is naturally transformable, making genetic manipulation easy as long as the DNA being transformed contains the DUS. It also requires the inclusion of resistance marker genes. However, the current approaches, such as restriction ligation cloning, can be time consuming and challenging, and use plasmids that are large in size, leading to a decreased transformation efficiency.

This project aimed to solve many existing problems with *N. gonorrhoeae* plasmid systems by using a Golden Gate assembly technique to design a modular cloning system for the genetic manipulation of *N. gonorrhoeae*. The pEG2 plasmid derived from Christodoulides et al., (2000) was found to be challenging for genetic manipulation after analysis in *N. gonorrhoeae*. Further characterisation confirmed that the pEG2 plasmid was >10kb in size and that its contents did not match the pEG2 plasmid map, making it clear that the pEG2 plasmid was not reliable or easy to manipulate. Therefore, the design of the Golden Gate assembly cloning system was created to make a simpler, more modular shuttle vector than pEG2 that can be transformed into both *E. coli* and *N. gonorrhoeae*. dsDNA fragment parts were designed for assembly: a promoter, an antibiotic resistance marker, a fluorescent protein, an origin of replication, and the

cryptic region from pEG2. From these parts, four plasmid constructs were made: NptIIGK, NptIIME, OpaGK, and OpaME, which were transformed successfully into *E. coli* and then *N. gonorrhoeae*. In *E. coli*, GFP expression was observed under control of both NptII and Opa promoters. However, *mCherry* expression was only observed under the control of the NptII promoter. In *N. gonorrhoeae*, *GFP* expression was observed only under the control of the Opa promoter, and expression of *mCherry* was not observed under any promoter.

Analysis of the OpaGK construct in *N. gonorrhoeae* suggested no significant difference in growth between *N. gonorrhoeae* WT and OpaGK strains. This finding indicated that the plasmid was stable with and without the presence of antibiotic. Further it was established that WT *N. gonorrhoeae* portrays very little background fluorescence, which is essential for a reporter system. Together these data show that the Golden Gate assembly cloning approach can successfully generate a modular system that allows for interchangeable features for genetic manipulation of gonococci.

After validation that the Golden Gate cloning approaches generated constructs with stable fluorescence in both *E. coli* and *N. gonorrhoeae*, further optimisation of individual fragment designs took place to improve assembly efficiency and ease of storage of DNA fragments. A construct was assembled to demonstrate the Golden Gate assembly version 2.0 design and was successfully transformed into *E. coli*, showing GFP expression, and the size validated via restriction enzyme digests.

The Golden Gate cloning system has the advantage of creating small, easy to manipulate, and efficient plasmids for the genetic manipulation of gonococci. The additional fragments in the version 2.0 design of this system will be useful for plasmid complementation for verification of phenotypes caused by mutations in specific genes. Using the inducible pTet + TetR promoter, kanamycin resistance (with a promoter and terminator) and a gene of interest with a mutation, a plasmid can be created that can turn the expression of the gene of interest on and off for analysis of its effects. The kanamycin resistance can also be independently turned on and off so that if expression of the gene of interest is stopped via the pTet + TetR promoter, the plasmid can still be maintained in the bacteria under antibiotic selection.

Despite the promise of the system, there are several areas in which further refinement could be made. For example, an analysis of which regions are essential versus non-essential to the stability and maintenance of the cryptic region could be undertaken to reduce the sequence size and improve transformation efficiencies. Additionally, analysis of the cryptic region fragment functionality after the BsaI recognition site was mutated during the version 2.0 design is still required. As the mutation falls within *cppA*, investigation of the effect of this mutation on the gene and plasmid stability will need to occur. If the mutation results in a non-functional cryptic region, there are other mutations that can be made in the BsaI site or alternative type IIS restriction enzymes can be used for the Golden Gate assembly.

This new system can be used to advance our understanding of *N. gonorrhoeae* biology through its ease of use and stable fluorescence in gonococci. For example, research involving mutagenesis of gonococcal genes generally requires genetic complementation to restore a normal phenotype to mutants. This plasmid-generating system can allow researchers to analyse mutations without integrating genes into the chromosome as usual, which can be complicated, and therefore will be a more efficient tool for research.

Secondly, this system can be used to analyse *N. gonorrhoeae* cell behaviour. For example, cell adhesion mutations can be effectively monitored using the stable fluorescence of the plasmids. The insertion of a Golden Gate plasmid containing a genetic mutation in a gene responsible for cell adhesion can be analysed by comparing fluorescence of cells in solution versus fluorescence of cells adhered to surfaces. It could also be used when treating infected mammalian cells that contain a Golden Gate plasmid in order to observe the effect of a given treatment, as fluorescence will either decrease or remain.

To date, there remains large gaps in our knowledge of *N. gonorrhoeae* biology and current tools for manipulation can be unfavourable. This thesis offers a new system that is an efficient tool for the genetic manipulation of *N. gonorrhoeae* with the hope to further understand its behaviour in the host and mechanisms of infection, therefore finding solutions to reliably treat this ‘superbug' pathogen.

Appendices

GMO approval numbers

For *E. coli*: GMD101146

For *N. gonorrhoeae*: GMD102338

A. First growth curve raw data

First growth curve raw data for *N. gonorrhoeae* WT strain. Data points are rounded to a maximum of two decimal places.

WT								
Replicate	**1**	**2**	**3**	**4**	**5**	**6**	**Average (x 10^6)**	**Standard Deviation**
Hours								
0	38	44					41.00	4.24
1.5	29	37	38	33	35	35	34.50	3.21
3	30	40	28	35	24	11	28.00	10.02
4.5	30	32	40	29	41	30	33.66	5.39
6	58	72	63	50	46	52	56.83	9.56
7.5	81	93	76	57	73	110	81.66	18.15
9	80	86	93	100	102	104	94.16	9.60
10.5	132	120	120	125	124	138	126.50	7.15
12	146	132	157	139	144	140	143.00	8.39
13.5	69	41	280	35	95	129	108.16	91.14

First growth curve raw data for *N. gonorrhoeae* OpaGK strain. Data points are rounded to a maximum of two decimal places.

OpaGK								
Replicate	**1**	**2**	**3**	**4**	**5**	**6**	**Average (x 10^6)**	**Standard Deviation**
Hours								
0	13	20					16.50	4.95
1.5	9	12	4	3	8	5	6.83	3.43
3	19	5	9	6	2	2	7.16	6.37
4.5	13	3	11	14	12	11	10.66	3.93
6	23	15	24	16	18	18	19.00	3.69
7.5	48	16	25	19	13	3	20.66	15.24
9	152	27	60	22	36	62	59.83	48.12
10.5	87	171	24	14	46	81	70.50	57.34
12	22	101	2	0	13	165	50.50	67.50
13.5	29	119	14	19	2	39	37.00	42.12

OD_{600} raw data for first *N. gonorrhoeae* growth curve WT strain. Data points are rounded to a maximum of two decimal places.

WT					
Replicate	**1**	**2**	**3**	**Average (x10)**	**Standard Deviation**
Hours					
0	0.05			0.05	0.03
1.5	0.09			0.09	0.05
3	0.11			0.11	0.06
4.5	0.11			0.11	0.06
6	0.17	0.18	0.19	0.18	0.01
7.5	0.22	0.25	0.21	0.23	0.02
9	0.24	0.22	0.24	0.23	0.01
10.5	0.26	0.26	0.24	0.25	0.01
12	0.25	0.26	0.28	0.26	0.02
13.5	0.28	0.3	0.29	0.29	0.01

OD_{600} raw data for first *N. gonorrhoeae* growth curve OpaGK strain. Data points are rounded to a maximum of two decimal places.

OpaGK					
Replicate	**1**	**2**	**3**	**Average (x10)**	**Standard Deviation**
Hours					
0	0.05			0.05	0.01
1.5	0.07			0.07	0.01
3	0.12			0.12	0.04
4.5	0.13			0.13	0.05
6	0.17	0.14	0.14	0.15	0.09
7.5	0.18	0.19	0.18	0.19	0.09
9	0.19	0.22	0.19	0.2	0.11
10.5	0.22	0.22	0.21	0.22	0.12
12	0.24	0.22	0.23	0.23	0.12
13.5	0.25	0.22	0.24	0.24	0.13

B. Subsequent growth curve raw data

Subsequent growth curve raw data for *N. gonorrhoeae* WT strain. Data points are rounded to a maximum of two decimal places.

WT								
Replicate	**1**	**2**	**3**	**4**	**5**	**6**	**Average (x 10^6)**	**Standard Deviation**
Hours								
0	20	9					14.50	7.78
1.5	17	12	29	24	17	23	20.33	6.12
3	18	18	16	10	10	3	12.50	5.92
4.5	12	17	10	14	14	14	13.50	2.35
6	14	7	8	2	13	10	9.00	4.38
7.5	10	10	8	11	7	9	9.17	1.47
9	3	3	3	3	2	5	3.17	0.98
10.5	5	3	3	6	9	4	5.00	2.28
12	1	1	2	2	3	4	2.17	1.17
13.5	1	1	0	0	0	0	0.33	0.52

Subsequent growth curve raw data for *N. gonorrhoeae* OpaGK + Kan strain. Data points are rounded to a maximum of two decimal places.

OpaGK + kan								
Replicate	**1**	**2**	**3**	**4**	**5**	**6**	**Average (x 10^6)**	**Standard Deviation**
Hours								
0	3	3					3.00	0.00
1.5	1	1	4	4	3	8	3.50	2.59
3	0	0	1	1	1	3	1.00	1.10
4.5	0	1	1	1	1	1	0.83	0.41
6	1	2	0	0	0	0	0.50	0.84
7.5	1	0	0	0	0	0	0.17	0.41
9	0	0	0	0	0	0	0.00	0.00
10.5	0	0	0	0	0	0	0.00	0.00
12	1	0	0	0	0	0	0.17	0.41
13.5	0	0	0	0	0	0	0.00	0.00

Subsequent growth curve raw data for *N. gonorrhoeae* OpaGK - Kan strain. Data points are rounded to a maximum of two decimal places.

OpaGK - kan								
Replicate	**1**	**2**	**3**	**4**	**5**	**6**	**Average (x 10^6)**	**Standard Deviation**
Hours								
0	4	2					3.00	1.41
1.5	1	1	3	2	4	5	2.67	1.63
3	0	0	0	1	1	2	0.67	0.82
4.5	0	0	0	1	1	1	0.50	0.55
6	0	0	0	0	1	1	0.33	0.52
7.5	1	0	0	0	0	0	0.17	0.41
9	1	0	0	0	0	0	0.17	0.41
10.5	0	0	0	0	0	0	0.00	0.00
12	0	0	0	0	0	0	0.00	0.00
13.5	0	0	0	0	0	0	0.00	0.00

Fluorescence raw data for *N. gonorrhoeae* WT strain. Data points are rounded to a maximum of two decimal places.

WT					
Replicate	**1**	**2**	**3**	**Average**	**Standard Deviation**
Hours					
0	0			0.00	0.00
1.5	0	0	0	0.00	0.00
3	0	0	0	0.00	0.00
4.5	0	0	0	0.00	0.00
6	0	0	0	0.00	0.00
7.5	2	0	0	0.67	1.15
9	0	0	0	0.00	0.00
10.5	0	0	0	0.00	0.00
12	0	0	1	0.33	0.58
13.5	0	0	0	0.00	0.00

Fluorescence raw data for *N. gonorrhoeae* OpaGK + kan strain. Data points are rounded to a maximum of two decimal places.

OpaGK + kan					
Replicate	**1**	**2**	**3**	**Average**	**Standard Deviation**
Hours					
0	0			0.00	0.00
1.5	19	1	3	7.67	9.87
3	12	0	8	6.67	6.11
4.5	8	6	6	6.67	1.15
6	0	0	4	1.33	2.31
7.5	0	1	1	0.67	0.58
9	2	1	0	1.00	1.00
10.5	0	8	8	5.33	4.62
12	0	0	4	1.33	2.31
13.5	0	0	0	0.00	0.00

Fluorescence raw data for *N. gonorrhoeae* OpaGK - kan strain. Data points are rounded to a maximum of two decimal places.

OpaGK - kan					
Replicate	**1**	**2**	**3**	**Average**	**Standard Deviation**
Hours					
0	12			12.00	0.00
1.5	4	0	4	2.67	2.31
3	6	4	4	4.67	1.15
4.5	2	0	10	4.00	5.29
6	5	1	0	2.00	2.65
7.5	6	3	1	3.33	2.52
9	2	0	2	1.33	1.15
10.5	0	0	0	0.00	0.00
12	5	8	0	4.33	4.04
13.5	1	0	1	0.67	0.58

Cell count raw data for *N. gonorrhoeae* WT strain. Data points are rounded to a maximum of two decimal places.

WT					
Replicate	**1**	**2**	**3**	**Average**	**Standard Deviation**
Hours					
0	5230			5230	0.00
1.5	149000	160000	86300	131766.7	39757.56
3	157000	154000	167000	159333.3	6806.859
4.5	139000	96800	220000	151933.3	62610.01
6	233000	170000	269000	224000	50109.88
7.5	186000	277000	160000	207666.7	61435.6
9	243000	222000	146000	203666.7	51032.67
10.5	96800	235000	157000	162933.3	69290.79
12	337000	188000	296000	273666.7	76969.69
13.5	238000	392000	290000	306666.7	78341.13

Cell count raw data for *N. gonorrhoeae* OpaGK + kan strain. Data points are rounded to a maximum of two decimal places.

OpaGK + kan					
Replicate	**1**	**2**	**3**	**Average**	**Standard Deviation**
Hours					
0	5230			5230	0.00
1.5	118000	107000	120000	115000	7000
3	146000	217000	75900	146300	70550.48
4.5	209000	259000	204000	224000	30413.81
6	191000	337000	241000	256333.3	74197.93
7.5	424000	68000	233000	241666.7	178158.2
9	201000	277000	251000	243000	38626.42
10.5	298000	256000	52800	202266.7	131134.3
12	332000	267000	264000	287666.7	38423.08
13.5	335000	246000	327000	302666.7	49237.52

Cell count raw data for *N. gonorrhoeae* OpaGK - kan strain. Data points are rounded to a maximum of two decimal places.

OpaGK - kan					
Replicate	**1**	**2**	**3**	**Average**	**Standard Deviation**
Hours					
0	20900			20900	0.00
1.5	194000	144000	196000	178000	29461.84
3	105000	173000	165000	147666.7	37166.29
4.5	107000	235000	220000	187333.3	69973.80
6	175000	180000	222000	192333.3	25813.43
7.5	217000	167000	173000	185666.7	27300.79
9	175000	348000	267000	263333.3	86558.27
10.5	183000	317000	141000	213666.7	91920.26
12	290000	152000	502000	314666.7	176298.99
13.5	484000	120000	382000	328666.7	187769.36

OD_{600} raw data for *N. gonorrhoeae* WT strain. Data points are rounded to a maximum of two decimal places.

WT					
Replicate	**1**	**2**	**3**	**Average (x 10)**	**Standard Deviation**
Hours					
0	0.05			0.05	0.00
1.5	0.1	0.1	0.06	0.09	0.02
3	0.11	0.1	0.11	0.11	0.01
4.5	0.11	0.1	0.12	0.11	0.01
6	0.11	0.12	0.13	0.12	0.01
7.5	0.1	0.16	0.12	0.13	0.03
9	0.11	0.12	0.13	0.12	0.01
10.5	0.12	0.12	0.11	0.12	0.01
12	0.12	0.12	0.11	0.12	0.01
13.5	0.08	0.09	0.1	0.09	0.01

OD_{600} raw data for *N. gonorrhoeae* OpaGK - kan strain. Data points are rounded to a maximum of two decimal places.

OpaGK + kan					
Replicate	**1**	**2**	**3**	**Average (x 10)**	**Standard Deviation**
Hours					
0	0.05			0.05	0.00
1.5	0.07	0.09	0.08	0.08	0.01
3	0.12	0.09	0.09	0.10	0.02
4.5	0.1	0.1	0.11	0.10	0.01
6	0.11	0.14	0.08	0.11	0.03
7.5	0.11	0.09	0.12	0.11	0.02
9	0.07	0.1	0.09	0.09	0.02
10.5	0.09	0.09	0.1	0.09	0.01
12	0.07	0.08	0.09	0.08	0.01
13.5	0.07	0.07	0.07	0.07	0.00

OD_{600} raw data for *N. gonorrhoeae* OpaGK - kan strain. Data points are rounded to a maximum of two decimal places.

OpaGK - kan					
Replicate	**1**	**2**	**3**	**Average (x 10)**	**Standard Deviation**
Hours					
0	0.05			0.05	0.00
1.5	0.11	0.11	0.09	0.10	0.01
3	0.11	0.09	0.09	0.10	0.01
4.5	0.09	0.09	0.09	0.09	0.00
6	0.11	0.08	0.12	0.10	0.02
7.5	0.1	0.12	0.08	0.10	0.02
9	0.08	0.09	0.09	0.09	0.01
10.5	0.08	0.09	0.09	0.09	0.01
12	0.11	0.09	0.11	0.10	0.01
13.5	0.08	0.08	0.07	0.08	0.01

C. Optimisation of inoculum OD_{600}

Inoculum dilutions for *N. gonorrhoeae* WT strain. Data points are rounded to a maximum of two decimal places.

WT				
Replicate	**1**	**2**	**Average (x 10^6)**	**Standard Deviation**
Inoculum				
0.05	61	22	41.5	27.58
0.075	55	80	67.5	17.68
0.1	101	90	95.5	7.78

Inoculum dilutions for *N. gonorrhoeae* OpaME strain. Data points are rounded to a maximum of two decimal places.

OpaME				
Replicate	**1**	**2**	**Average (x 10)**	**Standard Deviation**
Inoculum				
0.05	29	15	22	9.90
0.075	33	48	40.5	10.61
0.1	49	48	48.5	0.71

Inoculum dilutions for *N. gonorrhoeae* OpaGK strain. Data points are rounded to a maximum of two decimal places.

OpaGK				
Replicate	**1**	**2**	**Average (x 10)**	**Standard Deviation**
Inoculum				
0.05	13	7	10	4.24
0.075	7	12	9.5	3.54
0.1	14	8	11	4.24

References

Adamson, P. C., & Klausner, J. D. (2021). The Staying Power of Pharyngeal Gonorrhea: Implications for Public Health and Antimicrobial Resistance. *Clinical Infectious Diseases: An Official Publication of the Infectious Diseases Society of America*, *73*(4), 583–585. https://doi.org/10.1093/cid/ciab074

Bird, J. E., Marles-Wright, J., & Giachino, A. (2022). A User's Guide to Golden Gate Cloning Methods and Standards. *ACS Synthetic Biology*, *11*(11), 3551–3563. https://doi.org/10.1021/acssynbio.2c00355

Buckhout-White, S., Person, C., Medintz, I. L., & Goldman, E. R. (2018). Restriction Enzymes as a Target for DNA-Based Sensing and Structural Rearrangement. *ACS Omega*, *3*(1), 495–502. https://doi.org/10.1021/acsomega.7b01333

Burnstein, K. L., Dyer, D. W., & Sparling, P. F. (1988). Preferential Uptake of Restriction Fragments from a Gonococcal Cryptic Plasmid by Competent Neisseria gonorrhoeae. *Microbiology*, *134*(3), 547–557. https://doi.org/10.1099/00221287-134-3-547

Cehovin, A., & Lewis, S. B. (2017). Mobile genetic elements in Neisseria gonorrhoeae: Movement for change. *Pathogens and Disease*, *75*(6), ftx071. https://doi.org/10.1093/femspd/ftx071

Chao, R., Yuan, Y., & Zhao, H. (2015). Recent advances in DNA assembly technologies. *FEMS Yeast Research*, *15*(1), 1–9. https://doi.org/10.1111/1567-1364.12171

Chevreux, B., Wetter, T. and Suhai, S. (1999). *Computer Science and Biology: Proceedings of the German Conference on Bioinformatics (GCB)* (99th ed.).

Christodoulides, M., Everson, J. S., Liu, B. L., Lambden, P. R., Watt, P. J., Thomas, E. J., & Heckels, J. E. (2000). Interaction of primary human endometrial cells with Neisseria gonorrhoeae expressing green fluorescent protein. *Molecular Microbiology*, *35*(1), 32–43. https://doi.org/10.1046/j.1365-2958.2000.01694.x

Cohen, H. M., Tawfik, D. S., & Griffiths, A. D. (2004). Altering the sequence specificity of HaeIII methyltransferase by directed evolution using in vitro compartmentalization. *Protein Engineering Design and Selection*, *17*(1), 3–11. https://doi.org/10.1093/protein/gzh001

Costa-Lourenço, A. P. R. da, Barros dos Santos, K. T., Moreira, B. M., Fracalanzza, S. E. L., & Bonelli, R. R. (2017). Antimicrobial resistance in Neisseria gonorrhoeae: History, molecular mechanisms and epidemiological aspects of an emerging global threat. *Brazilian Journal of Microbiology*, *48*(4), 617–628. https://doi.org/10.1016/j.bjm.2017.06.001

Davies, J. K., & Normark, S. (1980). A relationship between plasmid structure, structural lability, and sensitivity to site-specific endonucleases in Neisseria gonorrhoeae. *Molecular & General Genetics: MGG*, *177*(2), 251–260. https://doi.org/10.1007/BF00267436

Dillard, J. P. (2011). Genetic Manipulation of Neisseria gonorrhoeae. *Current Protocols in Microbiology*, *0 4*, Unit4A.2. https://doi.org/10.1002/9780471729259.mc04a02s23

Edwards, J. L., & Apicella, M. A. (2004). The molecular mechanisms used by Neisseria gonorrhoeae to initiate infection differ between men and women. *Clinical Microbiology Reviews*, *17*(4), 965–981, table of contents. https://doi.org/10.1128/CMR.17.4.965-981.2004

Edwards, V. L., Wang, L.-C., Dawson, V., Stein, D. C., & Song, W. (2013). Neisseria gonorrhoeae breaches the apical junction of polarized epithelial cells for transmigration by activating EGFR. *Cellular Microbiology*, *15*(6), 1042–1057. https://doi.org/10.1111/cmi.12099

ESR. (n.d.). *New Zealand Sexually Transmitted Infection (STI) Surveillance Dashboard*. Retrieved July 18, 2023, from https://esr-cri.shinyapps.io/2021STIAnnualDashboard/#section-overview

Goodman, S. D., & Scocca, J. J. (1988). Identification and arrangement of the DNA sequence recognized in specific transformation of Neisseria gonorrhoeae. *Proceedings of the National Academy of Sciences of the United States of America*, *85*(18), 6982–6986.

Graves, J. F., Biswas, G. D., & Sparling, P. F. (1982). Sequence-specific DNA uptake in transformation of Neisseria gonorrhoeae. *Journal of Bacteriology*, *152*(3), 1071–1077. https://doi.org/10.1128/jb.152.3.1071-1077.1982

Green, L. R., Cole, J., Parga, E. F. D., & Shaw, J. G. (2022). Chapter Two—Neisseria gonorrhoeae physiology and pathogenesis. In R. K. Poole & D. J. Kelly (Eds.), *Advances in Microbial Physiology* (Vol. 80, pp. 35–83). Academic Press. https://doi.org/10.1016/bs.ampbs.2022.01.002

Guppy protocol. (n.d.). Oxford Nanopore Technologies. Retrieved December 11, 2023, from https://community.nanoporetech.com/protocols/Guppy-protocol/v/gpb_2003_v1_revax_14dec2018

Hilgarth, R. S., & Lanigan, T. M. (2020). Optimization of overlap extension PCR for efficient transgene construction. *MethodsX*, *7*, 100759. https://doi.org/10.1016/j.mex.2019.12.001

Kazi, T. A., Acharya, A., Mukhopadhyay, B. C., Mandal, S., Arukha, A. P., Nayak, S., & Biswas, S. R. (2022). Plasmid-Based Gene Expression Systems for Lactic Acid Bacteria: A Review. *Microorganisms*, *10*(6), 1132. https://doi.org/10.3390/microorganisms10061132

Kirkcaldy, R. D., Weston, E., Segurado, A. C., & Hughes, G. (2019). Epidemiology of Gonorrhea: A Global Perspective. *Sexual Health*, *16*(5), 401–411. https://doi.org/10.1071/SH19061

Korch, C., Hagblom, P., Ohman, H., Göransson, M., & Normark, S. (1985). Cryptic plasmid of Neisseria gonorrhoeae: Complete nucleotide sequence and genetic organization. *Journal of Bacteriology*, *163*(2), 430–438.

Kozlova, A. A., Verkhovskii, R. A., Ermakov, A. V., & Bratashov, D. N. (2020). Changes in Autofluorescence Level of Live and Dead Cells for Mouse Cell Lines. *Journal of Fluorescence*, *30*(6), 1483–1489. https://doi.org/10.1007/s10895-020-02611-1

Kuespert, K., Pils, S., & Hauck, C. R. (2006). CEACAMs: Their role in physiology and pathophysiology. *Current Opinion in Cell Biology*, *18*(5), 565–571. https://doi.org/10.1016/j.ceb.2006.08.008

Lendeckel, U., Venz, S., & Wolke, C. (2022). Macrophages: Shapes and functions. *Chemtexts*, *8*(2), 12. https://doi.org/10.1007/s40828-022-00163-4

Mayo Clinic. (n.d.). *Gonorrhea—Symptoms and causes*. Mayo Clinic. Retrieved July 17, 2023, from https://www.mayoclinic.org/diseases-conditions/gonorrhea/symptoms-causes/syc-20351774

Pryor, J. M., Potapov, V., Kucera, R. B., Bilotti, K., Cantor, E. J., & Lohman, G. J. S. (2020). Enabling one-pot Golden Gate assemblies of unprecedented complexity using data-optimized assembly design. *PLoS ONE*, *15*(9), e0238592. https://doi.org/10.1371/journal.pone.0238592

Pyhtila, B. (2016, March 1). *Plasmids 101: Gibson Assembly and Other Long-Homology Based Cloning Methods*. https://blog.addgene.org/plasmids-101-gibson-assembly

Ramsey, M. E., Hackett, K. T., Kotha, C., & Dillard, J. P. (2012). New Complementation Constructs for Inducible and Constitutive Gene Expression in Neisseria gonorrhoeae

and Neisseria meningitidis. *Applied and Environmental Microbiology*, *78*(9), 3068–3078. https://doi.org/10.1128/AEM.07871-11

Rand, K. N., Young, G. P., Ho, T., & Molloy, P. L. (2013). Sensitive and selective amplification of methylated DNA sequences using helper-dependent chain reaction in combination with a methylation-dependent restriction enzymes. *Nucleic Acids Research*, *41*(1), e15. https://doi.org/10.1093/nar/gks831

Rapid Sequencing gDNA (SQK-RAD004). (n.d.). Oxford Nanopore Technologies. Retrieved August 2, 2023, from https://community.nanoporetech.com/protocols/rapid-sequencing-sqk-rad004/v/rse_9046_v1_revad_14aug2019

Reece-Hoyes, J. S., & Walhout, A. J. M. (2018). Gateway Recombinational Cloning. *Cold Spring Harbor Protocols*, *2018*(1), pdb.top094912. https://doi.org/10.1101/pdb.top094912

Roth, T. L., Milenkovic, L., & Scott, M. P. (2014). A Rapid and Simple Method for DNA Engineering Using Cycled Ligation Assembly. *PLoS ONE*, *9*(9), e107329. https://doi.org/10.1371/journal.pone.0107329

Schlechter, R. O., Jun, H., Bernach, M., Oso, S., Boyd, E., Muñoz-Lintz, D. A., Dobson, R. C. J., Remus, D. M., & Remus-Emsermann, M. N. P. (2018). Chromatic Bacteria – A Broad Host-Range Plasmid and Chromosomal Insertion Toolbox for Fluorescent Protein Expression in Bacteria. *Frontiers in Microbiology*, *9*. https://www.frontiersin.org/articles/10.3389/fmicb.2018.03052

Smith, H. O., Gwinn, M. L., & Salzberg, S. L. (1999). DNA uptake signal sequences in naturally transformable bacteria. *Research in Microbiology*, *150*(9), 603–616. https://doi.org/10.1016/S0923-2508(99)00130-8

SnapGene (Director). (2022, January 18). *A Brief Look at Gibson Assembly*. https://www.youtube.com/watch?v=6bxuThtF828

Soriano, M. (2017, January 12). *Plasmids 101: Gateway Cloning*. https://blog.addgene.org/plasmids-101-gateway-cloning

Spencer-Smith, R., Roberts, S., Gurung, N., & Snyder, L. A. S. (2016). DNA uptake sequences in Neisseria gonorrhoeae as intrinsic transcriptional terminators and markers of horizontal gene transfer. *Microbial Genomics*, *2*(8), e000069. https://doi.org/10.1099/mgen.0.000069

Tóth, E., Huszár, K., Bencsura, P., Kulcsár, P. I., Vodicska, B., Nyeste, A., Welker, Z., Tóth, S., & Welker, E. (2014). Restriction Enzyme Body Doubles and PCR Cloning: On the General Use of Type IIS Restriction Enzymes for Cloning. *PLoS ONE*, *9*(3), e90896. https://doi.org/10.1371/journal.pone.0090896

Unemo, M., & Shafer, W. M. (2011). Antibiotic resistance in Neisseria gonorrhoeae: Origin, evolution, and lessons learned for the future. *Annals of the New York Academy of Sciences, 1230,* E19–E28. https://doi.org/10.1111/j.1749-6632.2011.06215.x

Vos, M. (2009). Why do bacteria engage in homologous recombination? *Trends in Microbiology*, *17*(6), 226–232. https://doi.org/10.1016/j.tim.2009.03.001

Walker, E., van Niekerk, S., Hanning, K., Kelton, W., & Hicks, J. (2023). Mechanisms of host manipulation by Neisseria gonorrhoeae. *Frontiers in Microbiology, 14*. https://www.frontiersin.org/articles/10.3389/fmicb.2023.1119834

Wang, L.-C., Yu, Q., Edwards, V., Lin, B., Qiu, J., Turner, J. R., Stein, D. C., & Song, W. (2017). Neisseria gonorrhoeae infects the human endocervix by activating non-muscle myosin II-mediated epithelial exfoliation. *PLOS Pathogens, 13*(4), e1006269. https://doi.org/10.1371/journal.ppat.1006269

Weber, E., Engler, C., Gruetzner, R., Werner, S., & Marillonnet, S. (2011). A Modular Cloning System for Standardized Assembly of Multigene Constructs. *PLoS ONE*, *6*(2), e16765. https://doi.org/10.1371/journal.pone.0016765

WHO. (n.d.). *Sexually transmitted infections (STIs)*. Retrieved July 17, 2023, from https://www.who.int/news-room/fact-sheets/detail/sexually-transmitted-infections-(stis)